Republic of Iraq

Ministry of Higher Education and Scientific Research

University of Babylon

College of Medicine

Department of Pharmacology

Potential Nephroprotective Effects of SGLT2 Inhibitors in Methotrexate-induced Nephrotoxicity in Animal Model

A thesis Submitted to the Council of the College of Medicine, the University of Babylon, as a Partial Fulfillment of the Requirements for the Degree of Master in Pharmacology /Pharmacology and Toxicology

By:

Rami Thamer Kareem Abdul Aimma Alhusseiny

BSc. Pharmacy (2016-2017)

Al-Rafidain university college

Supervised by:

Assist. Prof.

Majid Kadhim Abbas

MS.C Pharmacology

1445 A.H

Lect.

Dr. Ahmed Raji

FICMS. Pathology

2024 A.D

”بسم الله الرحمن الرحيم“

قَالُوا سُبْحَانَكَ لَا عِلْمَ لَنَا إِلَّا مَا عَلَّمْتَنَا إِنَّكَ أَنْتَ الْعَلِيمُ الْحَكِيمُ

صدق الله العلي العظيم

سوره البقره (ايه ٣٢)

Supervision Certificate

We certify that this thesis entitled **(Potential Nephroprotective Effects of SGLT2 Inhibitors in Methotrexate-induced Nephrotoxicity in Animal Model)** was prepared by (**Rami Thamer Kareem Abdul Aimma Alhusseiny**) under our supervision at the Department of Pharmacology. College of Medicine, University of Babylon (Iraq), in partial fulfillment of the requirements for the master's degree of sciences in pharmacology and toxicology.

Signature
Assistant Professor
Majid Kadhim Abbas
University of Babylon
Supervisor
Date:

Signature
Lecturer
Ahmed Raji
University of Babylon
Supervisor
Date:

The Recommendation of the Head of Department

In view of the available recommendation, I forward this thesis for debate by the examining committee.

Reyadh H. Al-Mosawi
Head of the Department of Pharmacology
College of Medicine
University of Babylon, Iraq

Examining Committee Certificate

We certify that we have read this thesis entitled "**Potential Nephroprotective Effects of SGLT2 Inhibitors in Methotrexate-induced Nephrotoxicity in Animal Model**" and as an examining committee examined the student "**Rami Thamer Kareem Alhusseiny**" in its contents and that in our opinion it meets the standard of a thesis for the degree of Master, in Pharmacology and Toxicology.

Prof.

Najah Rayish Hady

University of Al Kufa/ College of Medicine

Chairman

Assi. Prof.

Reyadh H. Al Mosawy

University of Babylon /

College of Medicine

Member

Prof.

Haider Abdul Rida

University of Babylon/

College of Medicine

Member

Assi. Prof.

Majid Kadhim Abbas

University of Babylon /

College of Medicine

Supervisor and Member

Lect. Dr.

Ahmed Raji

University of Babylon /

College of Medicine

Supervisor and Member

Approved for the college council

Prof.

Mohaned A.N. Alshalah

(Dean of the college of medicine)

Acknowledgment

I'm sincerely grateful to Allah. Through his grace, all good deeds are done. I would like to express my heartfelt gratitude to my esteemed professors and supervisors, Dr. Majed Kadhim Abass and Dr.Ahmed Raji, whose unwavering support, insightful guidance, and profound expertise have been invaluable throughout my research journey. Their dedication and mentorship have been pivotal to the successful completion of this thesis.

I am also deeply indebted to the Department of Pharmacology, under the exemplary leadership of Dr. Riyad Almosawy and to Dr. Salman M. Salman. The department has provided an inspiring and nurturing environment that has greatly enriched my academic and professional development.

To all my professors, colleagues, and the entire academic community, your encouragement and support have been a source of strength and motivation. Thank you for your contributions and for being an integral part of this significant achievement

Rami Thamer K. Alhusseiny

Dedication

I dedicate this work to my incredible parents, whose unwavering faith in me and constant support have been my bedrock. To my wonderful brother and cherished sisters, your encouragement and love have been sources of immense strength and inspiration.

I extend my heartfelt gratitude to my colleagues, friends, and mentors for their invaluable support and companionship throughout this journey.

I wish to express my deepest gratitude to Dr. Majid Kadim. His relentless support and tireless efforts have profoundly impacted me, and I will forever remember and appreciate all that he has done for me.

Finally, I wish to extend my sincere appreciation to all my teachers, whose guidance and wisdom have been instrumental in shaping my academic path. Thank you for your dedication and commitment to my education.

Rami Thamer K. Alhusseiny

Summary

Nephrotoxicity is the third most common cause of Acute Kidney Disease (AKD), which has gotten worse in recent decades as a result of drug use that carries a higher risk of kidney damage. Studies have shown that up to 20% of critically ill patients use nephrotoxic drugs. While safety tests are required before new pharmaceuticals can be released onto the market, adverse effects are frequently discovered only after the drug is on the market and being used by various populations worldwide. The kidney's excretion of drugs and metabolites exposes the kidneys' high-energy-requiring structures, the glomeruli and tubules, to large concentrations of foreign chemicals, which explains why drug-induced kidney injury rates are so high. The loss of GFR is a late marker of kidney injury, and other biomarkers are being researched to allow for an earlier intervention, which could improve the prognosis of these patients.

Sodium glucose co-transporter 2 inhibitors is a class of antidiabetic family that have kidney protection. This study explored the effects of (empagliflozin, dapagliflozin, and ertugliflozin) as an antioxidant, anti-inflammatory, and kidney protectors.

Fifty adult male albino rats were enrolled, and the selected rats were divided into five groups, with ten rats in each group. Group A (control) was neither exposed to MTX nor received any treatment, while group (B) was exposed to 10mg/kg of MTX I.P. on day ten of the experiment. Group (C) received 10mg/kg of empagliflozin by oral gavage for fourteen days and 10mg/kg of MTX I.P. on day 10 of the experiment. Group (D) was exposed to dapagliflozin 10mg/kg by oral gavage for fourteen days and MTX 10mg/kg I.P. on day ten of the experiment. Group (E) received 20mg/kg.

Of ertugliflozin by oral gavage for fourteen days and was exposed to 10mg/kg of MTX I.P. on day ten of the experiment.

The kidney protective effect of selected SGLT2I was evaluated by measuring the TNF-a, IL-1B, MDA, GSH, Total protein, Creatinine, and Urea serum levels using a specific kit for each parameter. In group (B), TNF-a, IL-1B, MDA, Urea, and creatinine were highly significantly ($p<0.001$) increased compared to group (A). However, Total protein and GSH were highly significantly ($p<0.001$) decreased compared to group (A). In groups (C, D, and E), TNF-a, IL-1B, MDA, Urea, and creatinine were significantly decreased (P- value <0.05), but Total protein and GSH were significantly (P- value >0.05) increased in comparison to group (B).

Exposed to MTX exhibits severe inflammation and notable morphological changes (marked vascular congestion, Chronic inflammatory cell infiltration, Bowman space widening, and Tubular cell vacuolation). Comparing group (B) to control group (A). Empagliflozin, dapagliflozin, and ertugliflozin have alleviated histopathological damage and mild inflammation compared to group (B).

In conclusion, the selected SGLT2I has anti-inflammatory, antioxidant, and renal protective effects, as depicted by biochemical tests and histopathological results.

List of content

List of Tables

List of Figures

List of Abbreviations

Abbreviations	Meanings
AIN	Acute Interstitial Nephritis
AKD	Acute Kidney Disease
CKD	Chronic Kidney Disease
CNI	Calcineurin Inhibitor
DCT	Distal Convoluted Tubule
DKD	Diabetic Kidney Disease
GFR	glomerular filtration rate
KIM-1	Kidney Injury Molecule-1
PCT	Proximal Convoluted Tubule
PTECS	Proximal Tubular Epithelial Cells
SBP	Systolic Blood Pressure
SGLT2I	Sodium-Glucose Cotransporter 2 Inhibitors
T2D	Type 2 Diabetes
UGE	Urinary Glucose Excretion

ATP	Adenosine triphosphate
BUN	Blood Urea Nitrogen
Cr	Creatinine
CVD	Cardiovascular Disease
DNA	Deoxyribonucleic Acid
GGT	Gamma-glutamyl transpeptidase
GPx	Glutathione peroxidase
GSH	Reduced Glutathione
GSSG	Glutathione Disulfide
H_2O_2	Hydrogen peroxide
HO-1	Heme Oxygenase-1
I.P.	Intraperitoneal
IL	Interleukin
IL-1B	Interleukin-1Beta
MDA	Malondialdehyde
MTX	Methotrexate
NADPH	Nicotinamide adenine dinucleotide phosphate
NF-kB	Nuclear factor kappa-light-chain enhancer of activated B cell
NrF2	Nuclear factor erythroid 2–related factor 2
OD	Optical Density
RNA	Ribonucleic Acid
ROS	Reactive Oxygen Species
SE	Side effects
TNF-α	Tumor Necrosis Factor-alpha
UACR	Urine Albumin/Creatinine Ratio

DAPA	Dapagliflozin
EMPA	Empagliflozin
ERTU	Ertugliflozin
IM	Intramuscular
PHD	Pharmacodynamics
PHK	Pharmacokinetics

Chapter One

Introduction & Literature Review

1.1. Introduction

In both inpatient and outpatient settings, as many as 60% of patients admitted to intensive care units have the diagnosis of acute kidney damage (AKI). Its incidence has increased in recent years, which is consistent with a rise in risk factors such as chronic kidney disease (CKD), diabetes mellitus, and senior age. Nephrotoxicity is the third most common cause of Acute Kidney Disease (AKD), which has gotten worse in recent decades, according to epidemiological studies. as a result of drug use that carries a higher risk of kidney damage. Studies have shown that up to 20% of critically ill patients use nephrotoxic drugs. While safety tests are required before new pharmaceuticals can be released onto the market, adverse effects are frequently discovered only after the drug is on the market and being used by various populations worldwide. The kidney's excretion of drugs and metabolites exposes the kidneys' high-energy-requiring structures, the glomeruli and tubules, to large concentrations of foreign chemicals, which explains why drug-induced kidney injury rates are so high. **(Sales & Foresto, 2020)**

Loss of glomerular filtration rate. (GFR) is a late sign of renal impairment, and additional indicators are being studied to allow for early management, perhaps improving the prognosis of these patients. Although high-quality studies prove no benefit, there are some promising candidates:

1. Kidney Injury Molecule (KIM-1), is an adhesion molecule generated in the proximal convoluted tubule (PCT). It has been shown that in cases of ischemia and drug toxicity, KIM-1 is elevated in urine concentration. This has been reliably established for cisplatin, gentamicin, and cyclosporine, and in some cases, it is raised 48 hours after the hazardous agent is administered and prior to GFR decline.

2. The production of beta-2 microglobulin, primarily by lymphocytes, raises the concentration of the protein in urine in inflammatory conditions, such as infections and autoimmune illnesses. It is thought to be a sign of tubular damage after glomerulus filtration and PCT reabsorption. A study on kidney transplantation showed a high degree of accuracy in differentiating rejection in patients with calcineurin inhibitor (CNI) toxicity before the decline in kidney function.

3. A protein called clusterin is present in many organs, including the kidney, and it plays a role in both apoptosis and antiapoptosis processes. It is not filtered and is created in the tubules during stressful conditions to stop cell death. Compared to creatinine, its higher diagnostic accuracy for tubular damage has been shown using cisplatin, vancomycin, tacrolimus, and gentamicin. It does not rise in patients with glomerular injury and has an early increase comparable to that of KIM-1.

4. All nucleated cells produce the protein cyclostatin C, which can be freely filtered. Since the proximal tubule entirely reabsorbs it, it is typically utilized to estimate GFR in cases with steady renal function, such as those involving cirrhosis when creatinine clearance is less accurate. Research on renal toxicity has demonstrated a stronger association between amphotericin B, polymyxin, vancomycin, and cisplatin than with creatinine. **(Griffin et al., 2019)**

Sodium-glucose co-transporter 2 inhibitors, often known as glucose-lowering medicines, work by decreasing the amount of glucose reabsorption from the renal filtrate, producing a glucosuric effect and eliminating excess glucose. Since the first SGLT2 inhibitor was introduced in 2012, the class of drugs has expanded to include canagliflozin, dapagliflozin, empagliflozin, and ertugliflozin in the Americas and Europe, with more drugs in the class starting to gain traction in other countries. Despite being intended to help with type 2 diabetes body weight control

and lower hyperglycemia, it is now recognized that SGLT2 inhibitors offer additional treatment alternatives to address the comorbidities and cardio-renal consequences associated with type 2 diabetes. Nephroprotective impacts of SGLT2I are class effects seen in individuals with normal or reduced GFR while using any of the approved medicines. **(Bailey et al., 2022)**

Aim of the Study

The current research sought to:

1. Highlight the effect of empagliflozin, dapagliflozin, and ertugliflozin on renal function biomarkers, Creatinine, Urea, and total protein in male rats.

2. Explore the anti-oxidant effects of empagliflozin, dapagliflozin, and ertugliflozin in male rats.

3. Investigate the anti-inflammatory effects of empagliflozin, dapagliflozin, and ertugliflozin in male rats.

1.2 The Kidney Pathophysiology

The kidney is the primary organ of mammals and has emerged as one of the main focus areas for drug research. Many human renal illnesses are fatal if the kidney is significantly damaged. **(Morya et al., 2018)**

The medulla, inner hilum, and outer cortex comprise the kidney. Nephrons, the functioning elements of the kidney located in the renal cortex, number about a million per kidney. Urine can be concentrated to 1-2 liters per day because of nephrons, which are tiny, functionally separate units that filter fluids and small molecules from the circulation. Nephrons also have a single tubule that secretes metabolic waste products and reabsorbs most purified molecules.**(Den Hartogh & Tsiani, 2019)**

There are two types of nephrons: cortical and juxtamedullary. The short Henle loop of the cortical nephron has a tip that dips into the outer medulla but stays outside the inner medulla. A lengthy loop of Henle descends into the medulla of the juxtamedullary nephron. **(Kardasz, 2015)**

The distal convoluted tubule (DCT), proximal convoluted tubule (PCT), loop of Henle, and collecting duct system are the components that make up the tubule. The first part of the renal tubule is the PCT. The PCT is continued in the Henle loop. The main processes are reabsorption and utilizing countercurrent multiplication to create a medullary interstitial osmolar gradient that will both concentrate and dilute urine. The distal convoluted tubule and the collecting duct make up the terminal nephron. An essential nephron component for regulating blood pressure and potassium (K+) balance is the distal convoluted tubule (DCT).**(Theodorou et al., 2021).**

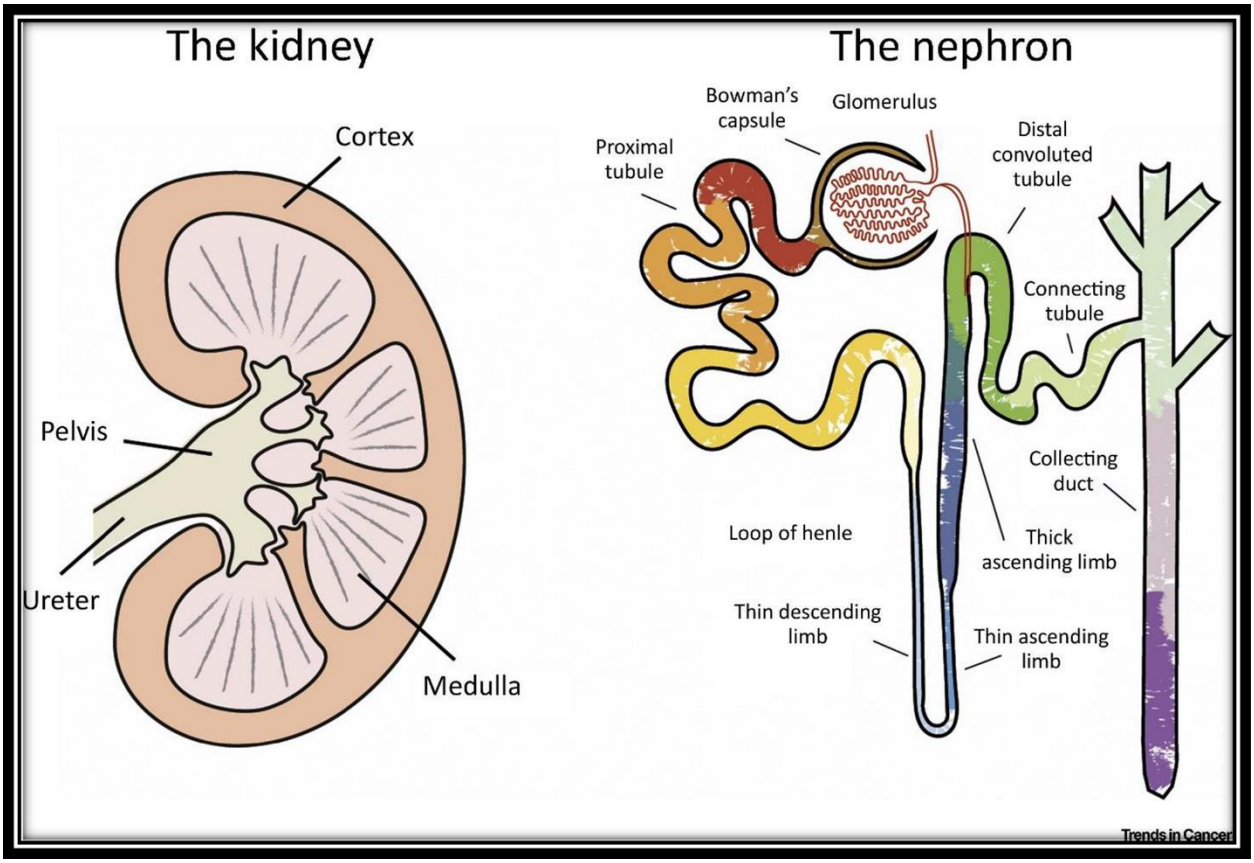

Figure 1.1 Structure of Kidney.**(Lindgren et al., 2018)**

1.3 Function of The Kidney

The kidney performs various tasks, including stimulating the creation of red blood cells, filtering and excreting metabolic waste products from the bloodstream, and regulating essential electrolyte levels. The renin-angiotensin-aldosterone system regulates water absorption, preserves the proper pH level, keeps the body's intravascular fluid, and helps control blood Pressure. Additionally, the kidney reabsorbs glucose and amino acids, which may have a role in the activation of vitamin D, calcitriol, and erythropoietin to regulate hormonal processes. **(Morya et al., 2018)**

1.4 Drugs Induce Nephrotoxicity

The term acute kidney injury (AKI) refers to the sudden drop in the glomerular filtration rate, which was previously known as acute renal failure.

Nephrotoxicity develops by one of the three below mechanisms:

1. Drug transfer from the apical surface, drug exudation from the basolateral surface into the tubular lumen, and apical contact with medicines or their metabolic products are the causes of proximal tubular injury and acute tubular necrosis (ATN), which is a dose-dependent mechanism. Medications that cause this kind of kidney damage include amphotericin B, gentamycin, kanamycin, streptomycin, tobramycin, vancomycin, cisplatin, cidofovir, and adenofovir. **(Kwiatkowska et al., 2021)**

2. Drug and metabolite crystals or casts might block the tubules (a dose-dependent mechanism): Certain medications, such as methotrexate, sulfadiazine triamterene, vancomycin, Indinavir, and ciprofloxacin, can result in this kind of kidney injury. The distal portions of the nephron get these medications after being eliminated via filtration and secretion into the tubules. **(Kwiatkowska et al.,2021).**

Methotrexate and its metabolite (7-OH methotrexate) are filtered and secreted into the urine via the tubules. Because methotrexate/7-OH is poorly soluble in acidic urine and has a decreased urine flow rate, crystal precipitation is encouraged. **(Luciano & Perazella, 2018)**

3- Acute interstitial nephritis (AIN) is an immune-mediated kidney injury marked by immune cell infiltration in the tubulointerstitial **(Boyer et al., 2022)**

Numerous processes are known to be responsible for drug-induced AIN. Immune complexes associated with medications accumulate in the renal interstitium. This leads to uncommon antibody-mediated reactions where drugs produce antibodies against the tubular basement membrane and a type 4 hypersensitivity reaction dominated by T cells. Antibiotics, nonsteroidal anti-inflammatory medicines (NSAIDs), immune checkpoint inhibitors (ICPIs), and proton pump inhibitors (PPIs) are the most common drugs associated with acute interstitial nephritis (AIN). AIN was first associated with antibiotics, which were responsible for over half of all AIN cases. These consist of rifampin, fluoroquinolones, sulfa-containing medications, and B-lactam antibiotics. **(Paueksakon & Fogo, 2017)**

1.4.1 Patient-related Risk Factors

A patient may be predisposed to drug-induced nephrotoxicity for a variety of reasons, some of which are mentioned below: Due to variations in hormones, which are often implicated in drug-induced nephrotoxicity. Susceptibility: men are more likely than women to experience the nephrotoxic effects of drugs. Heart failure, liver dysfunction, and dehydration are risk factors for drug-induced renal impairment. Acute kidney injury is more common in patients over 60 with diabetes mellitus, heart failure, dehydration, and chronic renal insufficiency. **(Al-Naimi et al., 2019).** Furthermore, because of the poor prerenal physiology linked to growing liver dysfunction, patients with advanced cirrhosis and acute hepatic failure are particularly vulnerable to drug-induced kidney impairment. Since hypoalbuminemia increases free drug concentrations and exposes cells to higher quantities, it escalates the risk associated with hepatic failure or nephrotic syndrome. **(Izzedine & Perazella, 2017)**

1.4.2 Drug-related Risk Factor

Nephrotoxicity is also a result of the pharmacological component of many medications, which is frequently enhanced in the renal microenvironment. For example, methotrexate causes crystalline nephropathy by decreasing urine flow rates and pH, encouraging crystal formation inside tubular lumens. Moreover, the kidney functions as a metabolic organ, using the renal parenchyma's cytochrome p450 and other enzyme systems to transform medications into metabolites. Many of these metabolites can damage the kidney by producing harmful reactive oxygen species and oxidative stress, among other methods. Certain medication classes necessitate the existence of extra risk factors, which can include, among other things, patient-related risk factors, specific disease states, and renal insufficiencies. **(Mody et al., 2020)**

1.5 Control of Blood Sugar

The kidneys regulate the balance of glucose via glucose synthesis, use, as well as absorption. The kidneys use gluconeogenesis to release the remaining 20% of endogenous glucose into circulation, with the liver accounting for 80% of this amount. This process occurs in the renal cortex, which houses all the enzymes required to synthesize glucose. In contrast, the renal medulla is where glucose utilization, or glycolysis, predominantly takes place. The kidneys need about 10% of the total glucose the body uses to eliminate waste from the blood, reabsorb essential nutrients, and carry out regulatory tasks. The kidneys are the body's second-most energy-demanding organ**.(Alsahli & Gerich, 2017)**

1.5.1 Sodium Glucose Co-Transporters

Daily, healthy kidneys filter 180 liters of blood, or around 180 grams of glucose, assuming an average plasma glucose concentration of 5.5 mmol/L. The amount of glucose in the blood and the glomerular filtrate are linearly correlated because the glomerulus easily filters glucose. Essentially, all of the filtered glucose will be reabsorbed prior to urine excretion in euglycemic conditions. Located in the proximal tubule of the nephron, sodium-glucose cotransporter-1 and -2 (SGLT1/2) are the primary mediators of glucose reabsorption in the kidneys (Figure 1.2). On the apical membrane of proximal tubular epithelial cells (PTECs) in the S1 and S2 segments of the proximal tubule, SGLT2 is a low-affinity, high-capacity transporter protein. Owing to its low affinity and initial role in glucose reabsorption, SGLT2 carries out approximately 97% of all glucose reabsorption in the kidneys, with SGLT1, which is situated on the apical membrane of PTECs in the S3 segment of the proximal tubule, handling the remaining ~3%. In a 1:1 ratio, SGLT2 moves salt and glucose from the proximal tubule lumen into the PTEC intracellular matrix. SGLT2 proteins exploit the electrochemical gradient of sodium to transport glucose against its concentration gradient into PTECs, linking the transport of sodium and glucose together. Glucose transporters (GLUT1 in the S3 segment and GLUT2 in the S1 and S2 segments) help move glucose from PTECs back into the bloodstream after it has been inside. This process continues until the kidneys' maximal capacity to reabsorp glucose is reached, at which point glucosuria develops on its own. The basolateral Na+ /K + adenosine triphosphatase (ATPase) pump expels three Na+ ions for every two K + ions entering the cell, maintaining the electrochemical gradient of sodium on the apical membrane. Consequently, preserving sodium-potassium homeostasis requires an energy-

intensive process that corresponds with the proximal tubule's reabsorptive activities. **(DeFronzo et al., 2017)**

1.6 History of SGLT2I

Kidneys are essential for maintaining glucose homeostasis, but therapeutic approaches for type 2 diabetes have recently begun to focus on them. As previously described, renal sugar control is an insulin-independent process regulated by passive transport via SGLT2 proteins. **(Vallon, 2011)**

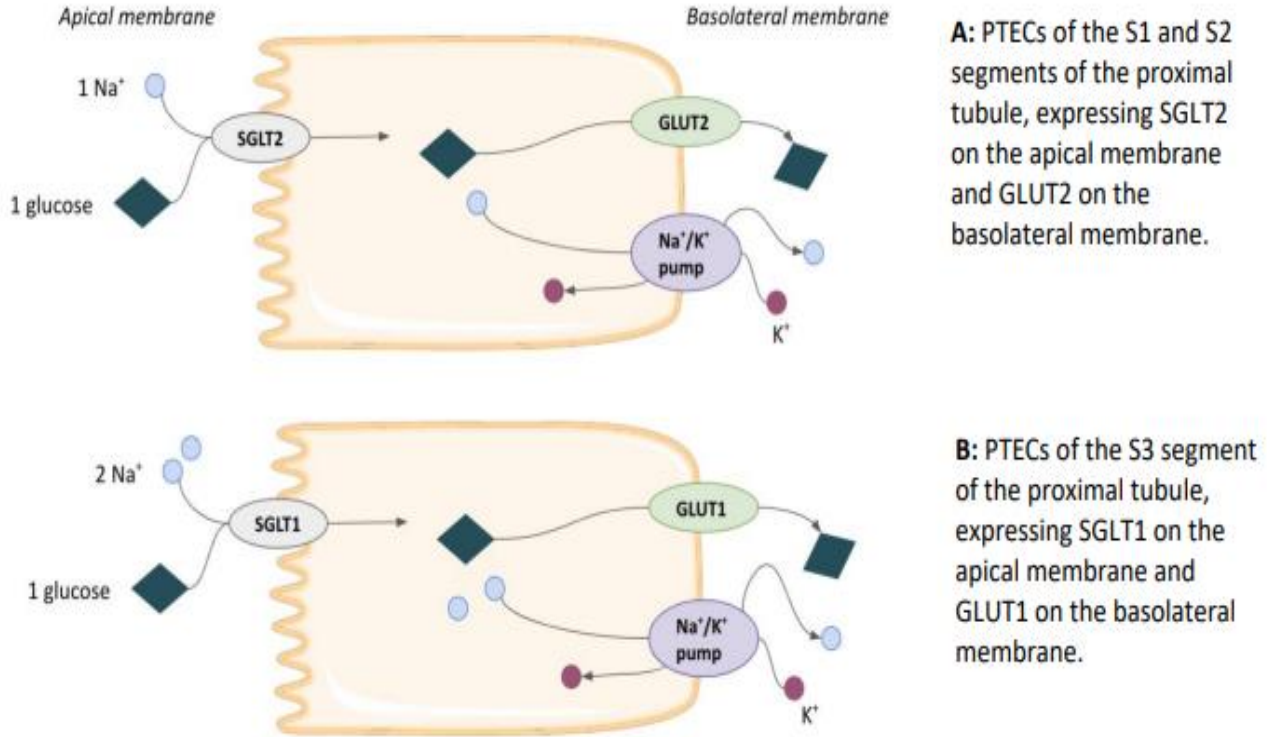

Figure 1.2: Co-transport of Suger and Sodium in the PT. **(DeFronzo et al., 2017)**

For those with T2DM who have historically used insulin and oral antihyperglycemics therapy and have a consistently high HbA1c, this offers a novel therapeutic option. Antihyperglycemic medications seek to increase endogenous insulin shortages, reinstate beta-cell activity, or enhance insulin sensitivity. Because of a steady reduction in the function of beta cells and persistent insulin resistance, these treatments eventually lose their ability to manage hyperglycemia. **(Vallon & Thomson, 2017)**

As a result, a large number of sick people are going to be on several antihyperglycemic drugs and might ultimately need insulin treatment. Developing T2D treatments that do not require insulin is critical in maintaining glycemic control and managing microvascular problems like diabetic kidney disease (DKD). A relatively new family of licensed antihyperglycemic drugs called SGLT2 inhibitors is safe and effective in treating type 2 diabetes (T2D) by reducing hyperglycemia without the need for insulin. **(J. Liu et al., 2012)**

Phlorizin is a chemical present in the fruit, leaves, shoots, and root bark of apple trees and was initially shown to have temporary glucosuric effects in 1885 by preventing the kidneys from reabsorbing glucose. Phlorizin was a potential treatment for diabetes at the time. Still, its limited oral bioavailability, poor water solubility, and lack of specific inhibition of SGLT2 and SGLT1 proteins have made it unsuitable for use in therapeutic settings. Therefore, phlorizin causes severe diarrhoea by inhibiting both renal glucose reabsorption and intestinal glucose-galactose absorption mediated by SGLT1. As a result, SGLT2 inhibitors that are more stable and specific have been developed. SGLT2 inhibitors regulate hyperglycemia without requiring insulin sensitivity or a functioning pancreas since they decrease renal glucose reabsorption and increase urine glucose excretion. Currently, available SGLT2 inhibitors for treating patients with T2D are

canagliflozin, dapagliflozin, empagliflozin, and most recently, ertugliflozin **(Rieg & Vallon, 2018).**

Table 1.1: Pharmacokinetics of the targeted SGLT2 inhibitors.

SGLT2 inhibitors	***t 1/2***	**Tmax**	**Max UGE**	**SGLT2 selectivity**
Empagliflozin	8-13 hrs	1.5-2.5 hrs	50-80 g/day	>2500-fold
Dapagliflozin	12.9 hrs	1 hrs	60 g/day	>1200-fold
Ertugliflozin	11-17 hrs	0.5-1hrs	70 g/day	>2000-fold

1.6.1 Empagliflozin

Empagliflozin (EMPA), an SGLT2I, belongs to the most recent group of oral hypoglycemic medications, including dapagliflozin and canagliflozin. The Food and Drug Administration authorized empagliflozin, the most recent drug in its class, in August 2014. The profile of empagliflozin negative impacts is minimal. When combined with other antidiabetic medications. Through its production, use, and—most importantly—its SGLT2-mediated reabsorption of glucose from the glomerular filtrate, the kidney is an essential component of glucose homeostasis. An estimated 90% of renal glucose reabsorption is facilitated by SGLT2. When

SGLT2 is inhibited, the kidneys excrete more glucose through the urine (UGE), which lowers plasma glucose levels without the need for insulin. Empagliflozin, a highly effective, competitive, and selective SGLT2 inhibitor, is approved to treat type 2 diabetes in individuals with normal renal function. Empagliflozin is an orally active tablet. C23H27ClO7 is an organic structure, and the molecular mass is 450.91 g/mol (Figure 1.3).In patients with T2DM, By 1) raising total glucose excretion, 2) enhancing beta-cell activity, and 3) changing substrate usage from glucose to lipid despite a compensatory rise in endogenous glucose synthesis, empagliflozin reduced fasting and postprandial glucose levels. **(Ndefo et al., 2015)**

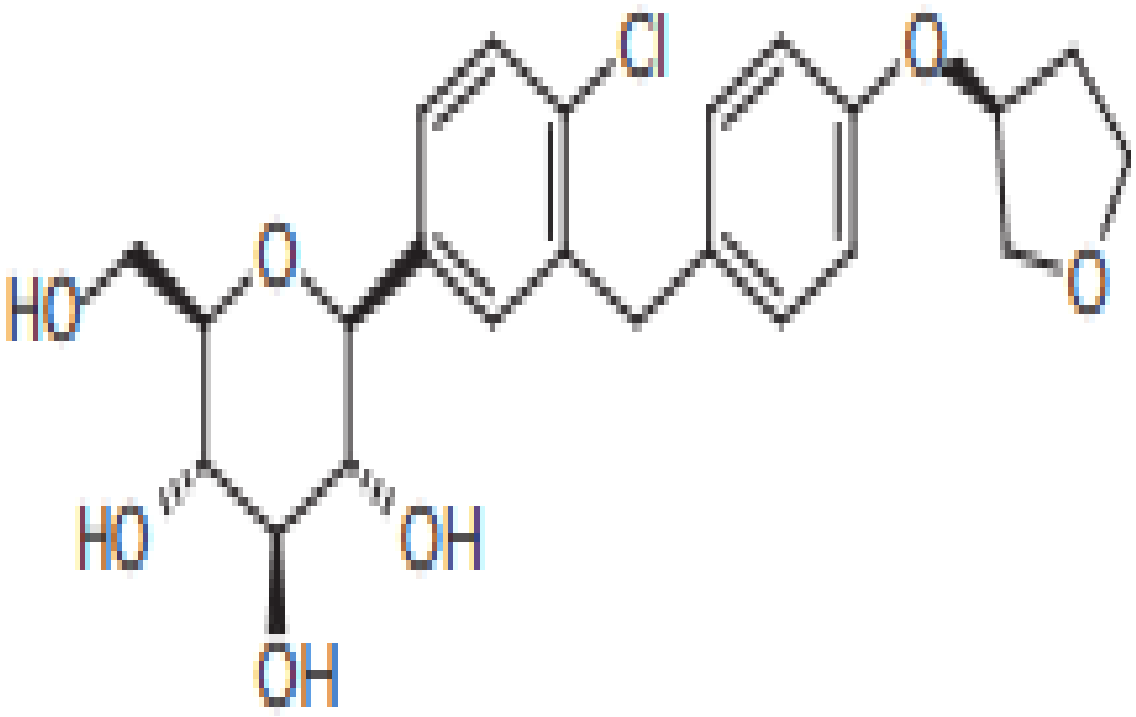

Figure 1.3: Structural formula of empagliflozin **(Ndefo et al., 2015).**

1.6.1.1 Pharmacokinetic

EMPA is a 78% bioavailable, selective SGLT2 inhibitor that can be used orally. It has no active metabolites and few drug-drug interactions. Empagliflozin absorbs quickly when taken orally; peak levels are reached 1.5 hours after a single dose. In healthy individuals, 86.2% of empagliflozin is protein-bound and dispersed throughout tissues and bodily fluids. The main glucuronidation method of empagliflozin metabolism is carried out by UGT2B7, UGT1A3, UGT1A8, and UGT1A9. Empagliflozin is excreted by the kidneys; of an oral dose of empagliflozin that was radiolabeled, about 54.4% was recovered in the urine, with half of that amount being recognized as an unmodified medication. **(Ndefo et al., 2015)**

1.6.1.2 Cardiovascular Effect

Empagliflozin has a cardioprotective effect; the relative risk of the primary composite outcome of death from cardiovascular causes, nonfatal MI, or nonfatal stroke was reduced by 14%; death from cardiovascular cause was reduced by 38%; death from any cause was reduced by 32%; and hospitalization for heart failure (HHF) was reduced by 35% in the empagliflozin-treated Patients. In addition to lowering HbA1c levels by 0.5%, empagliflozin reduced arterial stiffness, vascular resistance, and plasma urate levels. Empagliflozin also significantly reduced systolic blood pressure and blood volume without increasing heart rate. The caloric loss incurred by glucosuria resulted in moderate weight reduction in visceral adiposity. **(Steiner, 2016)**

1.6.1.3 Renal Effect

The mechanisms by which sodium-glucose cotransporter 2 (SGLT2) inhibitors

provide nephroprotection in nondiabetic models of chronic kidney disease (CKD) remain poorly understood. For this, there are numerous mechanisms:

1. Empagliflozin lowers blood creatinine, decreases proteinuria, increases the clearance of creatinine and ameliorates glomerulosclerosis, perivascular fibrosis, renal interstitial fibrosis, and renal interstitial inflammation in diabetic and nondiabetic nephropathy. **(Chen et al., 2023)**

2. Empagliflozin significantly raised the bcl2/bax and LC3-II/LC3-I ratios, demonstrating its advantageous effects on autophagy activation and apoptosis inhibition. Thus, by encouraging autophagy and mitochondrial biogenesis and reducing oxidative stress, inflammation, and apoptosis, empagliflozin reduced renal I/R injury**. (Ala et al., 2022)**

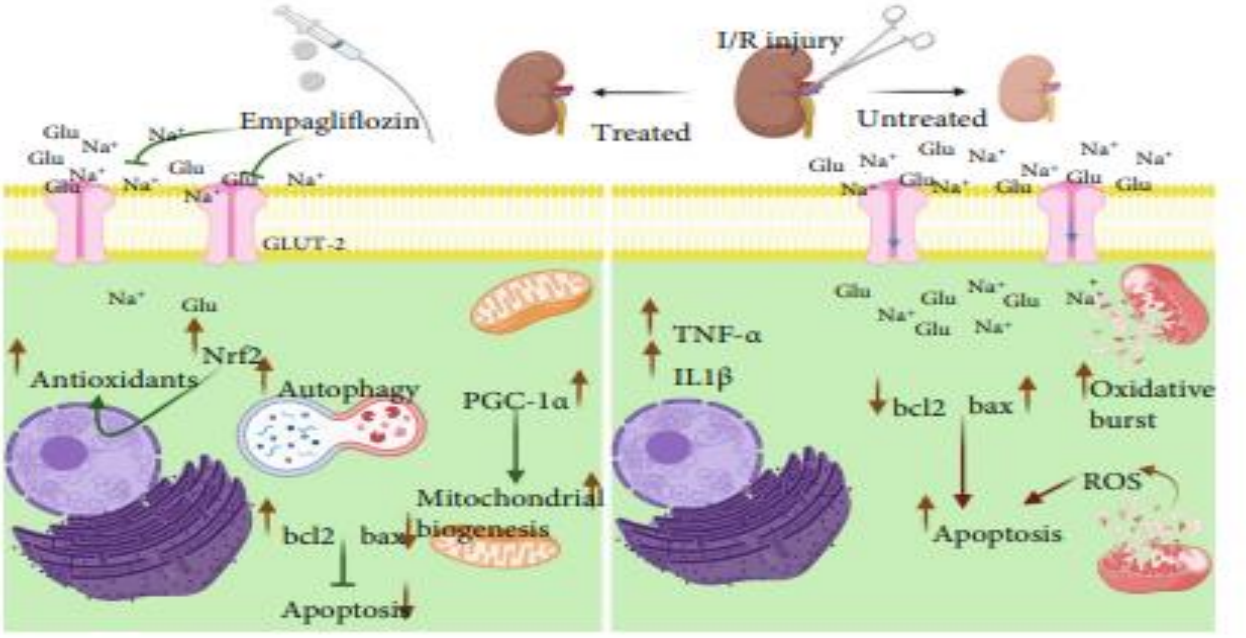

Figure 1.4: The Protective Impacts of EMPA on Renal I/R Injury. **(Ala et al., 2022)**

1.6.2 Dapagliflozin (DAPA)

Dapagliflozin's molecular structure makes sense and consists of a C-linked glucoside. Because of this, the aglycone component can form a carbon-carbon bond with glucose, giving it metabolic stability against the action of glucosidase enzymes. The molecular weight of dapagliflozin is 408.87. It is defined chemically as (2S,3R,4R,5S,6R)-2-[4-ethoxybenzyl)phenyl 4-chloro3-]The chemical formula for -6-(hydroxymethyl)tetrahydro 2H-pyran-3,4,5-triol is C21H25ClO6 (Figure 1.5).**(Kasichayanula et al., 2014)**

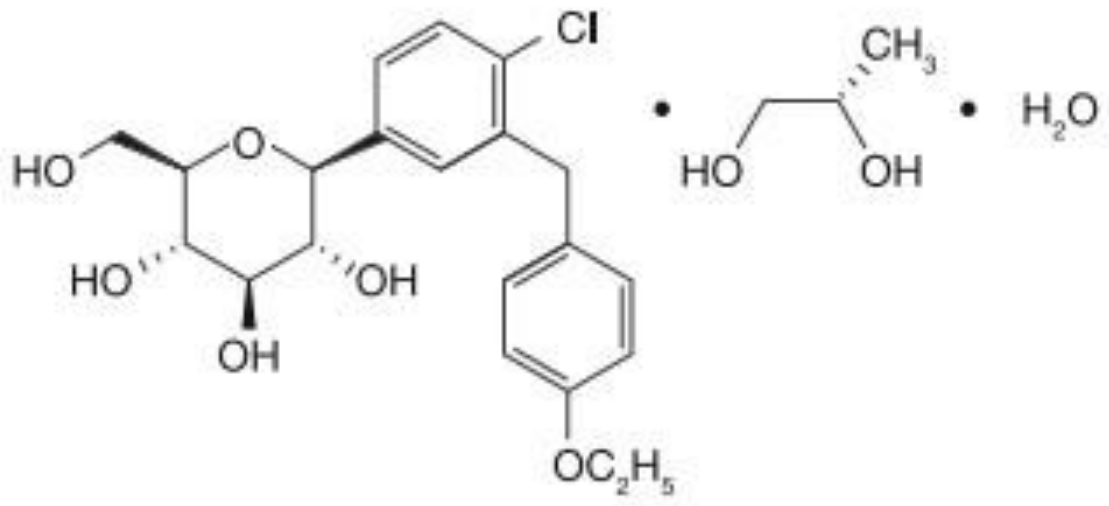

Figure 1.5: Dapagliflozin Propanediol Monohydrate's Chemical Makeup **(Kasichayanula et al., 2014)**

1.6.2.1 DAPA PhD and PhK

DAPA is an oral, highly selective, reversible, competitive, and potent inhibitor of human SGLT2. There's no proof that SGLT2 activity is upregulated after dapagliflozin exposure. Urinary glucose excretion increases in a dose-dependent manner when exposed to dapagliflozin. Oral bioavailability of dapagliflozin is 78%. **(Boulton et al., 2013)**. It is promptly and widely absorbed from the GI tract. In fasting, maximal peak concentrations were typically reached one to two hours after delivery. Dapagliflozin has a comprehensive distribution volume, and its overall absorption level was not significantly impacted by co-administration with meals. After taking 50 mg orally, dapagliflozin underwent significant metabolism. Dealkylation, oxidation, and glucuronidation were among the metabolic pathways.**(Kasichayanula et al., 2014)**

1.6.2.2 Cardiovascular Effect

Numerous research and trials have demonstrated the cardioprotective benefit of dapagliflozin. One such study, conducted on 17,160 patients in 2019, found that, when compared to a placebo, dapagliflozin lowers the The incidence of heart failure hospital stays and mortality. **(Wiviott et al., 2019).**

1.6.2.3 Renal Effect

Dapagliflozin significantly reduced the risk of end-stage kidney disease, a combination of a prolonged 50% decline in the estimated glomerular filtration rate (GFR) or mortality from renal causes in individuals with chronic kidney disease**(Heerspink et al., 2020).**

1.6.3 Ertugliflozin (ERTU)

Ertugliflozin is a mouth-engaged SGLT2I being investigated as a therapy for T2DM. In the United States, ertugliflozin was authorized in December 2017 to treat individuals with type 2 diabetes people in addition to nutrition and trains. **(Markham, 2018).**

1.6.3.1 Ertugliflozin Chemical Structure

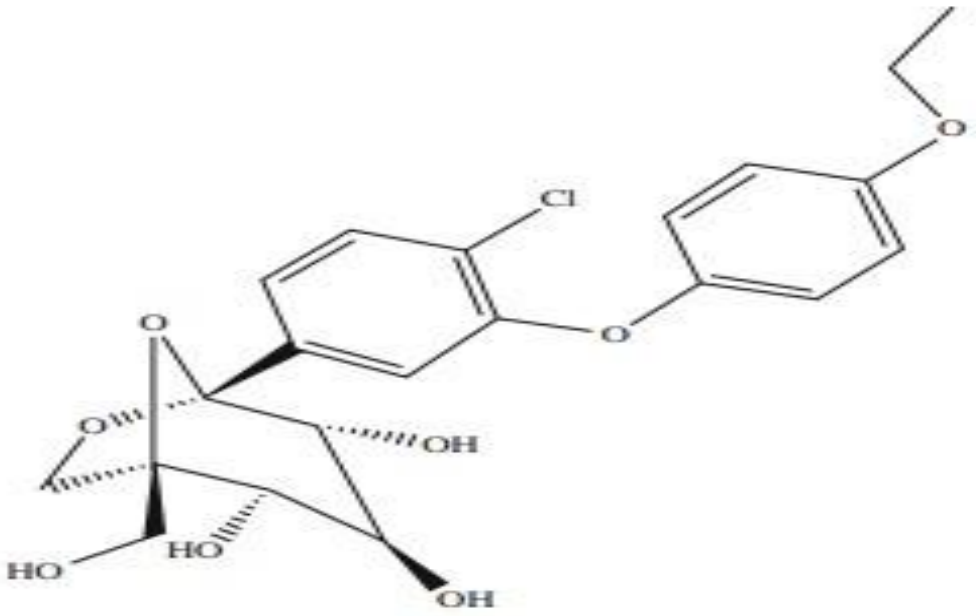

Figure 1.6: Structure of ERTU L-Pyroglutamate Co-crystal **(Markham, 2018).**

1.6.3.2 ERTU PHK and PHD

In people with type 2 diabetes, ertugliflozin enhanced UGE in a dose-dependent means; dose-response modeling indicates that 5 and 15 mg dosages resulted in a nearly maximal urinary glucose excretion response. **(Markham, 2018)**

Ertugliflozin pharmacokinetics are comparable in T2DM patients and healthy individuals. After 4–6 days of once-daily administration, the medication attained a

steady state, and its pharmacokinetic characteristics are not time-dependent. Peak plasma concentrations indicated rapid oral absorption at 1 hour (t max) after dosing. Ertugliflozin's t1/2 values are roughly 17 hours. Ertugliflozin excretion via urine and feces. **(Miao et al., 2013)**

1.6.3.3 Cardiac Effect of Ertugliflozin

Clinically significant decreases in mean 24-hour SBP, or systolic blood pressure and in-office sitting BP were observed in patients with T2DM and hypertension who were randomized to one of three dosages of ertugliflozin for four weeks. These reductions were comparable to hydrochlorothiazide and dapagliflozin 10 mg/day. Although Nothing altered in 24-hour plasma renin activity or aldosterone excretion, a slight diuretic impact and increased urinary glucose excretion (UGE) were noted. Therefore, the BP-lowering action of ertugliflozin is most likely due to osmotic diuresis. **(Amin et al., 2015)**

When ertugliflozin was administered at a supratherapeutic dose of 100 mg, QTc interval prolongation was not seen.**(Sahasrabudhe et al., 2018)**

1.6.3.4 Renal Effect of Ertugliflozin

Regardless of baseline renal function, ertugliflozin was linked to a sustained reduction of the indicator for tubular harm, kidney injury molecule-1 (KIM-1), in individuals with type 2 diabetes and stage 3 chronic kidney disease, indicating protecting benefits of tubules. Also, some study states that Ertugliflozin alleviates tubular hypoxia, which may lessen proximal tubular damage in diabetic kidney disease (DKD); in the same patient group, hematocrit was shown to rise following ertugliflozin medication, which provides more evidence that SGLT2 inhibitors may promote better oxygenation. **(H. Liu et al., 2021)**

A sensitive and precise biomarker of renal damage is KIM-1. KIM-1 is hardly expressed in human kidney tissue while the patient is healthy. However, KIM-1 expression is elevated in proximal tubular epithelial cells. Its extracellular portion is released into urine and systemic circulation when there is a hypoxic injury to the kidney's tubular cells, as occurs in diabetes**.** KIM-1 is also a marker of chronic tubular injury, correlating with the onset and progression of CKD. **(Song et al., 2019)**

Another study revealed that the benefits of ertugliflozin included decreased danger of the prespecified investigational renal composite, which showed a persistent 40% drop in estimated GFR, constant kidney substitution treatment, or renal mortality; significantly lower Urine albumin/creatinine ratio in individuals with baseline micro- or macroalbuminuria when compared to placebo; maintained renal health, particularly in those with macroalbuminuria who were most at risk of developing DKD; and renal health outcomes are in line with SGLT2 inhibitor side impacts. **(Cherney et al., 2021)**

1.6.3.5 Lung Effect of Ertugliflozin

Ertugliflozin reduces lung damage caused by endotoxemia in male mice by inhibiting the downstream signaling pathways for oxidative stress and Inflammation. **(Abd & Hassan, 2023)**

1.6.4 Adverse Drug Events of SLT2I

The adverse effects of empagliflozin, dapagliflozin,and ertugliflozin are summarized in figure

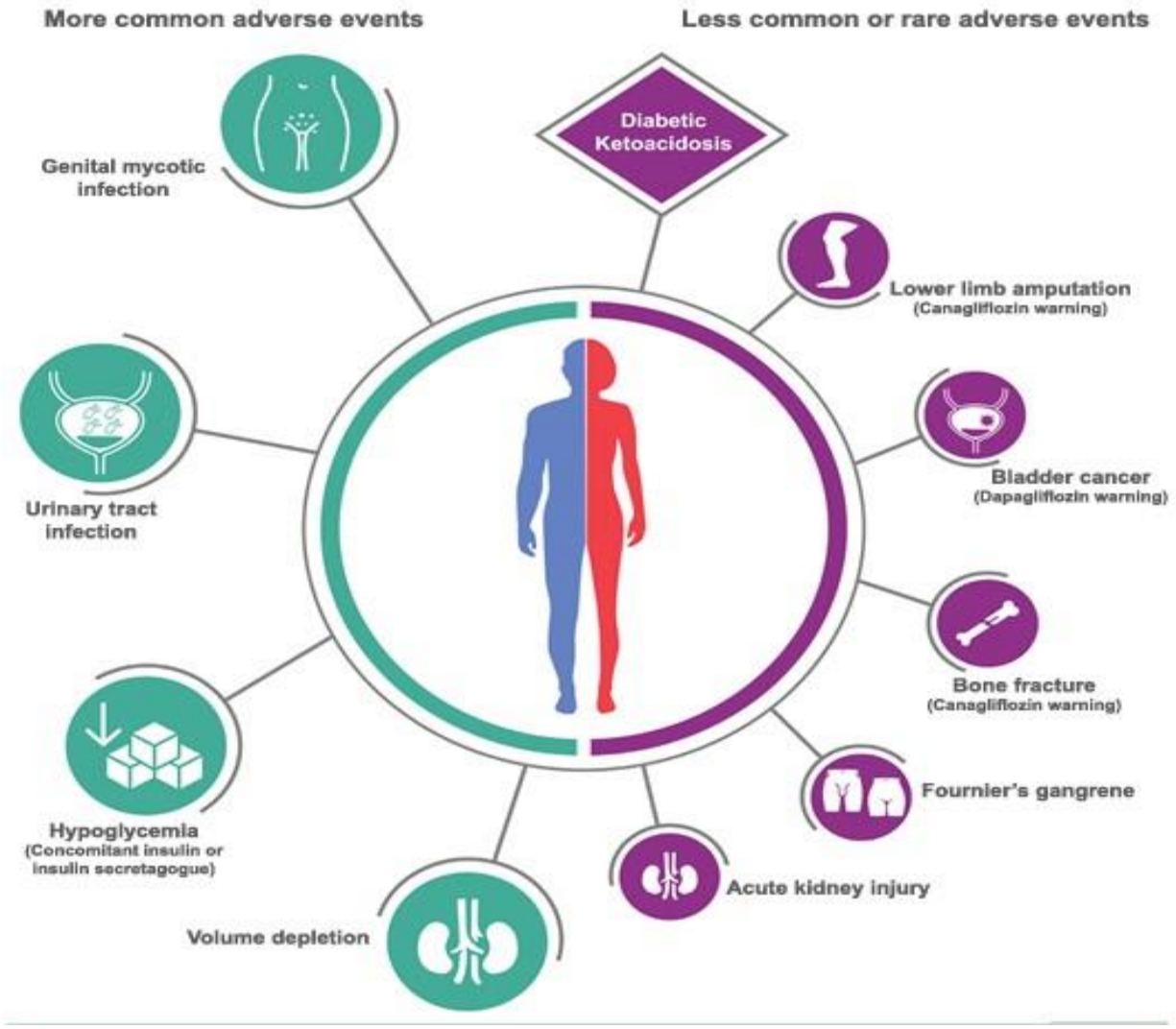

Figure 1.7: Summary of adverse events potentially associated with sodium-glucose co-transporter 2 inhibitors.**(Mcgill & Subramanian, 2019)**

1.7 Methotrexate

The first folate antagonist cytotoxic medication, methotrexate (MTX), treats solid tumors and blood cancer. More recently, it has also been used as an immunosuppressive medication in organ transplantation, treating some autoimmune illnesses and severe asthma. **(Rubino, 2001)**

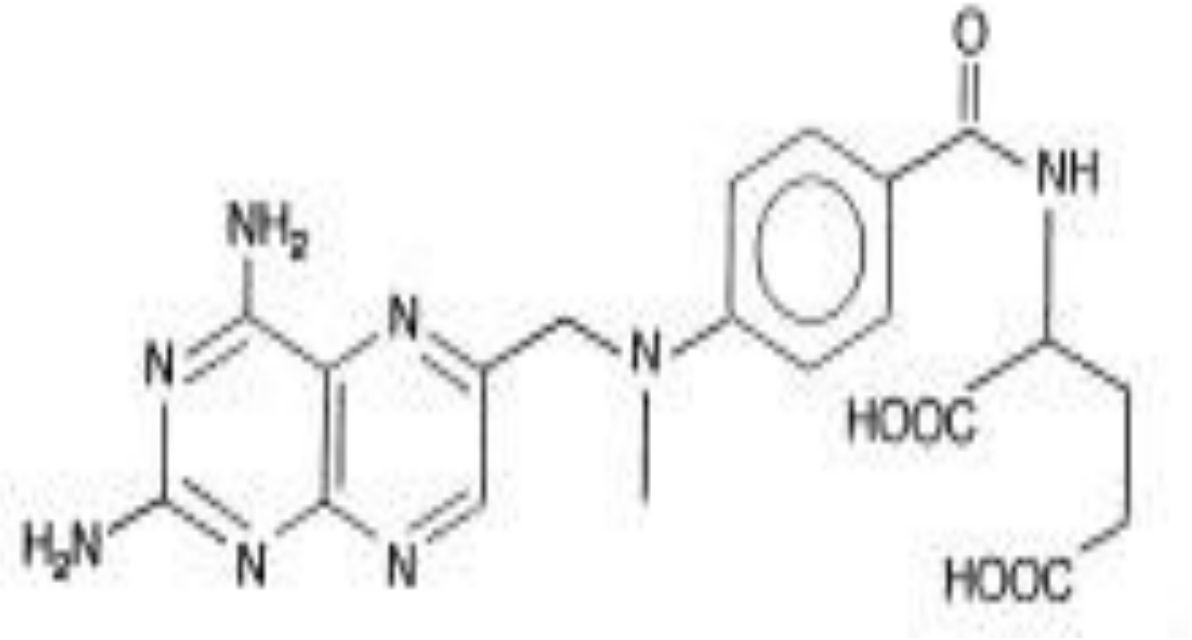

Figure 1.8: The chemical structure of MTX **(Rubino, 2001)**

1.7.1 Uses of Methotrexate

Methotrexate, a folic acid analog that was found to be a valuable treatment for psoriasis, rheumatoid arthritis, juvenile idiopathic arthritis (JIA) with a polyarticular course, and acute leukemia and other solid malignancies. Thanks to its advantageous anti-inflammatory and immunomodulatory properties. **(Hashkes et al., 2014)** it is also helpful in transplantation, Vascular inflammation, systemic

lupus erythematosus, multiple sclerosis, and other connective tissue illnesses. It is also beneficial in inflammatory bowel diseases. Additionally, MTX has spurred increased attention in managing virally caused arthritis. Numerous viruses are linked to arthritogenic disorders, such as Hepatitis B/C virus (HBV/HBC), Parvovirus B19, human immunodeficiency virus (HIV), and old-world alphaviruses**. (Bedoui et al., 2019)**

1.7.2 Mechanism of Action of Methotrexate

Methotrexate's capacity to restrict DNA and RNA synthesis by blocking dihydrofolate reductase and thymidylate synthase accounts for its medicinal and harmful effects. It binds to the enzyme and inhibits it once it enters cells via folate's active transport mechanism.

This enzyme recycles dihydro folic acid, created during the manufacture of thymidylate, to maintain decreased folate. Tetrahydrofolate, a crucial co-factor in producing purine nucleotides, is made when the enzyme dihydrofolate reductase reduces folic acid.

Thymidylate synthetase also needs reduced folates to supply methyl donors for the synthesis of thymidylate, which is necessary for DNA synthesis. Therefore, in tissues like the bone marrow and digestive tract that divide more quickly than other cells, methotrexate poisoning is most noticeable. As the medicine is absorbed, the liver receives more significant amounts of methotrexate through the portal circulation, so liver effects are frequently seen.**(Chan & Cronstein, 2013)**

1.7.3 Adverse Effect of Methotrexate

In addition to gastrointestinal side effects of MTX, which include (nausea, stomach pain, cramping, weight loss, vomiting, diarrhea, anorexia, abdominal

distress, and mucocutaneous ulcers in the mouth) there are many toxicities that MTX can cause, including (liver toxicity, kidney toxicity, Hematological Toxicity, including Megaloblastic anemia, leukopenia, neutropenia, and myelosuppression, Pulmonary Toxicity, increase risk of infection and dermatological harmfulness. **(Hamed et al., 2022).**

1.8 Oxidative Insults

From acute kidney injury (AKI) to irreversible persistence of renal damage, oxidative stress performs a critical service in the growth of kidney damage. The imbalance that promotes a higher generation of ROS and lower levels of the body's natural antioxidant defense systems is known as oxidative stress. Cells undergo continuous oxidation and reduction activities, but damage is typically prevented by several protective enzymatic and non-enzymatic anti-oxidative systems that maintain the equilibrium of these processes. Oxidative stress happens anytime the balance shifts in favor of more oxidation. The pathological transition to oxidative stress and damage to cells and tissues leads to changes in DNA, lipid, and protein structures, affecting their functions. Apart from producing immediate harm to tissue, oxidative stress can trigger various intracellular signalling pathways, which in turn triggers indirect effects such as cell death or proliferation, extracellular matrix synthesis and breakdown, oxygen detection, and inflammation. These outcomes can result in notable dysfunction of the kidneys, lungs, pancreas, and cardiovascular system. **(Zhang et al., 2020)**

1.8.1 Glutathione (GSH)

The amino acids glutamate, cysteine, and glycine combine to form the tripeptide molecule known as glutathione (GSH). Over 95% of GSH is found in its reduced form, making it the most prevalent thiol-containing antioxidant in the

human body. It can be found in both its reduced and oxidized forms in cells. The most pervasive thiol antioxidant in the human body, glutathione (GSH), is essential for numerous metabolic processes, including vitamin D, E, and C regulation and drug and toxin detoxification. GSH is a potent antioxidant that is especially crucial as a free radical scavenger that prevents oxidative damage to cellular components and as a regulator of mitochondrial metabolism. Numerous chronic pro-inflammatory disorders, including metabolic syndrome, cardiovascular, renal, and hepatic diseases, as well as autoimmune and neurological diseases, have been linked to low GSH levels. **(Hristov, 2022)**

1.8.2 Malondialdehyde (MDA)

Malondialdehyde (MDA) is produced when polyunsaturated fatty acids are peroxide. Lipid peroxidation's byproduct, MDA, has been employed as a biomarker to assess oxidative stress in a variety of biological samples, including blood, urine, and exhaled breath condensate, in patients affected with a variety of illnesses, such as cancer, cardiovascular, pulmonary, and neurological conditions**.** Moreover, identifying these end products in inflammatory diseases implies a significant involvement of lipid peroxidation in this kind of illness. The primary and best-researched substance obtained by lipid peroxidation that is known to have harmful and mutagenic properties is MDA. Furthermore, MDA can be generated as a byproduct of enzymatic thromboxane A2 production. **(Update et al., 2023)**

1.9 Renal Function Markers

1.9.1 Creatinine

In clinical practice today, the most commonly used indicator of renal function is serum creatinine concentration. Numerous unrelated factors, including glomerular

filtration, tubular secretion, endogenous production, food consumption, and extrarenal creatinine clearance, simultaneously affect serum creatinine levels. Locations and Sources of Creatinine Production are that the muscle creatine is dehydrated by nonenzymatic means, resulting in the formation of creatinine. About 98% of the body's entire creatine pool is found in muscle, which actively transports and largely synthesizes creatine in the liver. Every day, 1.6–1.7% of the whole pool of creatine is converted to creatinine**. (Heymsfield & Of, 2018)**

1.9.2 Urea

The glomeruli freely filter the tiny, water-soluble molecule known as urea, which is then absorbed by the kidney's proximal and distal tubules. Urea handling occurs along the nephron and involves many urea transporters. Traditionally, one measure used to assess kidney function is blood urea nitrogen (BUN), and there is an inverse relationship between BUN levels and kidney function. In addition to glomerular filtration, tubular resorption and urea synthesis impact BUN levels. Increased tubular reabsorption of urea due to neurohumoral activation resulting from the depletion of adequate circulating volume is a common cause of higher elevation of BUN compared to glomerular filtration rate (GFR), leading to higher BUN/creatinine ratio in acute illnesses, such as acute heart failure, acute pancreatitis, and extensive diuretic use. **(Kim et al., 2021)**

1.9.3 Total Protein

An increased plant protein diet appears to provide potential preventive benefits against chronic kidney disease (CKD). Furthermore, the fact that there is no correlation between the incidence of CKD and dietary total protein intake may emphasize the significance of protein sources compared to protein consumption volume.**(Alvirdizadeh et al., 2020)**

Another interesting fact is that people with Parkinson's disease (PD) who follow a diet higher in plant-based protein relative to total protein have decreased rates of cardiovascular disease (CVD) and all-cause mortality. This effect is particularly noticeable in older, female, and non-hypoalbuminemia patients. More research is necessary to determine the possible mechanisms underlying these occurrences. **(X. Liu et al., 2020)**

1.10 Interleukin-1Beta

Four major members make up the IL-1 family: IL-1α, IL-1β, IL-33, and IL-1 receptor antagonist (IL-1RA). Cytokine activators include IL-1α, IL-1β, and IL-33, whereas inhibitory cytokines include IL-1RA**(Garlanda et al., 2013)**.

The two genes that encode IL-1α and IL-1β have minimal sequence homology. Pro-IL-1α and pro-IL-1β are the first proteins that are produced. Whereas pro-IL-1α is active and can have its activity modulated by calpain cleaving it into IL-1α, pro-IL-1β must be transformed into IL-1β by inflammatory caspase cleavage. Two signals are needed for the carefully regulated manufacture and processing of IL-1β: one for "priming," which permits transcription of the IL1B gene, and another for activation, which triggers the activation of inflammasome complexes and inflammatory caspases, cleaving pro-IL-1β into mature IL-1β.**(Weber et al., 2010)**

IL-1β has been considered a partner of TNF in triggering chronic inflammatory diseases, but their functions in human disorders are distinct. **(Schett et al., 2015)**

1.11 Tumor Necrosis Factor-alpha (TNF-α)

One of the primary mediators of inflammatory tissue injury is tumor necrosis factor (TNF), a solid proinflammatory cytokine. It also performs critical immune-

regulatory tasks. According to numerous experimental research and clinical observations, TNF may have a role in the etiology of acute and chronic renal illness. However, TNF may mediate proinflammatory and immunosuppressive effects due to its dual roles in inflammation and immune modulation, especially in chronic renal disorders and systemic autoimmunity. Central mediators of renal disorders, both immunological and nonimmune, are cytokines. The classic proinflammatory cytokine is tumor necrosis factor-a (TNF-α), a type II transmembrane protein. Activated macrophages primarily secrete TNF, which is also released by mast cells, natural killer cells, antigen-stimulated T cells, and neutrophils. Additionally, TNF is produced by fibroblasts and intrinsic renal cells, including mesangial cells and glomerular and tubular epithelial cells.**(Vielhauer & Mayadas, 2007).**

Central (visceral) obesity, dysregulated lipid metabolism (dyslipidemia, hypertriglyceridemia, decreased high-density lipoprotein cholesterol), hypertension, and insulin resistance are among the risk factors that collectively characterize the metabolic syndrome. When taken as a whole, these variables raise the chance of developing metabolic non-communicable diseases such as type 2 diabetes, non-alcoholic fasting diabetes, heart disease, chronic renal disease, lung disease, and several types of cancer. Additional characteristics shared by all of these diseases include the following: they are all chronic conditions that frequently develop years before a clinical diagnosis; they involve significant tissue remodeling; they co-occur with a state of low-grade chronic inflammation, also known as meta inflammation; and this inflammation is initially localized to particular tissues, frequently at the site of tissue remodeling. Thus, it is not unexpected that TNF and related signaling networks, two frequent pro-inflammatory molecular actors, have been linked to promoting the

pathophysiology of numerous metabolic diseases Figure 1.8.**(Sethi & Hotamisligil, 2021)**

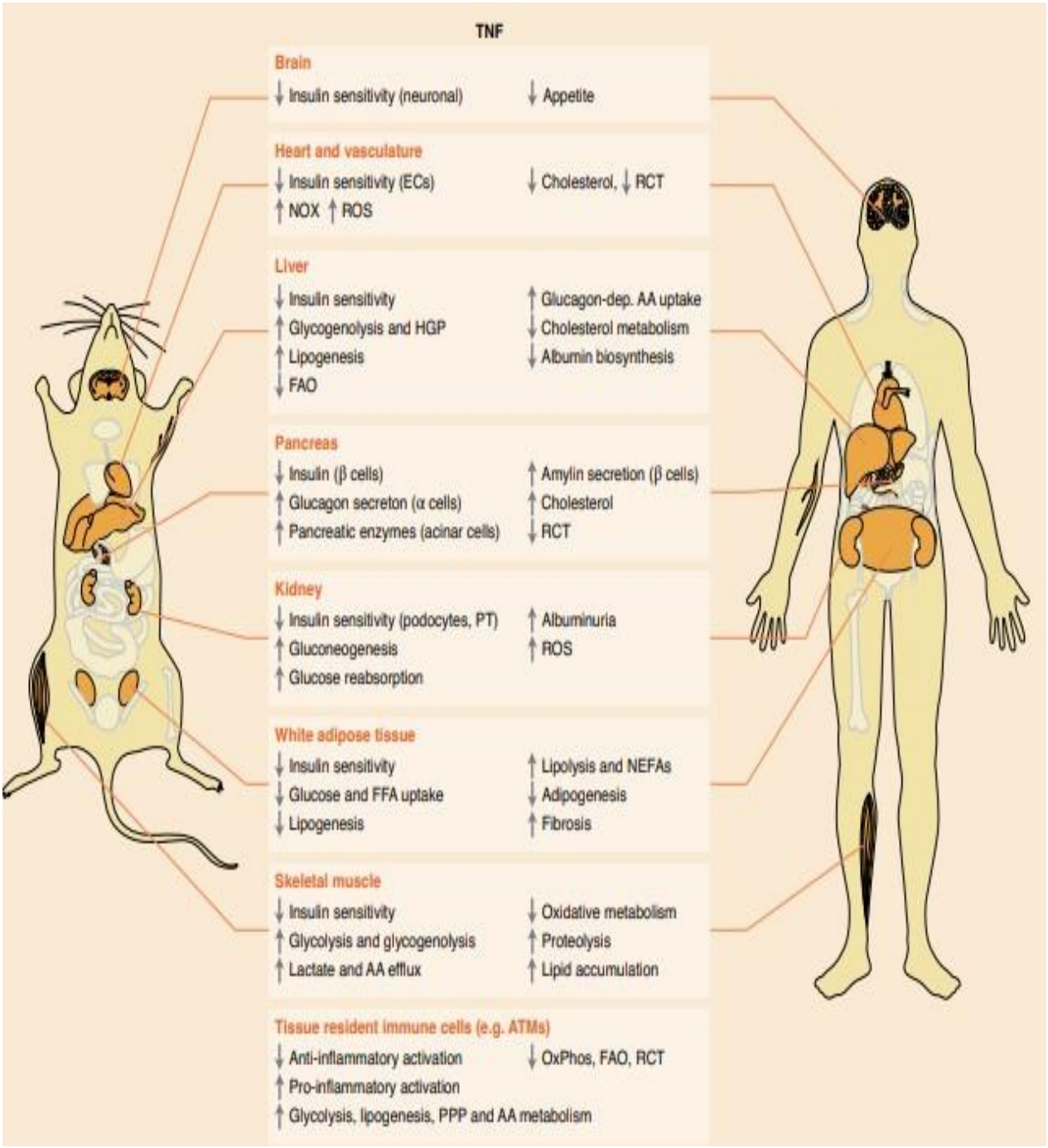

Figure 1.9: An Overview Explains the Target Tissues and Metabolic Activities of TNF. **(Sethi & Hotamisligil, 2021)**

Chapter Two

Materials and Methods

2.1 Materials

2.1.1 Drugs and Chemicals

A list of medications used in this study, along with information about their manufacture.

Table 2.1 Drugs, chemicals, Companies

No	Drugs and chemicals	Company/Country
1	Empagliflozin	Boehringer Ingelheim/Germany
2	Dapagliflozin	AstraZeneca/ Sweden
3	Ertugliflozin	Sami Pharma/Pakistan
4	Methotrexate	Health Step Pharma/Dubai
5	Xylazine	Alphatan/ Holand
6	Ketamine	Alphatan/ Holand
7	Formaldehyde	Iraq
8	Thio barbituric acid (TBA) ($C_3H_3SN_2$)	England
9	Tri Chloro Acetic acid (TCA) ($C_2HO_2Cl_3$)	England

2.1.2 Kits

All kits used in this study had high specificity and sensitivity, and their manufacture site.

Table 2.2 Kits, Companies

No.	Kits	Company/Country
1	Creatinine ELISA Kit	Elabscience biotechnology / China
2	Urea ELISA kit	Elabscience biotechnology/ China
3	BCA protein ELISA kit	Elabscience biotechnology/ China
4	Rat Tumor necrosis factor Alpha ELISA K	BT LAB /China
5	Rat Interleukin 1 Beta ELISA K	BT LAB /China
6	GSH and MDA	Manually calculated

2.1.3 Instruments and Equipment

All instruments and equipment used in this study are listed in Table 2.3

Table 2.3 Instruments, equipment, Companies

NO	Instruments and Equipment	Company/Country
1	Gel tube	SAIL BRAND/China
2	Plain tube	SAIL BRAND/China
3	Cotton	Pioneer/Iraq

4	Graduated cylinder	Wafi Medical Laboratory/Iraq
5	Disposable syringe 5cc	Iraq
6	Disposable syringe 1cc	Shanachuan/china
7	Intragastric tube	China
8	Gloves	Top glove/ Malaysia
9	Sensitive balance	Sartorius/ Germany
10	Beaker	Iraq
11	Automatic ELISA reader PKL PPC 230	Paramedical/Italy
12	Refrigerator	Concord/ Lebanon
13	Surgical set	China
14	Tube rack	China
15	Cooling box	China
16	Normal saline	Pioneer/Iraq
17	Distilled water	Iraq
18	Mortar and pestle	Iraq
19	Cup tube	Iraq
20	Stainless Steel Laboratory thermostat incubator	China
21	Multichannel micropipette	Labnet/ Germany
22	Biopette Variable Volume	Labnet/ Germany
23	Centrifuge	Hettich, Germany

2.1.4 Animal

The study included fifty adult male albino rats weighing 250-300 g and aged between 10 and 12 weeks. These rats were habituated in animal house conditions a room humidity of 60-65 percent, and a 14-hour light-dark cycle with a specified commercial feed and water.. The selected rats were randomly divided into five groups after ten days of acclimatisation. Ten rats have been involved in each group of experiments. This study started from 18/12/2023 to 1/1/2024 and was conducted at the Animal House in the College of Medicine/ University of Babylon.

2.2 Methods

2.2.1 Ethical Approval

This study was approved by the committee of publication ethics at the College of Medicine, University of Babylon, Iraq. A regional ethics committee examined and approved the study protocol, subject information, and permission form. Under document number 4-14. The document date was on 8/8/2023.

2.2.2 Study Design and Experimental Protocols

Animals: The picked rats were assigned at random into five groups of 10 rats each, as follows:

Group A is controlled negative and received only normal saline. I.P. for 14 days.

Group B is controlled positive and received 10mg/kg of methotrexate (MTX) I.P. on day 10 of the experiment.

Group C is the treated group and received 10mg/kg of empagliflozin orally by gavage for 14 days +10mg/kg of MTX was given I.P. on day 10 of the experiment. **(Ala et al., 2022)**

Group D is the treated group and received 10mg/kg of dapagliflozin orally by gavage for 14 days +10mg/kg of MTX was given I.P. on day 10 of the experiment. **(Mohamed et al., 2019)**

Group E is the treated group and received 20mg/kg of ertugliflozin orally by gavage for 14 days + 10mg/kg of MTX was given I.P. on day 10 of the experiment. **(Abd & Hassan, 2023)**

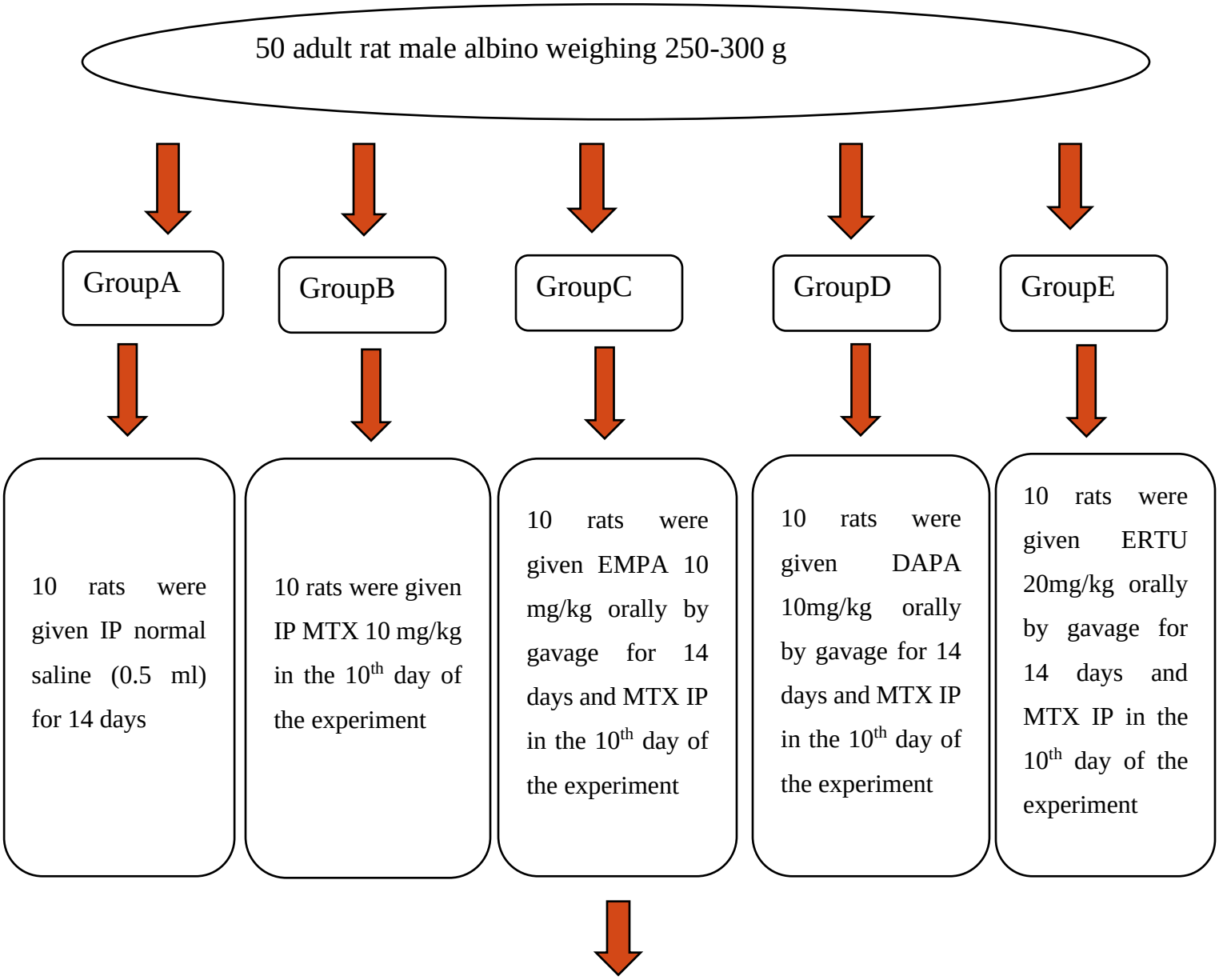

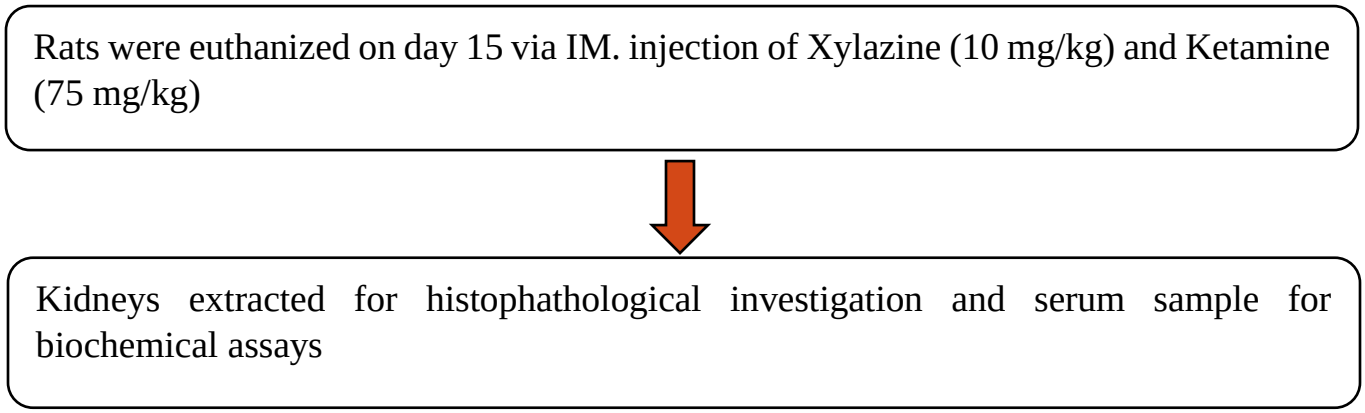

Figure 2.1 An overview of the study design and experimental protocol that has been done.

At the completion of the trial, on day fifteen, the rats were euthanized with a drug called xylazine (10 mg per kilogram of body and ketamine (75 mg per kilogram). The renal tissue samples and serum specimens have been gathered for biochemical and histological investigations.

2.2.3 Preparation of Serum Sample for Serology

The rat was dissected from its abdomen, and the diaphragm and the rib cage were cut off so that the heart was visible for blood to be drawn from it. After that, the blood was drawn by a 5cc syringe directly from the heart and was poured gradually and very slowly into a gel tube to avoid hemolysis. Then, the gel tube containing the whole blood was set in the centrifuge for ten minutes at 3,000 rpm. to get a clear serum. After that, all the samples of serum were put in a plain tube and then in the refrigerator at a temperature of 2-8C to be used later for biochemical assessment. Figure 2.2

2.2.4 Steps in the Preparation of Kidney Sample for Histopathological Studies

1. The rat was dissected from its abdomen, and the kidney was extracted and washed with normal saline to remove surplus blood.

2. Then, it was placed in a cup tube containing 10% formalin to avoid bacterial decomposition or autolysis.

3. The kidney tissue was cut into small pieces and put in a capsule cassette with labeling.

4. Fixation with 10% formalin (allowed up to 24 hours).

5. Dehydration of the kidney tissue started with 50% ethanol alcohol for one hour, then with 70% ethanol for two hours, then with 80% ethanol for two hours, then with 90% ethanol for two hours, and finally with 100% ethanol for two hours.

6. Then, pass the tissue into a xylene solution.

7. Then, embed the tissue into a container with paraffin wax.

8. the embedded tissue is cut into sections by microtome at three-micron thickness.

9. Staining: the first step is dewaxing by oven at 70C temperature for one hour.

10. After dewaxing, pass the tissue into a container with xylene for 45 minutes.

11. Again, pass it into ethanol alcohol 100%,90%,80%,70%, and 50%, respectively, for 10 minutes for each concentration.

12. Staining with hematoxylin for ten minutes, then washing with tap water.

13. Staining with eosin for two minutes, then washing with tap water.

14. They pass it into ethanol alcohol 50%,70%,80%,90% and 100%, respectively, for five minutes for each concentration.

15. pass it into a xylene container.

16. Finally, cover the tissue with DPX and put it on a cover slide for later microscopical examination.

Figure 2.2: Overview of a Rat Shows the Process of Drawing Blood from the Heart after an Abdominal Incision Operation.

2.3 Serology Assessments

2. 3.1 Interleukin-1Beta (IL-1B)

2.3.1.1 Test principle: The plate has been pre-coated with Rat IL-1B antibodies. IL-1B is introduced to the sample and binds to antibodies coated in the wells. After that, a biotinylated Rat IL-1B Antibody is added, which binds to IL-1B in the sample. Streptavidin-HRP is then added and bound to the biotinylated IL-1B antibody. During the washing process following incubation, all unbound Streptavidin-HRP is

removed. The substrate solution is added, and the color develops in accordance to the amount of Rat IL-1B. The reaction is ended by adding an acidic stop solution, and the absorbance is measured at 450 nm. Post-inserting stop solution to bring the enzymatic reaction to an end, the hues change from Blue to yellow. Figure 2.3

Figure 2.3 An Overview of IL-1B Kit After Insertion of Stop Solution

2.3.1.2 Reagent Preparation

1-All reagents should be brought to room temperature before use.

2-Standard Reconstitute the 120µl of the standard (80ng/ml) with 120µl of standard diluent to generate a 40ng/ml standard stock solution. Allow the standard to sit for 15 minutes with gentle agitation before diluting. Prepare duplicate standard points by serially diluting the standard stock solution (40ng/ml) 1:2 with standard diluent to produce 20ng/ml, 10ng/ml, 5ng/ml, and 2.5ng/ml solutions. Standard diluent serves as the zero standard (0 ng/ml). Any remaining solution should be frozen at -20°C and used within one month. Dilution of standard solutions suggested are as follows:

Table 2.4: Explain the Reagents Preparation.

40ng/ml	Standard No.5	120µl Original Standard + 120µl Standard Diluent
20ng/m	Standard No.4	120µl Standard No.5 + 120µl Standard Diluent
10ng/m	Standard No.3	120µl Standard No.4 + 120µl Standard Diluent
5ng/ml	Standard No.2	120µl Standard No.3 + 120µl Standard Diluent
2.5ng/ml	Standard No.1	120µl Standard No.2 + 120µl Standard Diluent

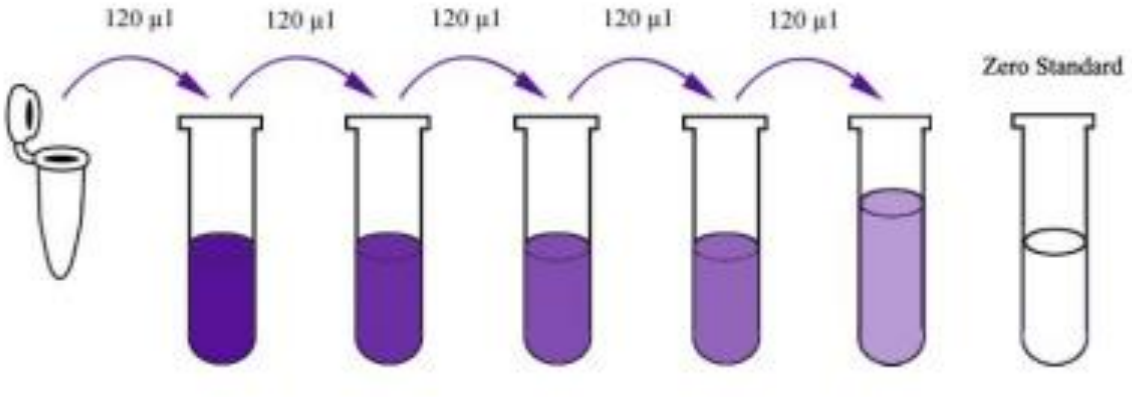

Figure 2.4: Explain the Dilution Process.

Table 2.5: Explain the Conc. of Each Standard

Standard Concentration	Standard No.5	Standard No.4	Standard No.3	Standard No.2	Standard No.1
80ng/ml	40ng/ml	20ng/ml	10ng/m	5ng/m	2.5ng/ml

3- Wash Buffer: Dilute 20 mL of wash buffer. Concentrate 25x in deionized or distilled water to make 500 mL of 1x Wash Buffer. If crystals were created in the concentrate, mix it lightly until they are fully dissolved.

2.3.1 .3 Assay Process

1. Prepare all reagents, standard solutions, and samples as instructed. Bring all reagents to room temperature before use.

2. Determine the number of strips required for the assay. Insert the strips in the frames for use. The unused strips should be stored at 2-8°C.

3. Add 50µl standard to the standard well. Do not add biotinylated antibody to the standard well because the standard solution contains a biotinylated antibody.

4. Add 40µl sample to sample wells, 10µl anti-IL-1B antibody to sample wells, and 50µl streptavidin-HRP to sample wells and standard wells (Not blank control well). Mix well. Cover the plate with a sealer. Incubate 60 minutes at 37°C.

5. Remove the sealer and wash the plate five times with wash buffer. Soak wells with 300ul wash buffer for 30 seconds to 1 minute for each wash. Aspirate or decant each well and wash five times with wash buffer for automated washing. Blot the plate onto paper towels or other absorbent material.

6. Add 50µl substrate solution A to each well and then add 50µl substrate solution B to each well. Incubate plate covered with a new sealer for 10 minutes at 37°C in the dark.

7. Add 50µl Stop Solution to each well; the blue color will change into yellow immediately.

8. Determine each well's optical density (OD value) immediately using a microplate reader set to 450 nm within 10 minutes after adding the stop solution.

$$y = d + \frac{a - d}{1 + (\frac{x}{c})^b}$$

a	b	c	d
0.26688	1.187879	35.832197	3.951381

$R^2 = 0.998$

a: Theoretical response at zero concentration
b: Slope factor
c: Inflection point (EC50/IC50)
d: Theoretical response at infinite concentration

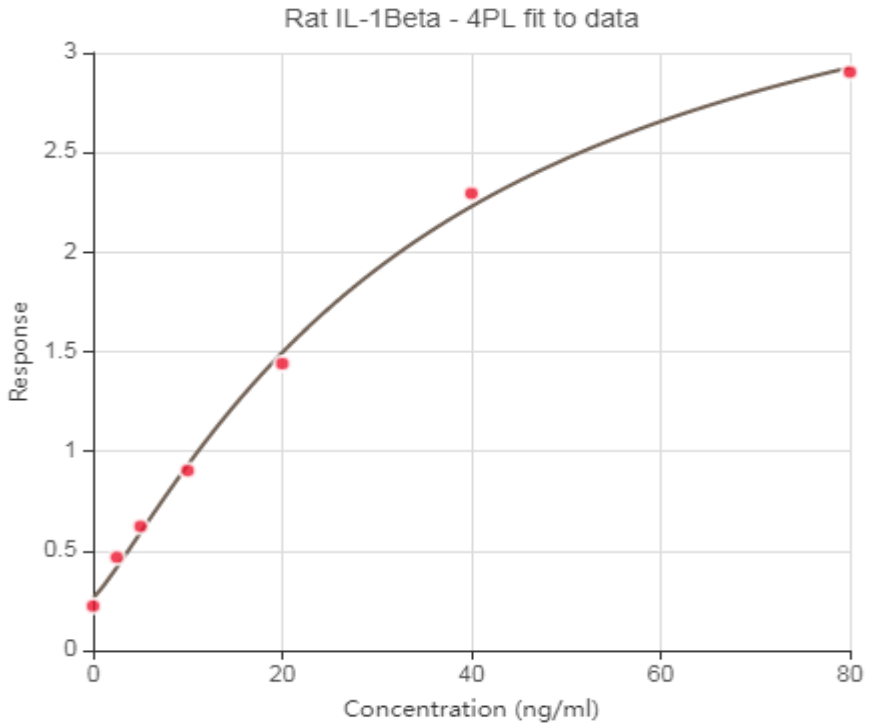

2.3.2 Rat Tumor Necrosis Factor Alpha (TNF-α) ELISA KIT

2.3.2.1 Test Principle: An enzyme-linked immunosorbent assay (ELISA) is what this kit is for. Rat TNF- α antibody has been pre-coated on the plate. When TNF- α from the sample is added, it attaches itself to the coated antibodies on the wells. Next, a biotinylated rat TNF- α antibody is introduced to the sample, where it binds to TNF- α. Streptavidin-HRP is then joined and bonded to the TNF- α antibody that has been biotinylated. During a washing step following incubation, unbound Streptavidin-HRP is removed. Following the addition of a substrate solution, color changes in accordance with the amount of Rat TNF- α. Absorbance is measured at

450 nm, and the reaction is stopped by introducing an acidic stop solution. After inserting the stop solution to bring the enzymatic reaction to an end, the hue changes from Blue to yellow. Figure 2.4

Figure 2.4 An Overview of TNF-α Kit After adding of Stop Solution

2.3.2.2 Reagent Preparation

1. All reagents should be brought to room temperature before use.

2. Standard Reconstitute the 120µl of the standard (1280ng/L) with 120µl of standard diluent to generate a 640ng/L standard stock solution. Allow the standard to sit for 15 minutes with gentle agitation before diluting. Prepare duplicate standard points by serially diluting the standard stock solution (640ng/L) 1:2 with standard diluent to produce 320ng/L, 160ng/L, 80ng/L, and 40ng/L solutions. Standard diluent serves as the zero standard (0 ng/L). Any remaining solution should be frozen at -20°C and used within one month. Dilution of standard solutions suggested are as follows:

Table 2.6: Explain the Reagents Preparation.

640ng/L	Standard No.5	120µl Original Standard + 120µl Standard Diluent
320ng/L	Standard No.4	120µl Standard No.5 + 120µl Standard Diluent
160ng/L	Standard No.3	120µl Standard No.4+ 120µl Standard Diluent
80ng/L	Standard No.2	120µl Standard No.3 + 120µl Standard Diluent
40ng/L	Standard No.1	120µl Standard No.2 + 120µl Standard Diluent

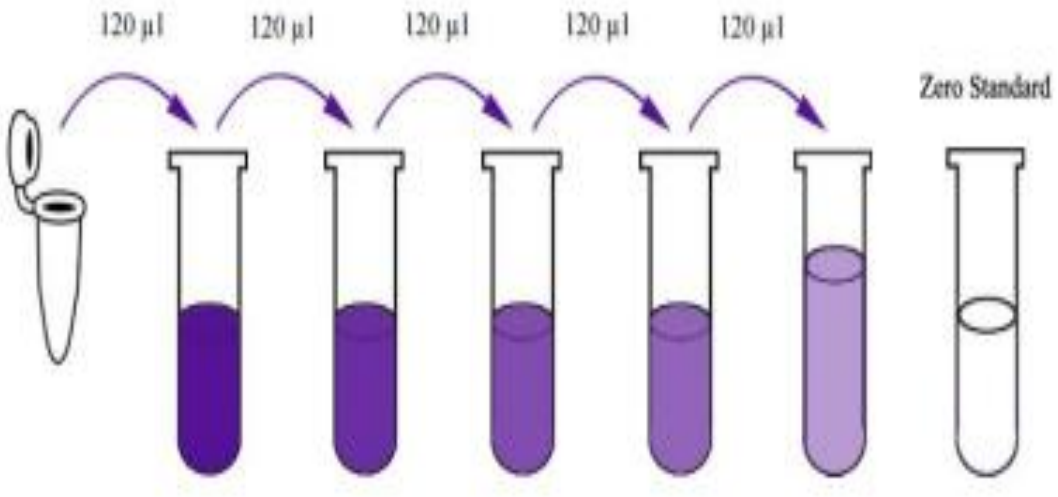

Figure 2.6: Explain the Dilution Process

Table 2.7: Explain the Conc. of Each Standard

Standard Concentration	Standard No.5	Standard No.4	Standard No.3	Standard No.2	Standard No.1

1280ng/L	640ng/L	320ng/L	160ng/L	80ng/L	40ng/L

3. Wash Buffer Dilute 20ml of Wash Buffer Concentrate 25x into deionized or distilled water to yield 500 ml of 1x Wash Buffer. If crystals have formed in the concentrate, mix gently until the crystals have completely dissolved.

2.3.2.3 Assay Process

1. Prepare all reagents, standard solutions, and samples as instructed. Bring all reagents to room temperature before use. The assay is performed at room temperature.

2. Determine the number of strips required for the assay. Insert the strips in the frames for use. The unused strips should be stored at 2-8°C.

3. Add 50µl standard to the standard well. Note: Don't add biotinylated antibody to standard well because the standard solution contains biotinylated antibody.

4. Add 40µl sample to sample wells and 10µl anti-TNF-α antibody and 50µl streptavidin-HRP to sample wells and standard wells (Not blank control well). Mix well. Cover the plate with a sealer. Incubate 60 minutes at 37°C.

5. Remove the sealer and wash the plate five times with wash buffer. Soak wells with 300ul wash buffer for 30 seconds to 1 minute for each wash. Aspirate or decant each well and wash five times with wash buffer for automated washing. Blot the plate onto paper towels or other absorbent material.

6. Add 50µl substrate solution A to each well and then add 50µl substrate solution B to each well. Incubate plate covered with a new sealer for 10 minutes at 37°C in the dark.

7. Add 50µl Stop Solution to each well; the blue color will change into yellow immediately.

8. Determine each well's optical density (OD value) immediately using a microplate reader set to 450 nm within 10 minutes after adding the stop solution.

$$y = d + \frac{a - d}{1 + (\frac{x}{c})^b}$$

a	b	c	d
0.23885	1.062153	576.922676	3.735665

$R^2 = 0.997$

a: Theoretical response at zero concentration
b: Slope factor
c: Inflection point (EC50/IC50)
d: Theoretical response at infinite concentration

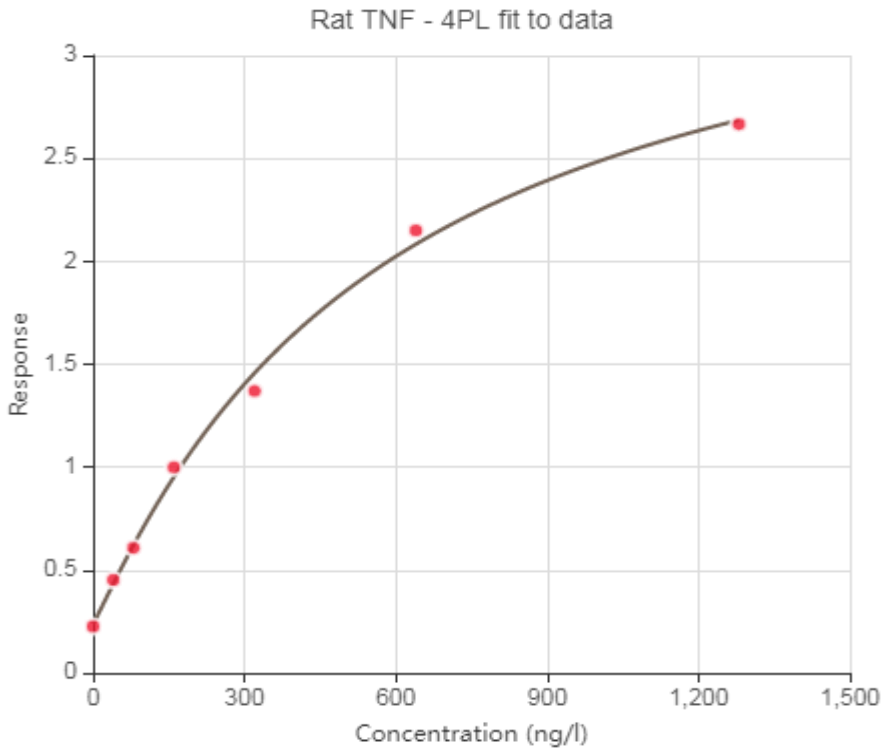

2.3.3 Creatinine (Cr) ELISA Kit

2.3.3.1 Test principle: This ELISA kit uses the Competitive-ELISA principle. The micro-ELISA plate provided in this kit has been pre-coated with Cr. During the reaction, Cr in the sample or standard competes with a fixed amount of Cr on the solid phase supporter for sites on the Biotinylated Detection Ab specific to Cr. Excess conjugate and unbound samples or standard are washed from the plate, and Avidin conjugated to Horseradish Peroxidase (HRP) is added to each microplate well and incubated. Then, a TMB substrate solution is added to each well. The addition of stop solution terminates the enzyme-substrate reaction, and the color change is measured spectrophotometrically at a wavelength of 450 nm ± 2 nm. The concentration of Cr in the samples is then determined by comparing the OD of the samples to the standard curve.

2.3.3.2 Reagent preparation

1. Bring all reagents to room temperature (18~25℃) before use. Follow the Microplate reader manual for set-up and preheat it for 15 min before OD measurement.

2. Wash Buffer: Dilute 30 mL of Concentrated Wash Buffer with 720 mL of deionized or distilled water to prepare 750 mL of Wash Buffer. Note: if crystals have formed in the concentrate, warm it in a40℃ water bath and mix it gently until the crystals have completely dissolved.

3. Standard working solution: Centrifuge the standard at 10,000×g for 1 min. Add 1.0 mL of Reference Standard &Sample Diluent, let it stand for 10 min, and invert it gently several times. After it dissolves fully, mix it thoroughly with a pipette. This reconstitution produces a working solution of 80μg/ml. Then, make serial dilutions

as needed. The recommended dilution gradient is as follows: 80,40,20,10,5,2.5,1.25,0μg/ml.

Dilution method: Take 7 EP tubes, and add 500uL of Reference Standard & Sample Diluent to each tube. Pipette 500 of the 80μg/mL working solution to the first tube and mix up to produce a 40μg/mL working solution. Pipette 500uL of the solution from the former tube into the latter according to this step. The illustration below is for reference. Note: the last tube is regarded as a blank. Don't pipette solution into it from the former tube.

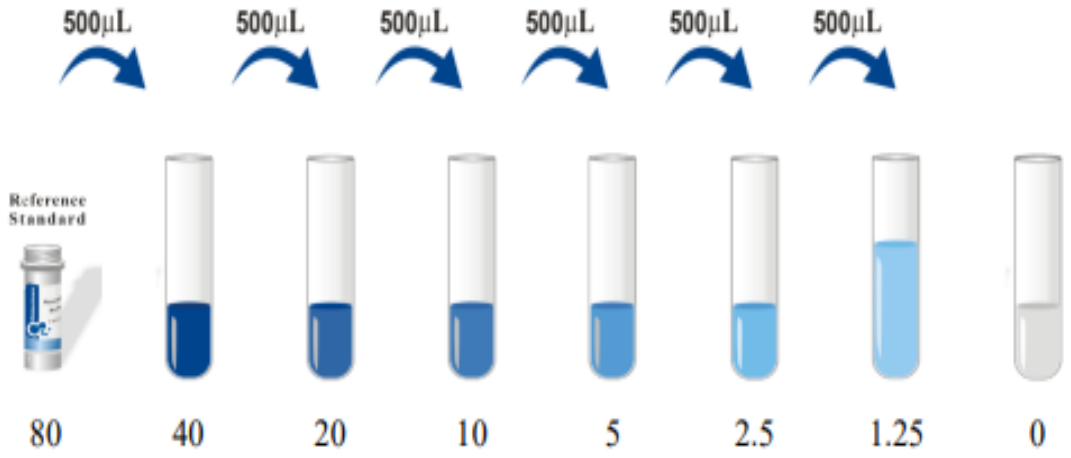

Figure 2.7: Explain the dilution process

4. Biotinylated Detection Ab working solution: Calculate the required amount before the experiment (50μL/well). In preparation, slightly more than calculated should be prepared. Centrifuge the stock tube before use, and dilute the 100× Concentrated Biotinylated Detection Ab to 1×working solution with Biotinylated Detection Ab Diluent.

5. Concentrated HRP Conjugate working solution: Calculate the required amount before the experiment (100μL/well). In preparation, slightly more than calculated

should be prepared. Dilute the 100× Concentrated HRP Conjugate to 1× working solution with Concentrated HRP Conjugate Diluent.

2.3.3.3 Assay Process

1. Add the standard working solution to the first two columns: Each solution concentration is duplicated side by side (50uL for each well). Add the samples to the other wells (50uL for each well). Immediately add 50μL of Biotinylated Detection Ab working solution to each well. Cover the plate with the sealer provided in the kit. Incubate for 45 min at 37℃. Note: solutions should be added to the bottom of the micro-ELISA plate well; avoid touching the inside wall and causing foaming as much as possible.

2. Aspirate or decant the solution from each well, and add 350uL of wash buffer to each well. Soak for 1~2 min, aspirate or decant the solution from each well, and pat it dry against clean absorbent paper. Repeat this wash step 3 times. Note: a microplate washer can be used in this step and other wash steps.

3. Add 100μL of HRP Conjugate working solution to each well. Cover with the Plate sealer. Incubate for 30 min at 37°C.

4. Aspirate or decant the solution from each well, repeat the wash process five times as conducted in step 2. 5. Add 90μL of Substrate Reagent to each well. Cover with a new plate sealer. Incubate for about 15 min at 37°C. Protect the plate from light. Note: the reaction time can be shortened or extended according to the color change, but not more than 30 minutes.

6. Add 50 μl of Stop Solution to each well. Note: The stop solution should be added in the same order as the substrate solution.

7. Determine each well's optical density (OD value) simultaneously with a micro-plate reader set to 450 nm.

$$y = \frac{A - D}{1 + \left(\frac{x}{C}\right)^{B}} + D$$

A	B	C	D
0.13183	-0.76332	11.44469	2.92283

A: Theoretical Response At Zero Concentration
B: Slope Factor
C: Inflection Point (EC50/IC50)
D: Theoretical Response At Infinite Concentration

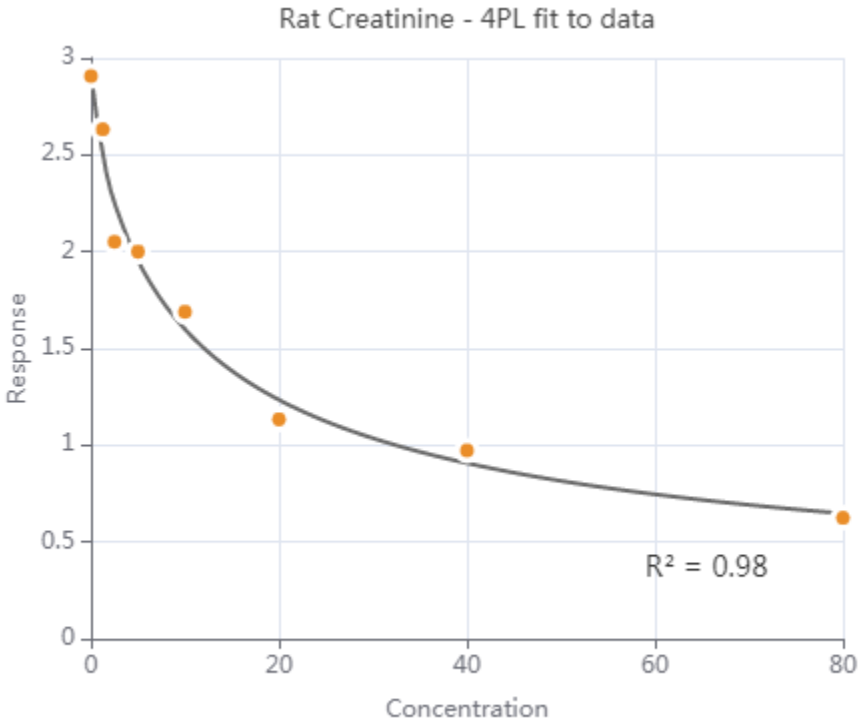

2.3.4 Urea Colorimetric Assay ELISA Kit

2.3.4.1 Test Principle: urease can decompose Urea into ammonia ions and carbon dioxide. Ammonia ions can react with amyl, forming a green substance in an alkaline medium. The production of a green substance is proportional to the urea content, which can be calculated with a colorimetric assay at 580 nm.

2.3.4.2 Reagent Preparation

Table 2.8: Types of reagents, each with (its components, specifications, and storage)

Items	Components	Specifications	Storage
Reagent 1	100 mmol/L Urea Standard	2 ml, one vial	2-8 °C, 12 months
Reagent 2	Enzyme Stock Solution	0.05 ml, one vial	2-8 °C, 12 months shading light
Reagent 3	Enzyme diluent	15 ml, one vial	2-8 °C, 12 months
Reagent 4	Chromogenic agent	15 ml, one vial	2-8 °C, 12 months shading light
Reagent 5	Alkaline NaCIO	15 ml, one vial	2-8 °C, 12 months shading light
	Microplate	96 wells	No requirement
	Plate sealer	Two pieces	

Note: The regent must be stored strictly according to the preservation conditions in the above table. The regent in different kits cannot mixed.

1. Prepare fresh enzyme working solution according to the ratio of reagent 2: reagent 3=1:3000 before use.

2. Sample preparation: The sample should be prepared using conventional methods, and heparin ammonium should not be used as an anticoagulant.

3. Dilution of the sample: it is recommended to take 2-3 samples with an expected significant difference to do a pre-experiment before the formal experiment and dilute the sample according to the result of the pre-experiment and the detection range (0.28-35 mmol/L).

4. The preparation of standard curve: Dilute 100 mmol/L urea standard with deionized water to a serial concentration. The recommended dilution gradient is as follows: 0, 5, 10,15, 20, 25, 30, and 35 mmol/L

2.3.4.3 Assay process

1. Standard wells: Add 4uL of standard solution with different concentrations to the corresponding wells.

Sample wells: Add 4uL of sample to the corresponding wells.

Control wells: Add 4uL of sample to the corresponding wells.

2. Add 50uL of enzyme working solution to standard and sample wells. Add 50uL of reagent 3 to control wells, mix thoroughly with the microplate reader for 10 seconds, then react at 37°C for 10 minutes accurately.

3. Add 125uL of reagent four and 125uL of reagent 5 to each well, mix thoroughly with the microplate reader for 10 s, and accurately react at 37°C for 10 min.

4. Measure the OD value of each well at 580 mm with a microplate reader.

2.3.5 Protein BCA Colorimetric Assay Kit

2.3.5.1 Test principle: Copper Cu+2 can be reduced to Cu+ by protein in alkaline conditions. Cu+ can combine with BCA reagent, forming a purple complex with a maximum absorption peak of 562 nm. The absorbance value is proportional to the protein concentration. Therefore, the protein concentration can be calculated according to the OD value.

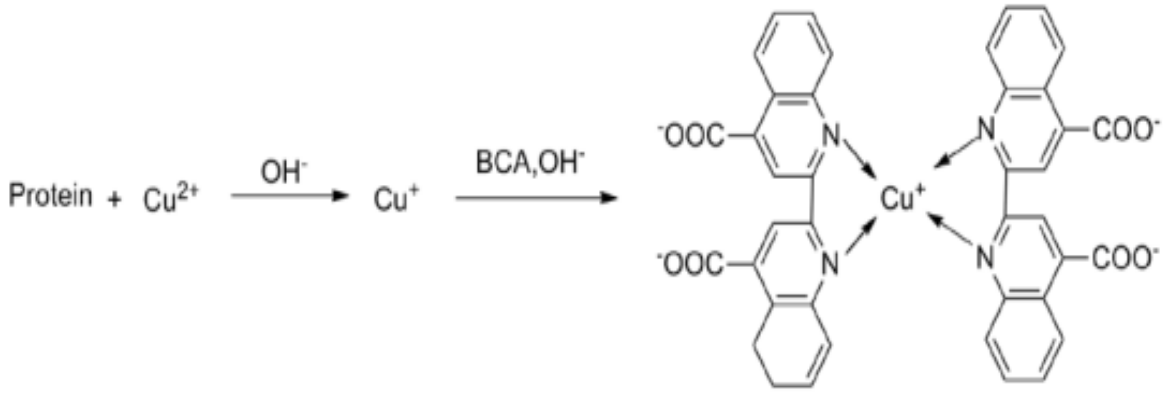

Figure 2.8: Explain the test principle of the Protein BCA Colorimetric Assay Kit

2.3.5.2 Reagent preparation

Table 2.9: Types of reagents, each with (its components, specifications, and storage)

Item	Component	Specification	Storage
Reagent 1	BCA reagent	25 ml, one vial	RT, 12 months
Reagent 2	Copper salt solution	0.5 ml, one vial	RT, 12 months
Reagent 3	Standard	1 mg, one vial	RT, 12 months
Reagent 4	Standard diluent	15 ml, one vial	RT, 12 months
	Microplate	96 wells	No requirement
	Plate sealer	2 Pieces	

1. Preparation of BCA working solution: Mix reagents one and two thoroughly at a ratio of 50:1. Prepare the needed amount of solution before use. The prepared working solution can be stored at four °C for 24 h.

2. Preparation of 1 mg/mL standard solution: Dissolve a vial of reagent three powder with 1 mL reagent four and mix thoroughly before use. It is recommended that the prepared solution be aliquoted, which can be stored at 20 °C for three months.

3. Sample preparation: The sample should be prepared according to conventional methods. The sample should not contain chelating agents (EGTA, EDTA) and reductive substances (DDT, 2-mercaptoethanol)

4. Dilution of sample: It is recommended to take 2-3 samples with an expected significant difference to do a pre-experiment before the formal experiment and dilute the sample according to the result of the pre-experiment and the detection range (0.0165-1 mg/mL).

5. The preparation of standard curve: Dilute 1 mg/mL standard solution with normal saline to a serial concentration. The recommended dilution gradient is as follows: 0, 0.2, 0.3, 0.4, 0.6, 0.7, 0.9, 1 mg/ml.

2.3.5.3 Assay Process

1. Standard well: add 20uL of standard solution with different concentrations.

2. Sample well: add 20pL of tested samples.

3. Add 200pL of BCA working solution to the wells of Step 1.

4. Oscillate for 20 to mix thoroughly and incubate at 37°C for 30 min.

5. Measure the OD value of each well at 562 m with a microplate reader.

2.3.6 Calculation of Malondialdehyde (MDA)

2.3.6.1 Test Principle: The concentration of MDA in serum was determined according to the Buege and Aust method **(Alam et al., 2013)**.MDA formed from the

breakdown of polyunsaturated fatty acids serves as a convenient index of peroxidation reaction. The thiobarbituric acid method was used to estimate the MDA, which reacts with thiobarbituric acid (TBA), giving a pink color read at λ max 535 nm .

2.3.6.2 Reagent Preparation

Thiobarbituric acid 0.188 gm. of (0.013 N) and 7.5 gm. trichloro acetic acid (TCA) (0.46 N) was dissolved in a suitable volume of hydrochloric acid (HCl) (0.25 N), the mixture was shaken and heated at 70 °C until dissolved completely then the volume was made up 100 ml with HCL (0.25N).

2.3.6.3 Assay Process

1. One ml of the reagent was added to 0.5 ml of serum sample.

2. The tube was mixed well by vortex and then heated at 70 °C for 20 min.

3. After cooling, the mixture was centrifuged for 10 min at (6000 rpm) using a microfuge centrifuge.

4. The clear supernatant was read at λ max 535 nm against the blank, which contains 1ml of D.W and 0.5 ml of reagent.

$$\text{Serum MDA concentration (μmol/l)} = \frac{\text{Abs} \times \text{D.F}}{\varepsilon \times \text{d}}$$

Abs: Absorbance

d: Light path = 1 cm

D. *f*: Dilution factor = 3

ε: Extinction coefficient = $1.56 \times 10^5 M^{-1}\ cm^{-1}$

2.3.7 Calculation of Serum GSH Concentration

2.3.7.1 Test Principle: The thiol concentration was measured according to the Ellman method.**(Ellman, 1959)**

2.3.7.2 Reagent Preparation

a. H_2NaPO_4 (0.2M) was prepared by dissolving (0.2gm) in (100ml) D.W.

b. HNa_2PO_4 (0.2M) was prepared by dissolving (0.2gm) in (100ml) D.W.

1. Reagent A: [Phosphate buffer (0.2M); pH= 7] was prepared by mixing 41 ml of (b)with 9 ml of (a). Volume was completed to 100ml by D.W., and pH was adjusted.
2. Reagent B: [Phosphate buffer (0.2M); pH= 8] was prepared by mixing 5 ml of a. with 45 ml of (b) and completed to 100 ml by D.W. pH was adjusted before and after adding D.W.
3. Reagent C (DTNB reagent): This solution was prepared by dissolving 39.6 mg of DTNB in 10 ml of reagent A with a tiny amount of Na_2CO_3.

2.3.7.3 Assay Process

1. In a test tube, 20 µl of serum was included to 1000 µl of D.W.
2. Reagent B (1000 µl) was next added and thoroughly mixed.
3. 200 µl of reagent C was added after 1500 µl of the aforementioned mixture was extracted. After a thorough mixing, the solution was incubated for sixty minutes at 37°C.
4. The exact same processes as in steps 1, 2, and 3 were followed to prepare the blank; however, in step 1, the same volume of D.W. was included in place of serum.
5. At 420 nm, the absorbance was taken into account.

$$GSH\ con.in\ \text{serum}\ \ \mu\text{mol/L} = (\text{T} - \text{B}) \times \frac{d.f}{\varepsilon} \times 10^6$$

T: Test absorbance

ε: Extinction coefficient = 13600 $M^{-1}.cm^{-1}$

B: Blank absorbance

d.f: Dilution factor =102.

2.3.8 Statistical Analysis

Data was expressed as Mean±SD. The statistical significance of the difference between various groups was decided by one-way analysis of variance (ANOVA). Examining data statistically were performed with Statistical Package for Social Sciences (SPSS) version 26.0 software. A *p-value of* < *0.05* was considered to be statistically significant.

Chapter Three

Results

3.1 Biochemical Test Results

The following results were appears in different studied groups and presented as a tables and bar charts.

Table 3-1: Biochemical Variables in the Studied Groups

Dependent Variable	Group A N=10	Group B N=10	Group C N=10	Group D N=10	Group E N=10
Urea mmol/l	0.44 ± 0.11	2.79 ± 0.32**	1.69 ± 0.96**	1.43 ± 0.79 **	1.39 ± 0.85 **
Creatinine Ug/ml	27.55± 9.48	37.97±5.44**	31.24±4.27 *	31.48±2.45*	32.24±7.24 *
MDA µmol/l	1.58 ± 0.24	2.11 ± 0.5**	1.75 ± 0.2 *	1.82 ± 0.1*	1.85 ± 0.13 *
GSH µmol/l	649.5±64.8	579±48.03**	625.35±26.3*	636.3±38.7*	622.0±47.18*
Total protein mg/ml	36.99±2.29	34.35±1.03**	36.14±1.84*	35.92±1.14*	36.19±2.27*
IL-I Beta ng/ml	6.4±1.07	8.32±1.06 **	7.26±0.68 *	7.18±0.99 *	7.13±0.833 *
TNF-α ng/l	115.8±8.77	139.4±9.63**	123.59±5.9 *	119.3±10.9 **	124.3±17.9 *

*significant (*P- value <0.05)*; ** highly significant (p<0.001).group A is controlled negative(only NS was given for 14 days); group B is controlled positive (10mg/kg of MTX was given on day 10); group C is the treated group (10mg/kg of empagliflozin was given for 14 days +MTX was given on day 10 of the experiment); group D is the treated group (10mg/kg of dapagliflozin was given for 14 days +MTX was given on day 10); group E is the treated group (20mg/kg of ertugliflozin was given for 14 days + MTX was given on day 10).

3.1.1 Urea Biomarker

Results (n=10) are expressed as the mean±SD. It has been shown that group (B) increased urea levels significantly compared to group (A). Moreover, in groups (C), (D), and (E), a highly significant decrease in urea was detected compared to the group B.

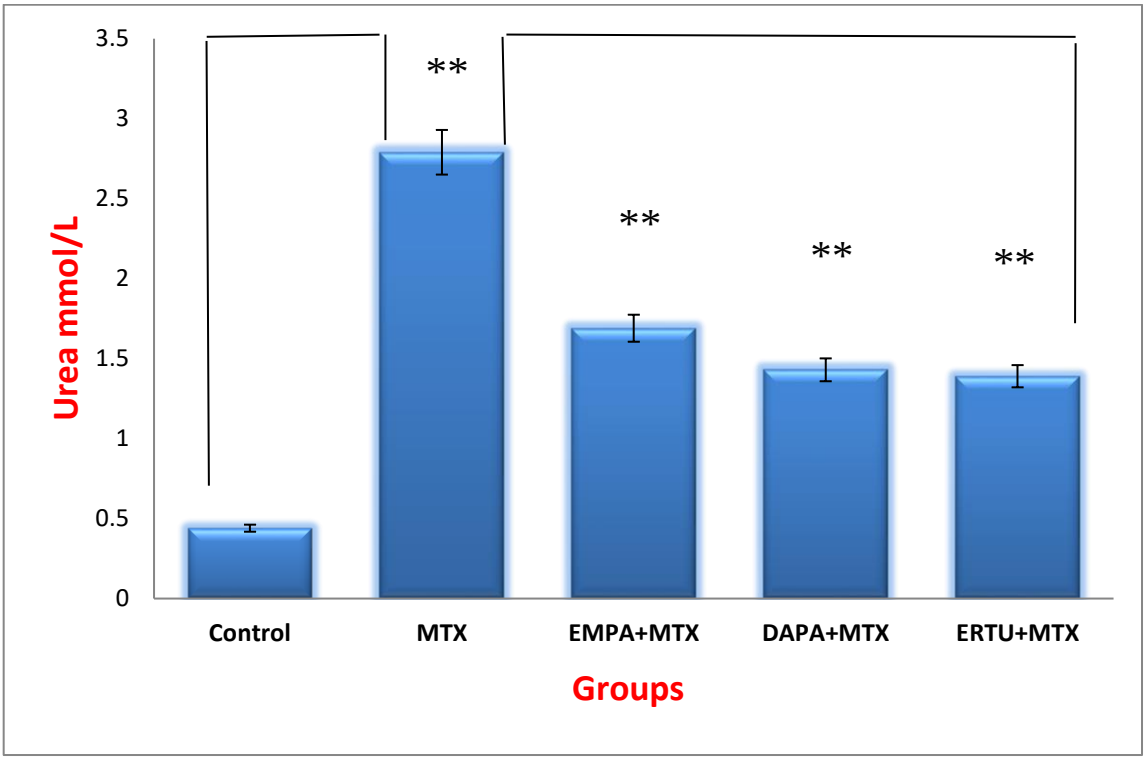

Figure 3-1: Effects of MTX, pretreatment EMPA+MTX, DAPA+MTX, and ERTU+MTX on Urea level (mmol/L) in rats kidneys. (*p<0.05), (**p<0.001).

Table 3-2: Comparison between the effect of treatment on urea level in group (A) and group (B).

Dependent Variable	Group	Study group	No.	Mean ±SD	P- value
Urea mmol/l	Group C	Group A	10	0.44 ± 0.11	**0.001**
		Group B	10	2.79 ± 0.32	**0.003**
	Group D	Group A	10	0.44 ± 0.11	**0.006**
		Group B	10	2.79 ± 0.32	**0.000**
	Group E	Group A	10	0.44 ± 0.11	**0.009**
		Group B	10	2.79 ± 0.32	**0.000**

3.1.2 Creatinine Biomarker

Results (n=10) are expressed as the mean± SD. This figure shows a highly significant increase in creatinine levels in group B compared to group A. However, in groups C, D, and E, creatinine levels decreased significantly compared to the B group.

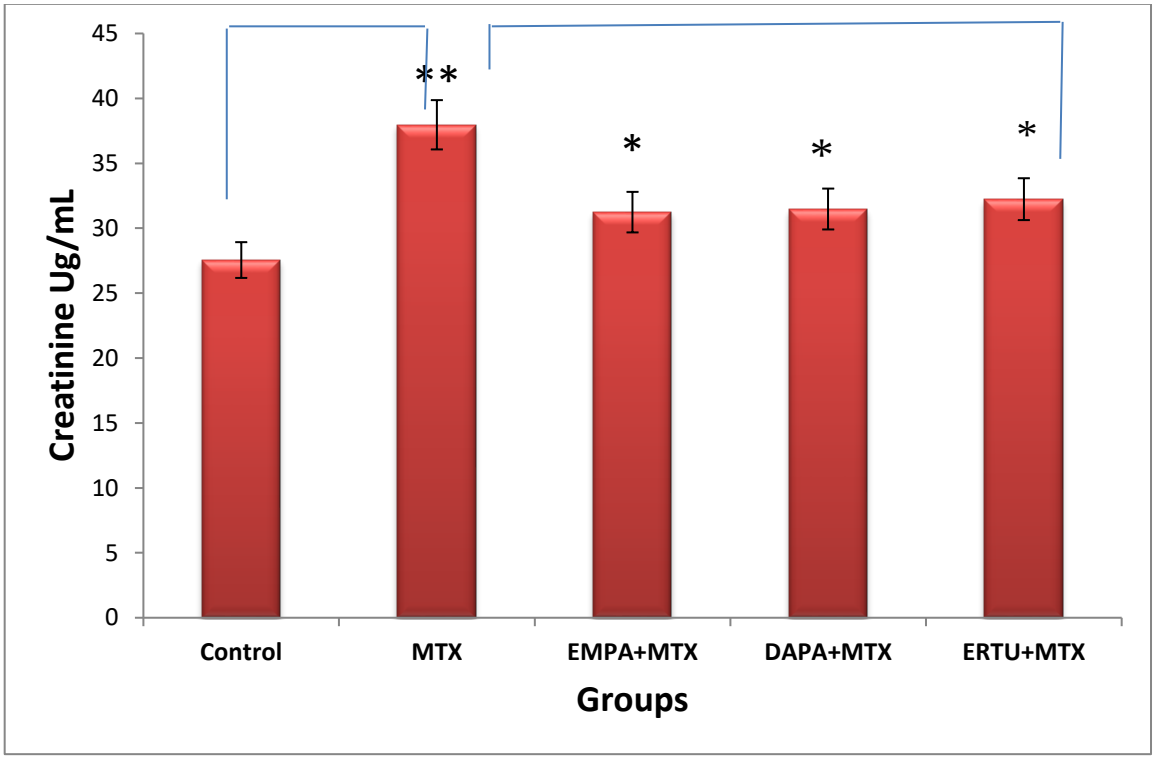

Figure 3-2: Effects of MTX, pretreatment EMPA+MTX, DAPA+MTX, and ERTU+MTX on Creatinine level (Ug/mL) in rats kidneys. (*p<0.05), (**p<0.001).

Table 3-3: Comparison between the effect of treatment on creatinine levels in groups A and B

Dependent Variable	Group	Study group	No.	Mean ±SD	P- value
Creatinine Ug/ml	Group C	Group A	10	27.55 ± 9.48	0.195
		Group B	10	37.97 ± 5.44	**0.021**
	Group D	Group A	10	27.55 ± 9.48	0.168
		Group B	10	37.97 ± 5.44	**0.025**
	Group E	Group A	10	27.55 ± 9.48	0.101
		Group B	10	37.97 ± 5.44	**0.047**

3.1.3 Malondialdehyde Biomarker

Results (n=10) are expressed as the mean±SD. This figure shows a highly significant increase in MDA level in the B group compared to group A and group C compared to group B. The MDA level decreased significantly in groups D and E compared to the B group.

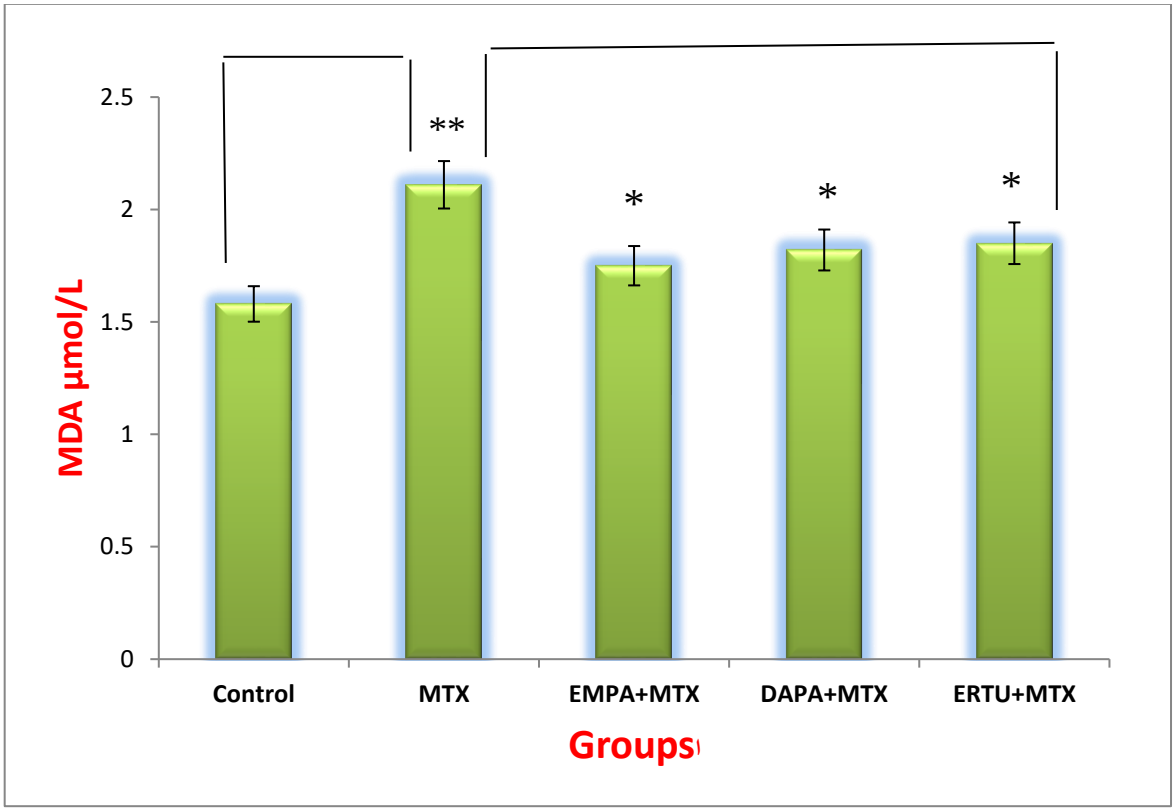

Figure 3-3: Effects of MTX, pretreatment EMPA+MTX, DAPA+MTX, and ERTU+MTX on MDA level (umol/L) in rats kidneys. (*p<0.05), (**p<0.001).

Table 3-4: Comparison between the effect of treatment on Malondialdehyde level in groups A and B

Dependent Variable	Group	Study group	No.	Mean ±SD	P- value
MDA µmol/l	Group C	Group A	10	1.58± 0.24	0.193
		Group B	10	2.11 ± 0.5	**0.005**
	Group D	Group A	10	1.58± 0.24	0.063
		Group B	10	2.11 ± 0.5	**0.023**
	Group E	Group A	10	1.58± 0.24	**0.037**
		Group B	10	2.11 ± 0.5	**0.041**

3.1.4 Glutathione Biomarker:

Results (n=10) are expressed as the mean±SD. This figure shows a highly significant decrease in GSH levels in the B group compared to group A. On the other hand, groups C and E showed a substantial increase in GSH levels, while group D showed a highly significant increase compared to the B group.

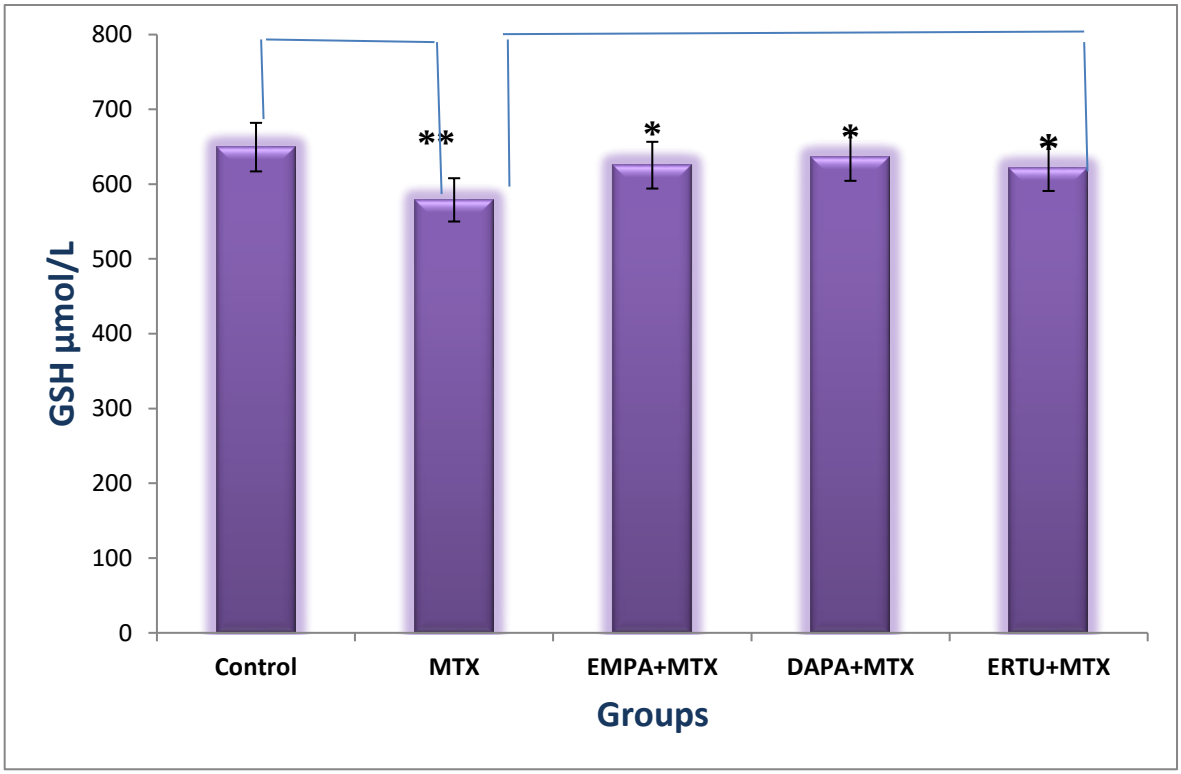

Figure 3-4: Effects of MTX, pretreatment EMPA+MTX, DAPA+MTX, and ERTU+MTX on GSH level (umol/L) in rats kidneys. (*p<0.05), (**p<0.001).

Table 3-5: Comparison between the effect of treatment on Glutathione level in groups A and B

Dependent Variable	Group	Study group	No.	Mean ±SD	P- value
GSH µmol/l	Group C	Group A	10	649.5 ± 64.8	0.254
		Group B	10	579 ± 48.03	**0.032**
	Group D	Group A	10	649.5 ± 64.8	0.529
		Group B	10	579 ± 48.03	**0.009**
	Group E	Group A	10	649.5 ± 64.8	0.195
		Group B	10	579 ± 48.03	**0.046**

3.1.5 Total Protein Biomarker

Results (n=10) are expressed as the mean±SD. This figure shows a highly significant decline in total protein level in the B group compared to group A. Conversely, total protein levels surged significantly in groups C, D, and E compared to the B group.

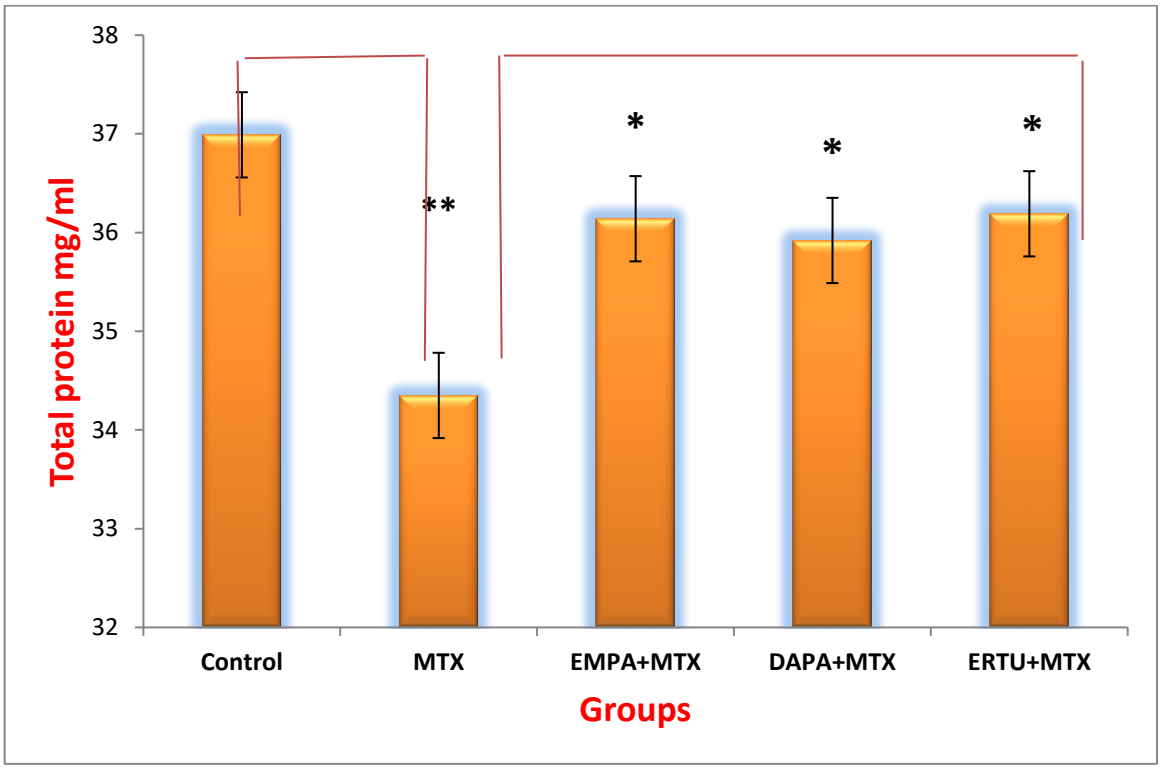

Figure 3-5: Effects of MTX, pretreatment EMPA+MTX, DAPA+MTX, and ERTU+MTX on Total protein level (mg/ml) in rats kidneys. (*p<0.05), (**p<0.001).

Table 3-6: Comparison between the effect of treatment on Total protein level in groups A and B

Dependent Variable	Group	Study group	No.	Mean ±SD	P- value
Total protein mg/ml	Group C	Group A	10	36.99 ± 2.29	0.296
		Group B	10	34.35 ± 1.003	**0.031**
	Group D	Group A	10	36.99 ± 2.29	0.189
		Group B	10	34.35 ± 1.003	**0.057**
	Group E	Group A	10	36.99 ± 2.29	0.324
		Group B	10	34.35 ± 1.003	**0.027**

3.1.6 IL-1 Beta Biomarker

Results (n=10) are expressed as the mean±SD. This figure shows a highly significant increase in IL-1Beta level in the B group compared to the A group. However, in groups C, D, and E, IL-1Beta levels decreased significantly compared to the B group.

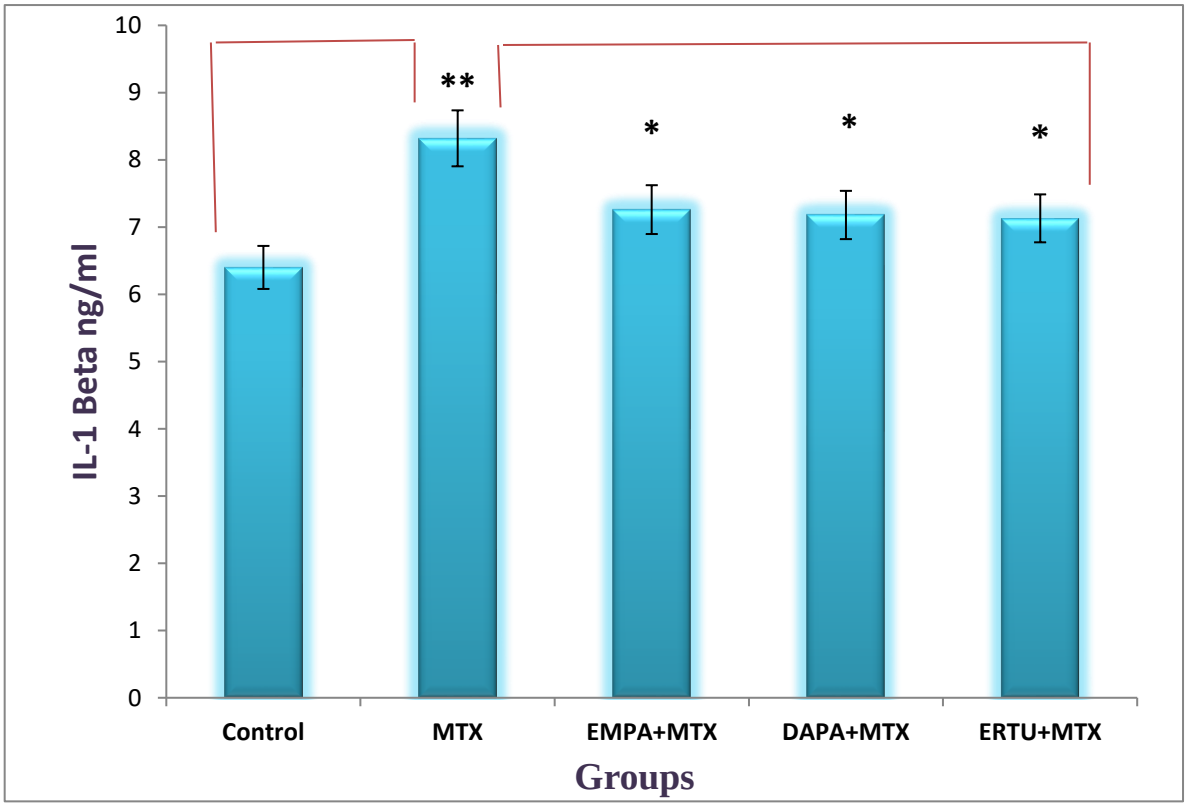

Figure 3-6: Effects of MTX, pretreatment EMPA+MTX, DAPA+MTX, and ERTU+MTX on IL-1B level (ng/ml) in rats kidneys. (*p<0.05), (**p<0.001).

Table 3-7: Comparison between the effect of treatment on IL-1 Beta level in groups A and B

Dependent Variable	Group	Study group	No.	Mean ±SD	P- value
IL-I Beta ng/ml	Group C	Group A	10	6.4 ± 1.07	**0.047**
		Group B	10	8.32 ± 1.06	**0.016**
	Group D	Group A	10	6.4 ± 1.07	0.073
		Group B	10	8.32 ± 1.06	**0.009**
	Group E	Group A	10	6.4 ± 1.07	**0.09**
		Group B	10	8.32 ± 1.06	**0.007**

3.1.7 TNF-α Biomarker

Results (n=10) are expressed as the mean±SD. It has been shown that TNF-α level increased highly significantly in group B compared to A group. In addition, in groups C, D, and E, a highly significant decrease of TNF-α was detected compared to the B group.

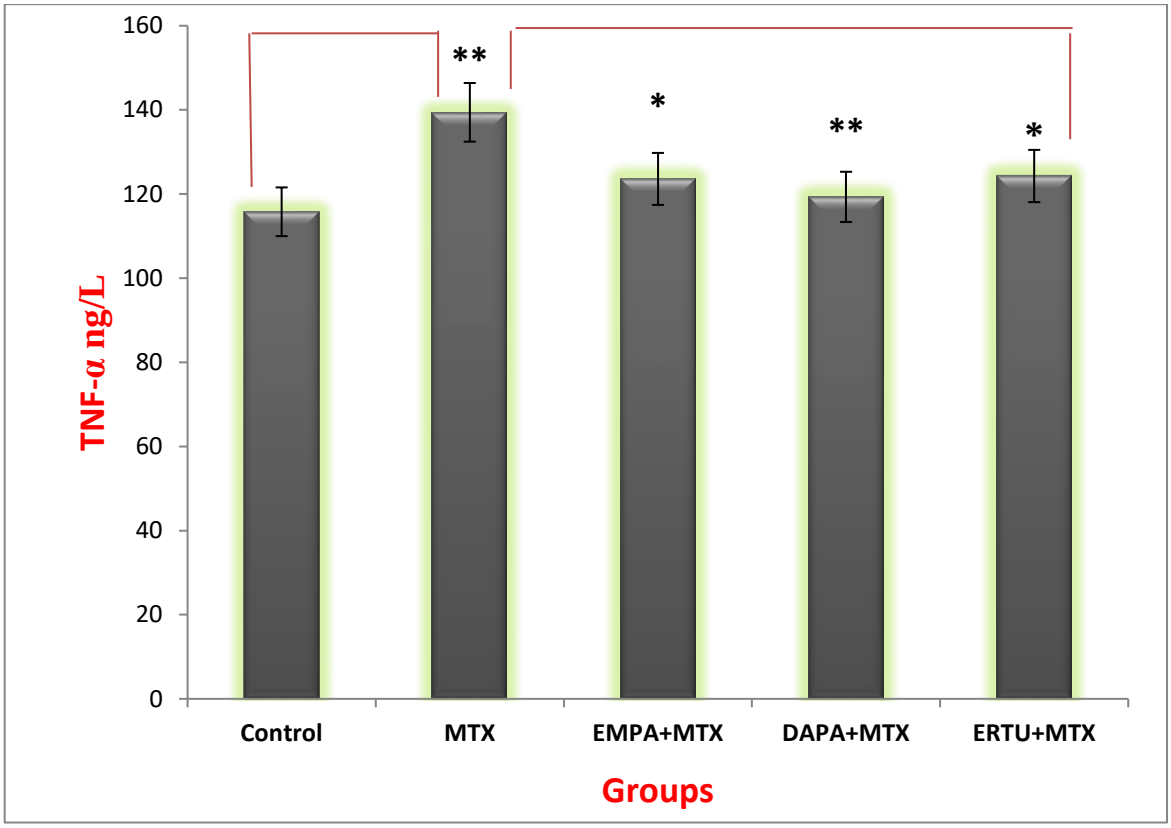

Figure 3-7: Effects of MTX, pretreatment EMPA+MTX, DAPA+MTX, and ERTU+MTX on TNF- α level (ng/L) in rats kidneys. (*p<0.05), (**p<0.001).

Table 3-8: Comparison between the effect of treatment on TNF-α levels in groups A and B

Dependent Variable	Group	Study group	No.	Mean ±SD	P- value
TNF-α ng/l	Group C	Group A	10	115.78 ± 8.77	0.131
		Group B	10	139.42 ± 9.63	**0.003**
	Group D	Group A	10	115.78 ± 8.77	0.49
		Group B	10	139.42 ± 9.63	**0.000**
	Group E	Group A	10	115.78 ± 8.77	0.101
		Group B	10	139.42 ± 9.63	**0.005**

Table 3-9: Comparison Between the Effect of the Treatment in Groups C, D, and E

Dependent Variable	Group	Study group	No.	Mean ±SD	P- value
Urea mmol/l	**Group C**	**Group D**	10	1.43 ± 0.79	0.456
		Group E	10	1.39 ± 0.85	0.396
	Group D	**Group C**	10	1.69 ± 0.96	0.456
		Group E	10	1.39 ± 0.85	0.917
Creatinine Ug/ml	**Group C**	**Group D**	10	31.48±2.45	0.933
		Group E	10	32.24±7.24	0.723
	Group D	**Group C**	10	31.24±4.27	0.933
		Group E	10	32.24±7.24	0.787
MDA µmol/l	**Group C**	**Group D**	10	1.82 ± 0.1	0.561
		Group E	10	1.85 ± 0.13	0.41
	Group D	**Group C**	10	1.75 ± 0.2	0.561
		Group E	10	1.85 ± 0.13	0.806
GSH µmol/l	**Group C**	**Group D**	10	636.3±38.7	0.605
		Group E	10	622.0±47.18	0.873
	Group D	**Group C**	10	625.35±26.3	0.605
		Group E	10	622.0±47.18	0.499
Total protein mg/ml	**Group C**	**Group D**	10	35.92±1.14	0.783
		Group E	10	36.19±2.27	0.953
	Group D	**Group C**	10	36.14±1.84	0.783
		Group E	10	36.19±2.27	0.738
IL-I Beta ng/ml	**Group C**	**Group D**	10	7.18±0.99	0.837
		Group E	10	7.13±0.833	0.76
	Group D	**Group C**	10	7.26±0.68	0.837
		Group E	10	7.13±0.833	0.92
TNF-α ng/l	**Group C**	**Group D**	10	119.3±10.9	0.404
		Group E	10	124.3±17.9	0.893
	Group D	**Group C**	10	123.6±5.86	0.404
		Group E	10	124.3±17.9	0.333

P- value >0.05 considered non-significant

P- value <0.05 considered significant

3.2 Histological Results

The histopathology results can be described in sections from control cases (group A) that showed bland-looking glomerular and tubular structures with no significant changes.

Other Sections from methotrexate-treated cases (group B) showed Bowman space widening, tubular cell vacuolar degeneration, intratubular hemorrhage, chronic inflammatory cell infiltration, and marked vascular congestion.

Another section from the C, D, and E groups showed bland-looking glomeruli, few glomeruli with mild Bowman space widening, no significant tubular changes, and foci of vascular congestion.

The Following are photomicrographs describing tissue changes in each group:

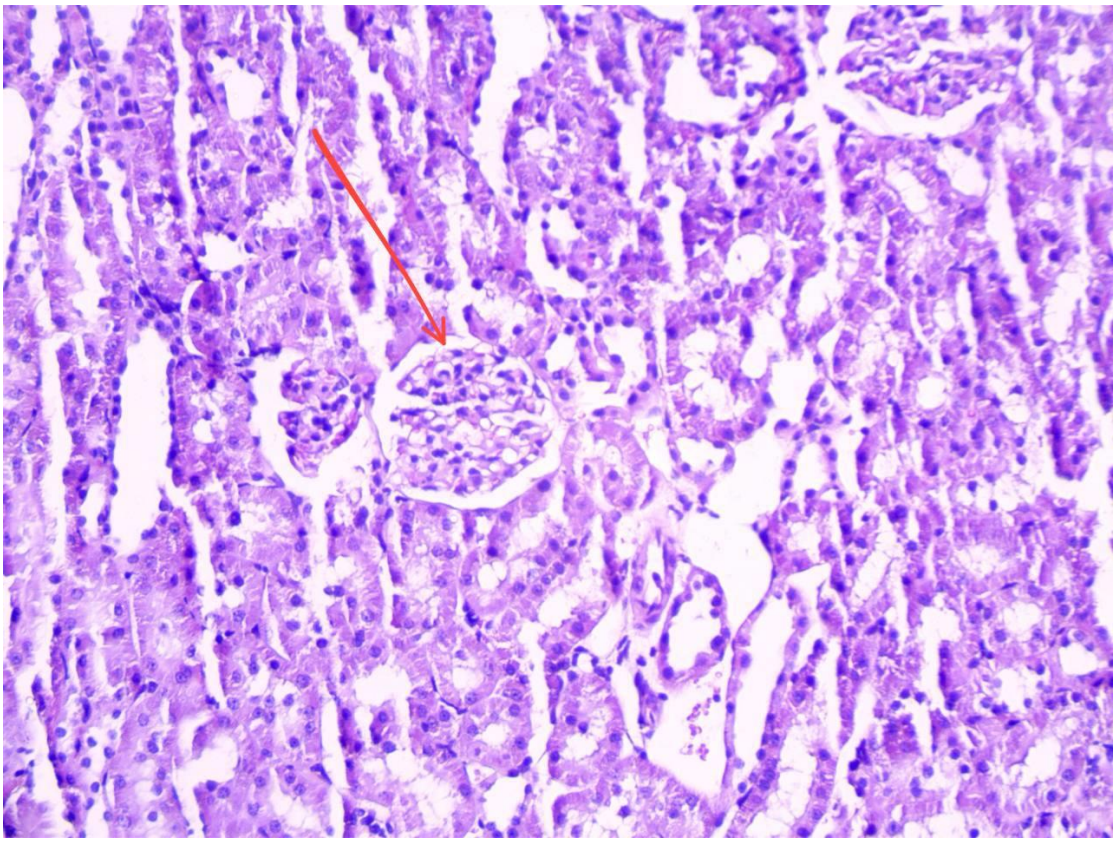

Figure 3.8: A photo micro-graph of the kidney of a Rat Treated with Normal Saline for 14 days (Group A) Shows a Bland Look of the Glomerulus (red arrow), hematoxylin, and eosin, x 20.

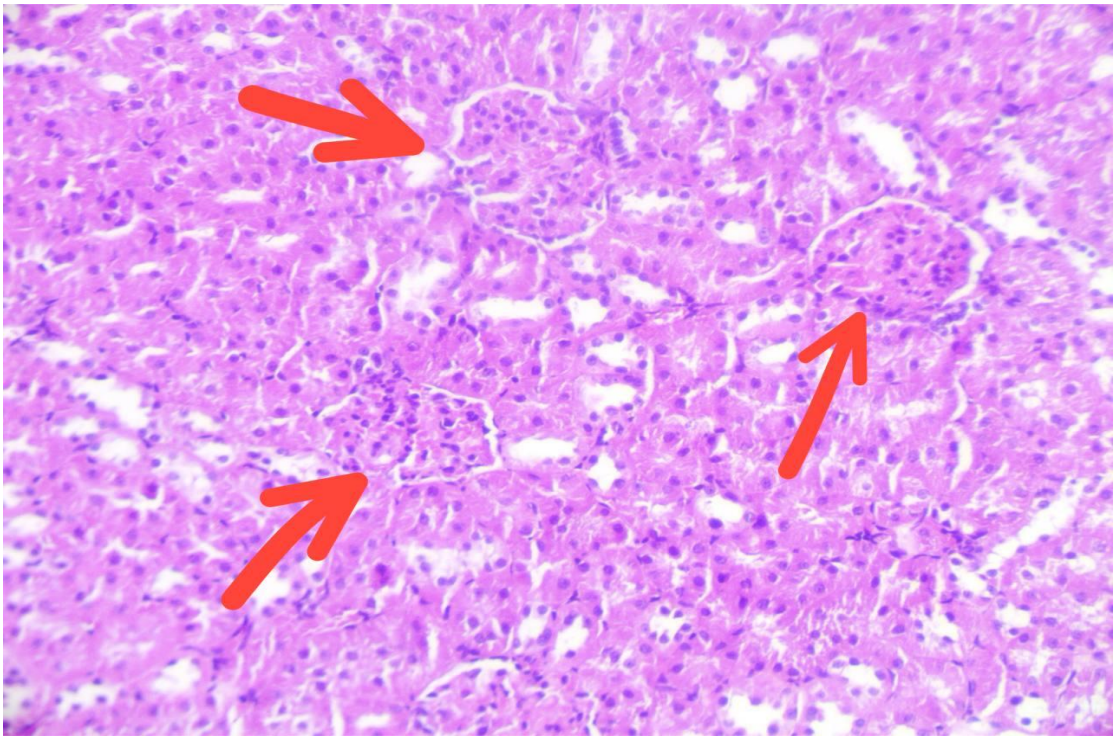

Figure 3.9: A photo micro-graph of the kidney of a Rat Treated with Normal Saline for 14 days (Group A) Shows a Bland Look of the Glomeruli (red arrow), hematoxylin, and eosin, x 20.

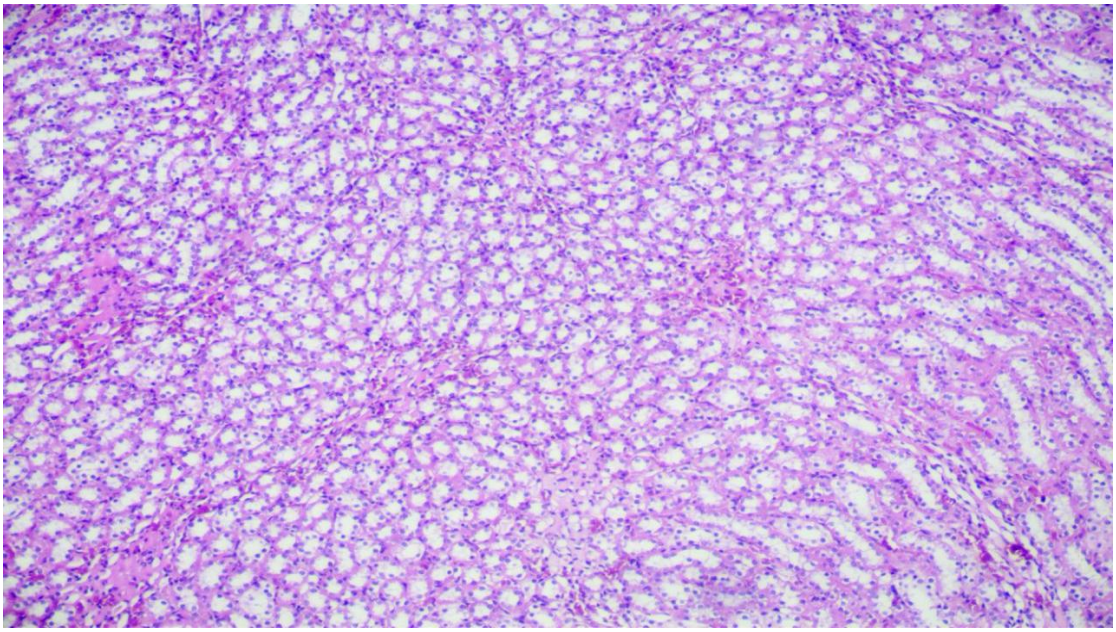

Figure 3.10: A photo micro-graph of the kidney A Slice of the Tissue of a Rat Treated with Normal Saline for 14 days (Group A) Shows a Bland Look of the Tubules, hematoxylin, and eosin, x 4.

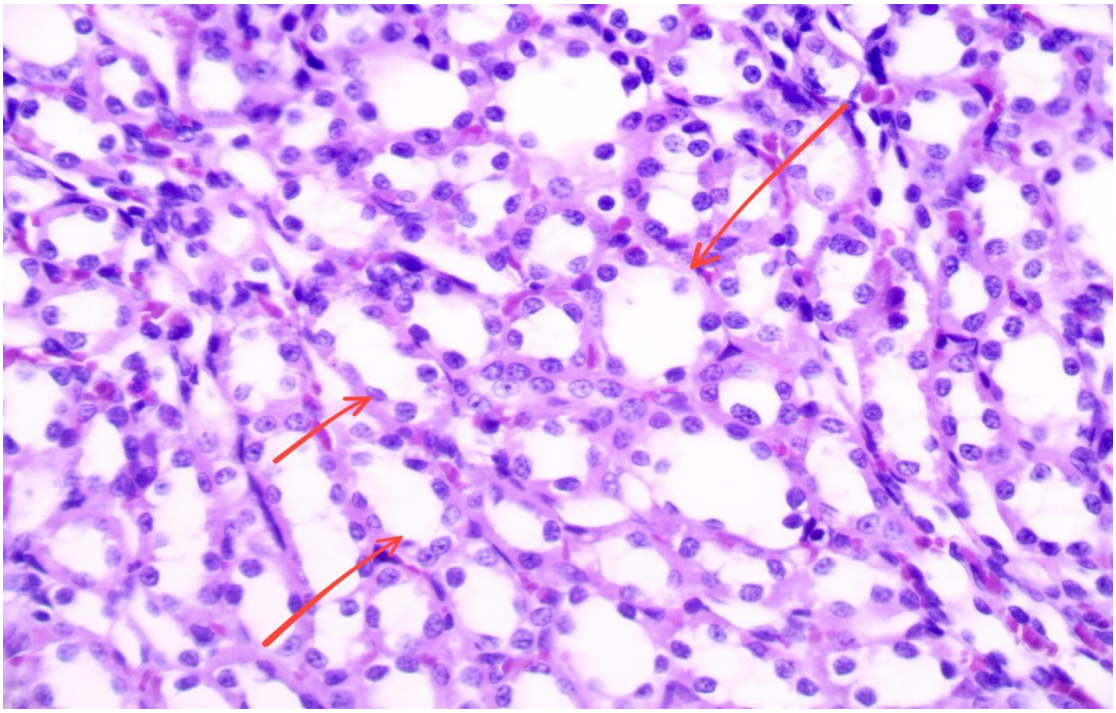

Figure 3.11: A photo micro-graph of the kidney of a Rat Treated with Normal Saline for 14 days (Group A) Shows a Bland Look of the Tubules (red arrow), hematoxylin, and eosin, x 40.

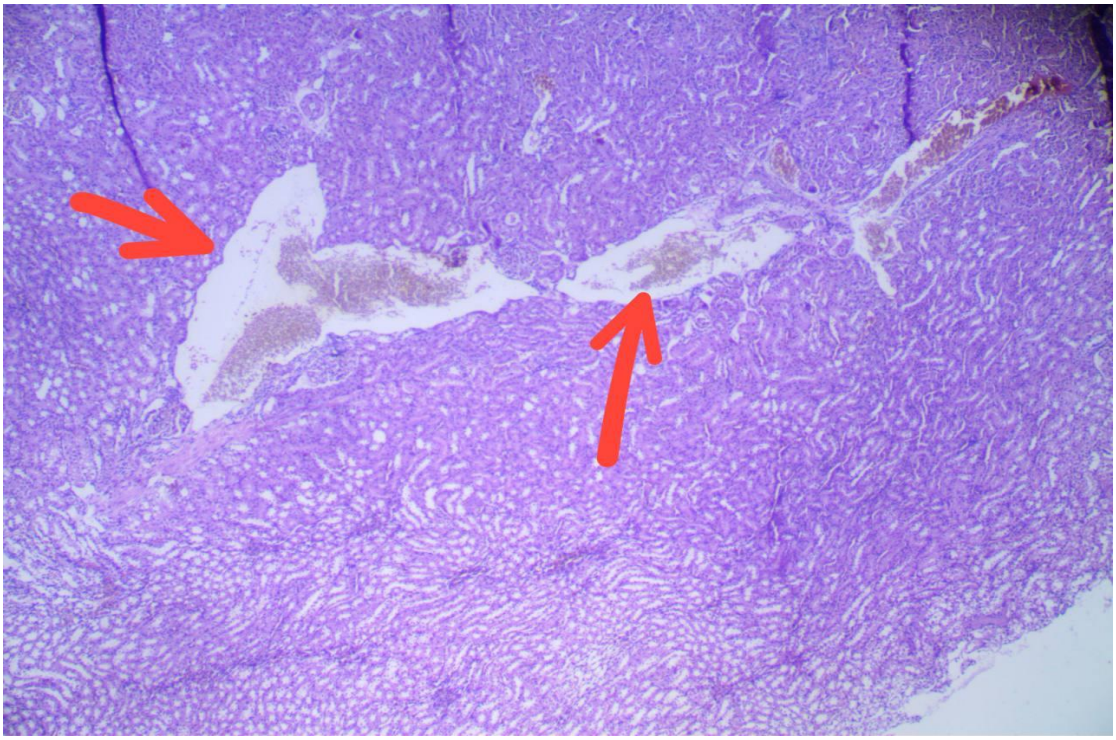

Figure 3.12: A photo micro-graph of the kidney of a Rat Treated with MTX on day 10 of the Experiment (Group B) Shows Marked Vascular Congestion (red arrow), hematoxylin, and eosin, x 4.

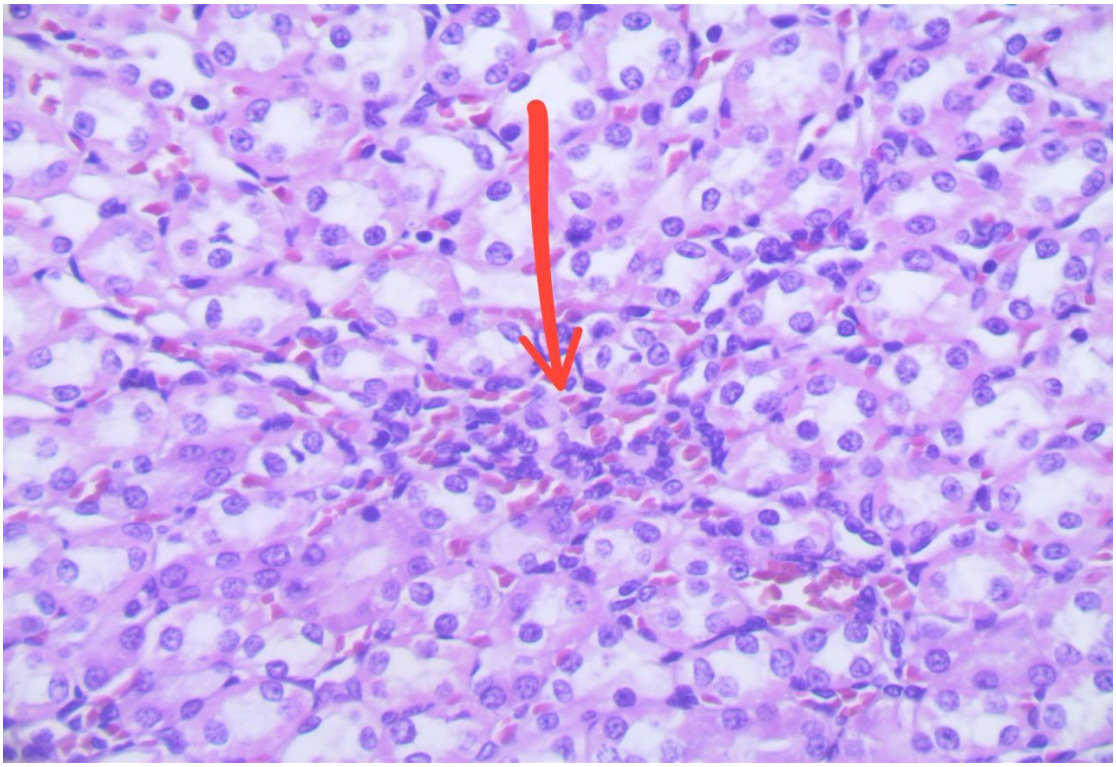

Figure 3.13: A photo micro-graph of the kidney of a Rat Treated with MTX on day 10 of the Experiment (Group B) Shows Chronic Inflammatory Cell Infiltration (red arrow), hematoxylin, and eosin, x 40.

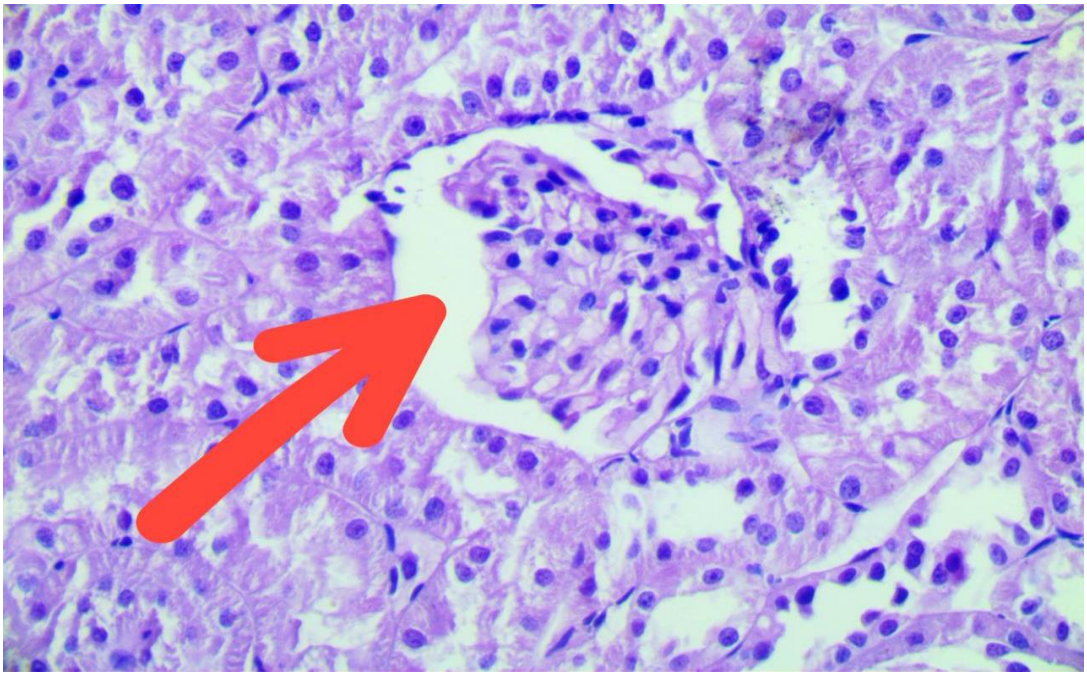

Figure 3.14: A photo micro-graph of the kidney of a Rat Treated with MTX on day 10 of the Experiment (Group B) Shows Bowman Space Widening (red arrow), hematoxylin, and eosin x 40.

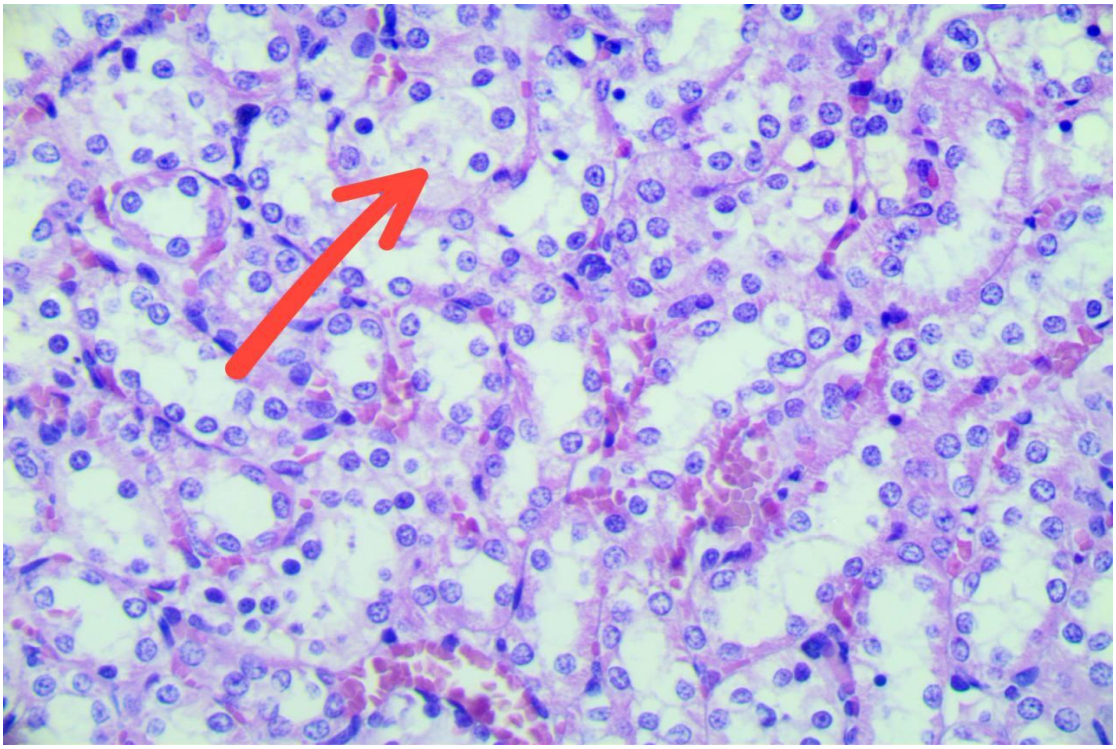

Figure 3.15: A photo micro-graph of the kidney of a Rat Treated with MTX on day 10 of the Experiment (Group B) Shows Tubular Cell Vacuolation (red arrow), hematoxylin, and eosin x 40.

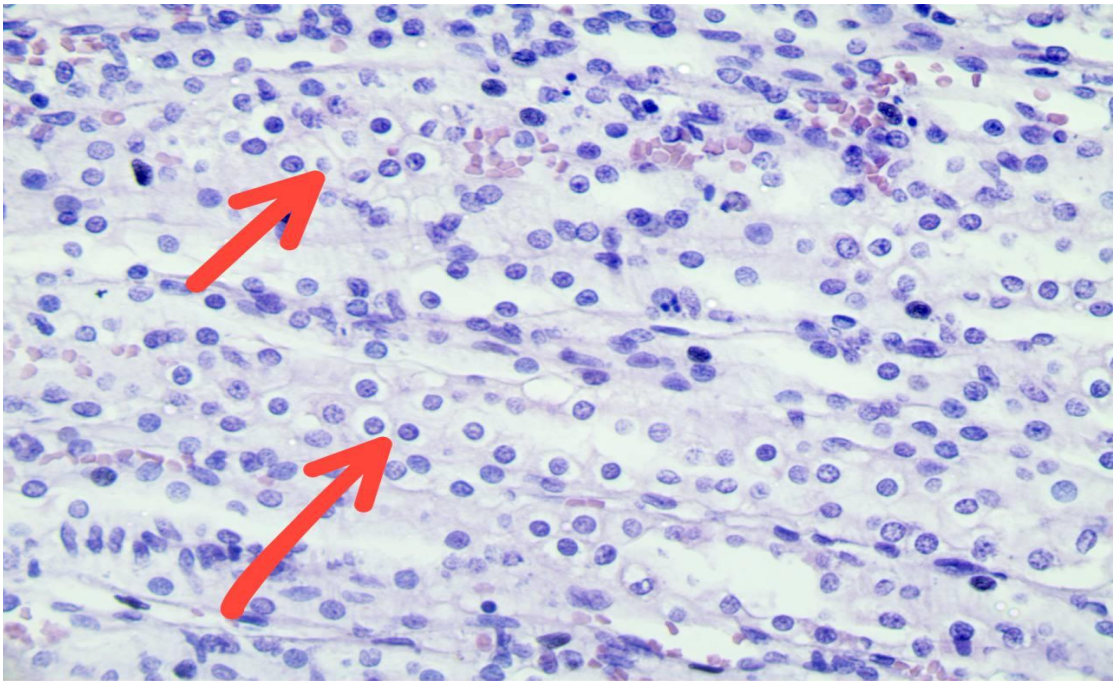

Figure 3.16: A photo micro-graph of the kidney of a Rat Treated with MTX on day 10 of the Experiment (Group B) Shows Tubular Cell Vacuolation (red arrow), hematoxylin, and eosin x 40.

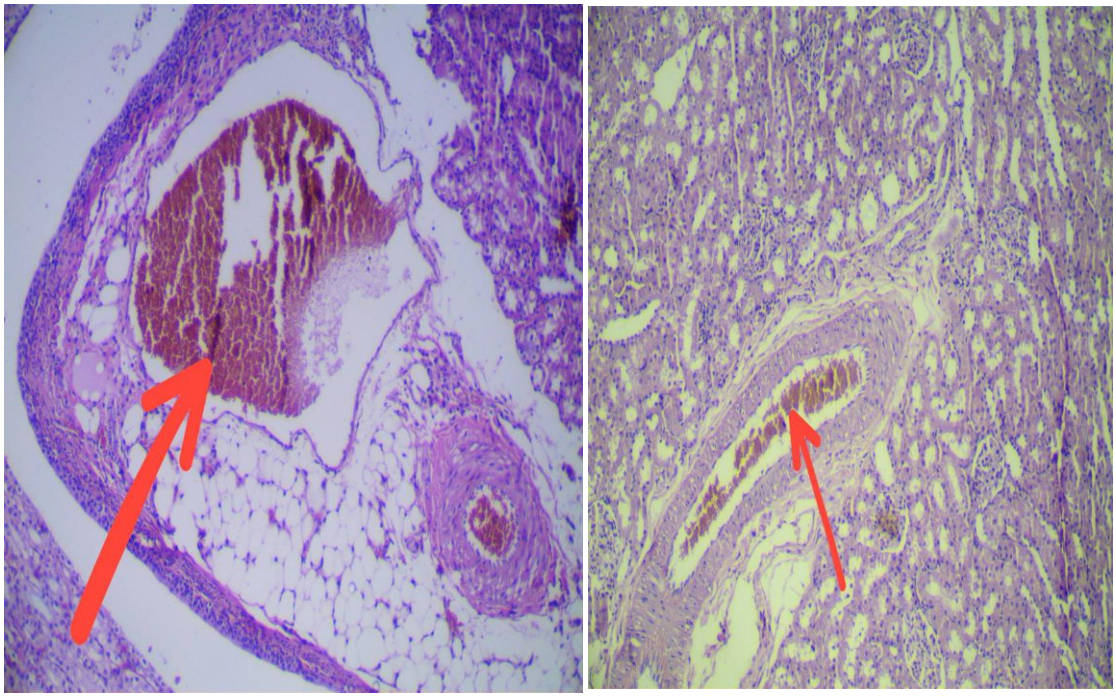

Figure 3.17: A photo micro-graph of the kidney of a Rat Treated with Empagliflozin for 14 days (Group C) Shows Vascular Congestion (red arrow), hematoxylin, and eosin x 10.

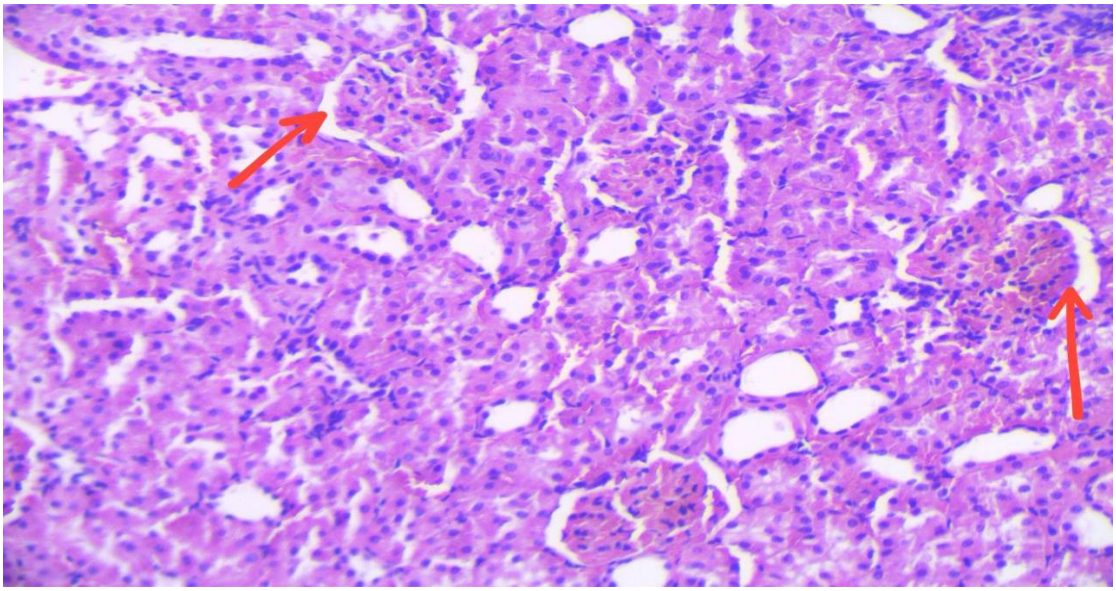

Figure 3.18: A photo micro-graph of the kidney of a Rat Treated with Empagliflozin for 14 days (Group C) Shows Normal Glomeruli to Mild Bowman Space Widening (red arrow), hematoxylin and eosin x 20.

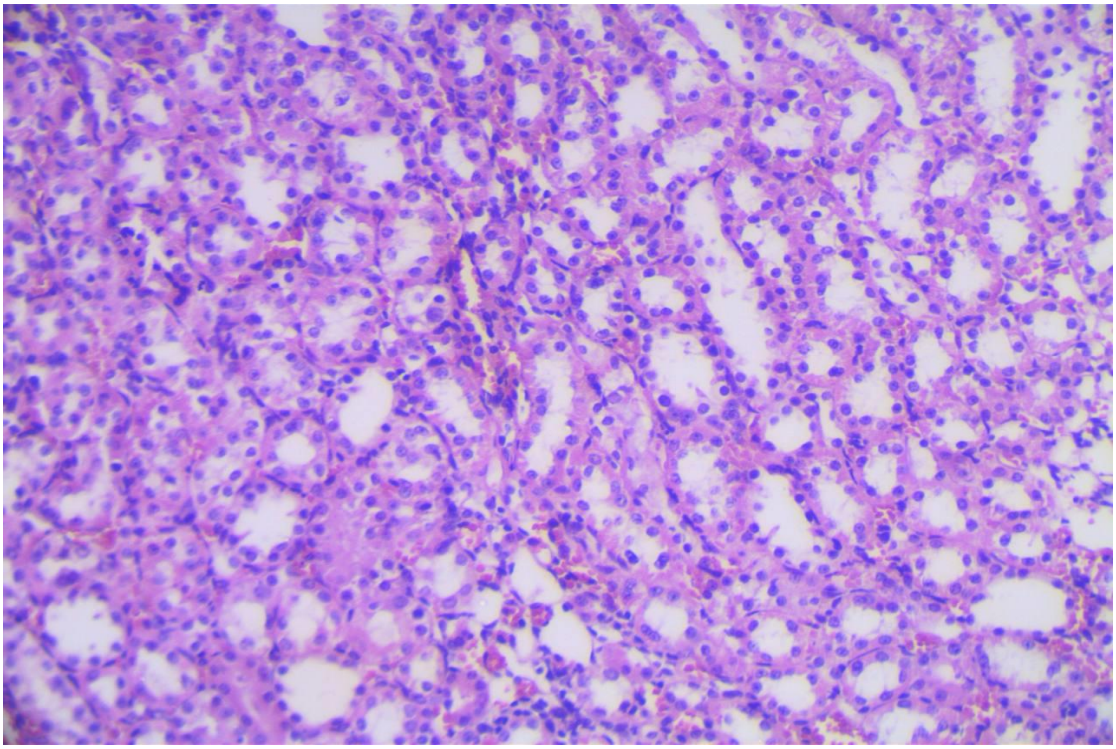

Figure 3.19: A photo micro-graph of the kidney of a Rat Treated with Empagliflozin for 14 days (Group C) Shows Bland-Look of the Tubular Structures x 20.

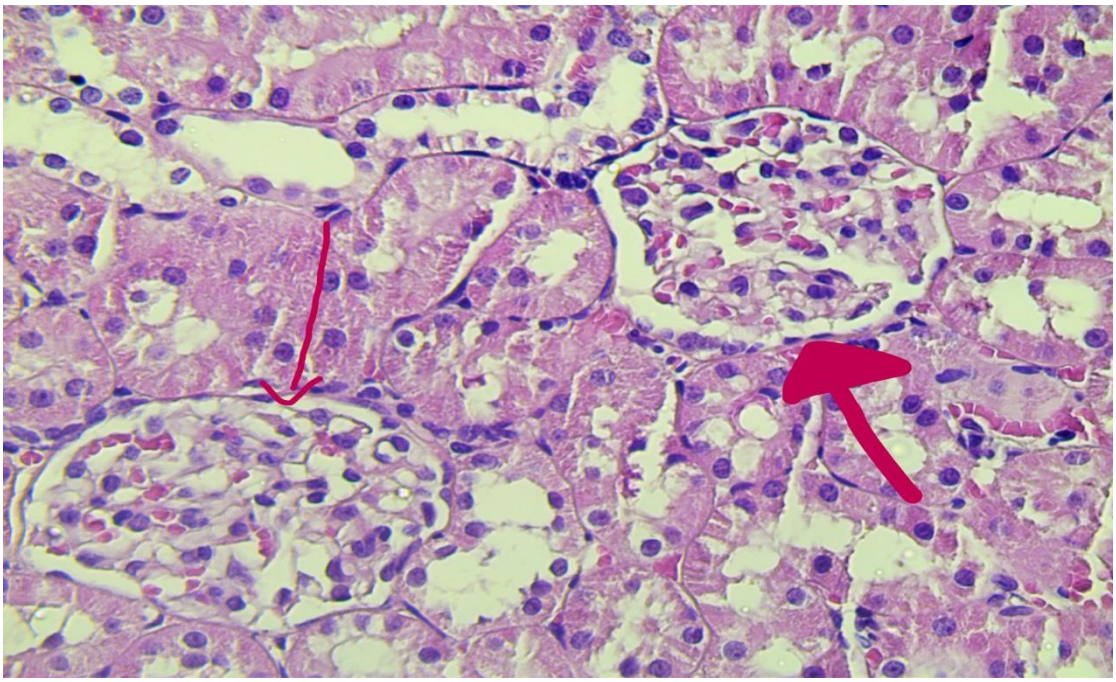

Figure 3.20: A photo micro-graph of the kidney of a Rat Treated with Dapagliflozin for 14 days (Group D) Shows Bland-Look of the Glumerular and Tubular Structures (red arrows) x 40.

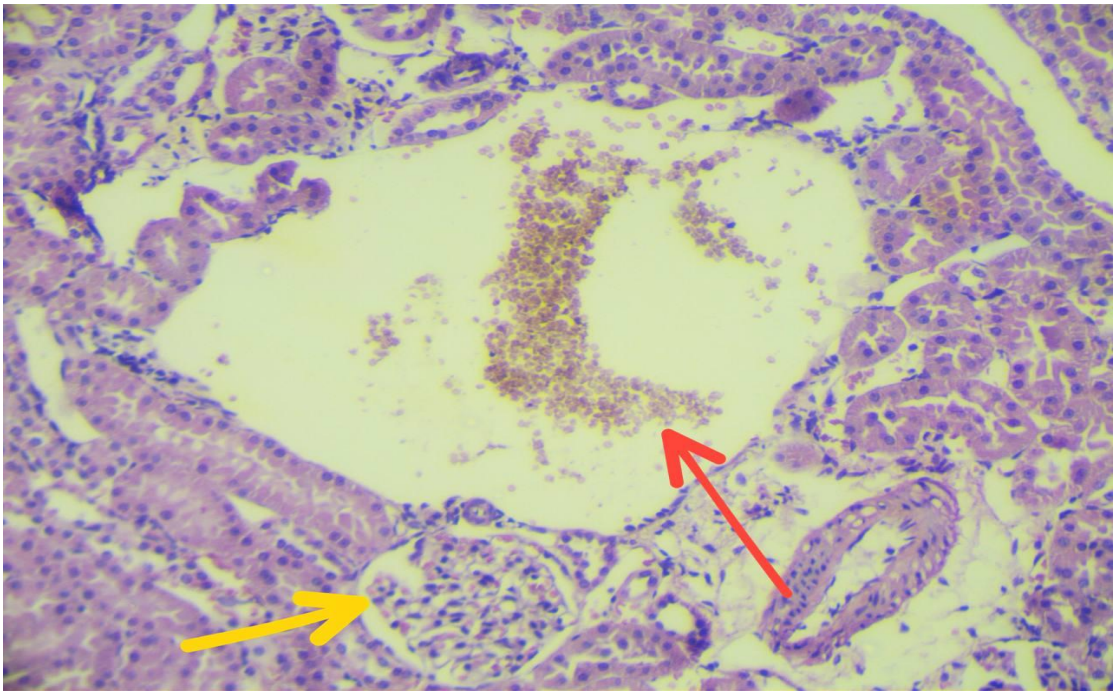

Figure 3.21: A photo micro-graph of the kidney of a Rat Treated with Dapagliflozin for 14 days (Group D) Shows Bland-Look of the Glumerular and Tubular Structures (red and yellow arrows) x 20.

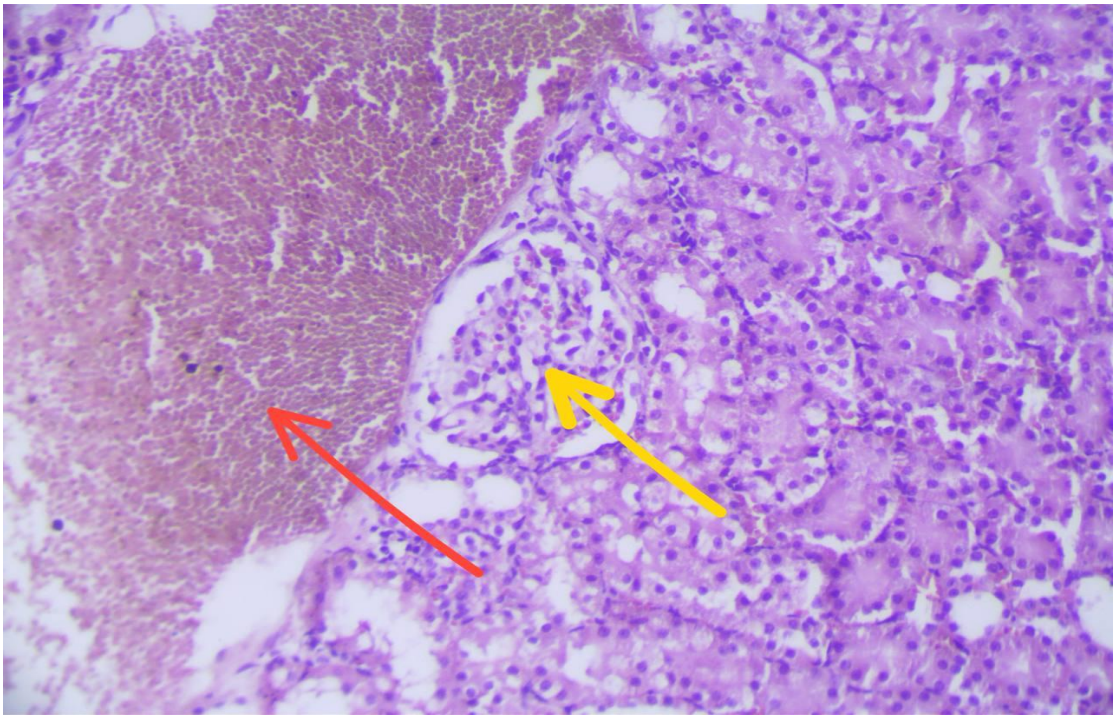

Figure 3.22: A photo micro-graph of the kidney of a Rat Treated with Ertugliflozin for 14 days (Group E) Shows Bland-Look of the Glumerular and Tubular Structures (red and yellow arrows) x 20.

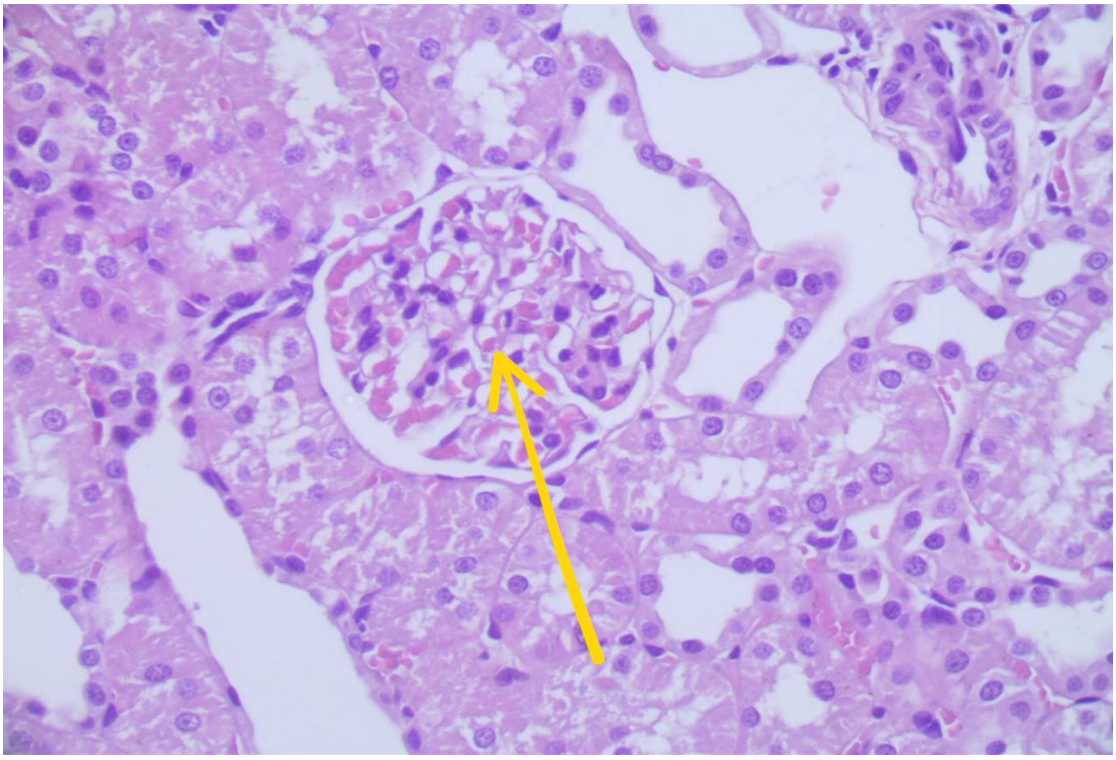

Figure 3.23: A photo micro-graph of the kidney of a Rat Treated with Ertugliflozin for 14 days (Group E) Shows a Bland Look of the Glomerular and Tubular Structures (yellow arrow) x 40.

Chapter Four

Discussion

4. Discussion

Maintaining the extracellular environment's equilibrium largely depends on the renal system's ability to detoxify and remove harmful substances and their byproducts. **(Alshanwani *et al.*, 2021)**

Nephrotoxicity, characterized by a dramatic decrease in kidney function, can result from exposure to environmental contaminants directly or as a side effect of certain medications. **(Sharma *et al.*, 2020)**

Methotrexate has been linked to many mechanisms of kidney injury, including increased oxidative stress and elevated renal function tests that result in kidney cell damage. Renal damage caused by MTX was examined using renal histology, biochemical testing, and oxidative assays.

The present study focused on the protective effect of selected SGLT2 inhibitors (empagliflozin, dapagliflozin, and ertugliflozin) on MTX-induced renal damage in rats by:

1. Reducing creatinine and urea levels and increasing the total protein level.

2. Suppressing the oxidative stress parameters by reducing MDA and increasing GSH.

3. Decreasing the inflammation by decreasing TNF-alpha and interleukin 1B.

4. Repairing the histopathological damage of the kidneys.

4.1 Effect of Methotrexate, Empagliflozin, Dapagliflozin, and Ertugliflozin on the Oxidative Stress Parameters

4.1.1 Effects on MDA Level

According to earlier research, MTX causes renal tissue damage by suppressing

the body's natural defense mechanism against free radicals. This increases reactive oxygen species (ROS) production and lipid peroxidation. Lipid peroxidation is one of the main processes via which free radicals cause tissue damage. **(Sahindokuyucu-Kocasari *et al.*, 2021)(Asci *et al.*, 2017)**

When antioxidant systems are depleted, reactive oxygen species cause polyunsaturated fatty acids to peroxide, forming MDA, a highly reactive molecule. MDA comes in two forms: endogenous, which comes from lipid peroxidation, and exogenous, which is distributed through food.**(Kapusta, Kuczyńska and Puppel, 2018)**

The current study highlighted that MTX led to a significant surge in oxidative insults as evidenced by a significant increase in the concentration of MDA, which reflected the increase in ROS compared to group A, as shown in Figure (3.3). This result is consistent with previous studies.**(Al-Abdaly, Saeed and Al-Hashemi, 2021)(Moodi *et al.*, 2020)**

Additionally, Reactive oxygen species increase permeability, which alters endothelium and epithelial cells. As a result, interacting with nucleic acids, sulfhydryl bonds, and unsaturated fatty acids of cell membranes can cause tissue damage brought on by MTX-induced OS. Treatment with MTX may indirectly release mitochondrial enzymes, impairing mitochondria and reducing antioxidant activity.**(Jalili *et al.*, 2020)**

Empagliflozin was found to suppress MTX-inducing renal damage via modulating oxidative stress in (group C) pretreatment; empagliflozin significantly decreased the level of MDA when compared to group B, as presented in Figure (3.3) as in the previous study **(Yaribeygi *et al.*, 2023).**

Dapagliflozin + MTX (group D) presented the effect of dapagliflozin in reducing oxidative stress via significantly decreasing the level of MDA compared with (group B) as shown in Figure (3.3). These findings went well with other study. **(Bora *et al.*, 2021).**

By altering pro-oxidant enzymes, including xanthine oxidase and endothelial nitric oxide synthase, dapagliflozin therapy reduces oxidative stress. Furthermore, recent research has demonstrated that SGLT2 inhibitors stop mitochondrial malfunction combined with a better redox state. **(Yaribeygi *et al.*, 2019).**

In the present study, ertugliflozin + MTX (group E) was found to alleviate lipid peroxidation MDA compared to (group B), as explained in Figure (3.3); these results were consistent with another previous study, which indicates that ertugliflozin has been found to modulate mitochondrial dysfunction and oxidative stress in high-fat, high-sucrose-fed mice by preventing hydrogen peroxide release and preserving ATP production.**(Croteau *et al.*, 2021)**

4.1.2. Effects on GSH Level

Tripeptide glutathione (γ-l-glutamyl-l-cysteinyl glycine) is an essential antioxidant in all mammalian tissues, ranging from 1 to 10mM. The peptide bond that connects glutamate and cysteine in GSH is called a glutamate γ-carboxyl group instead of the more common α-carboxyl group. This gives GSH its distinct structure. The only enzyme capable of hydrolyzing this peculiar bond is gamma-glutamyl transpeptidase (GGT), which is only found on the surface of specific kinds of cells. **(Lu, 2013)**. Given its ability to rescue the body from free radical damage, repair damaged molecules by supplying hydrogen atoms, reducing peroxides, and preserve protein thiols in their reduced form, glutathione (GSH) is a versatile and worldwide antioxidant **(Owumi, Ajijola and Agbeti, 2019).**

The current study demonstrated that MTX produced a highly significant decrease in GSH levels in group (B) compared to group (A) (control negative), as shown in Figure (3.4). These results agreed with other recent studies demonstrating a significant reduction in GSH levels in the methotrexate-treated group.**(Safaei *et al.*, 2018)(Ali *et al.*, 2017)(Ahmed, Zaki and Nabil, 2015).**

Lipid peroxidation caused MTX to inhibit the NADP malic enzyme and cytosolic nicotinamide adenosine diphosphate (NADP) dependent dehydrogenase, which decreased the availability of NADPH. NADPH is necessary to maintain the essential cytosolic antioxidant glutathione by glutathione reductase enzyme in the reduced state. **(Santhakumar *et al.*, 2021).**

Maintaining the equilibrium of the antioxidant system is crucial for preventing oxidative stress, and GSH plays a major part in this process. One significant antioxidant system in cells is the GSH redox cycle. By inhibiting the synthesis of cytosolic NADPH, MTX increases oxidative stress and lowers glutathione in its storage form. **(Azadnasab *et al.*, 2021)**

Rather than directly neutralizing free radicals, empagliflozin modulates oxidative stress in the renal cortex via upregulating Nrf2, stimulating the activity of antioxidant enzymes such as GSH-Px and catalase. Furthermore, through its involvement in the elimination of lipoperoxidation products, elevated GSH-Px activity can contribute to the reduction of lipid peroxidation. Increased glutathione levels, a sensitive indicator of oxidative damage, were likewise associated with increased GSH-Px activity in the renal cortex after empagliflozin administration. **(Malínská *et al.*, 2022)**. In the present study, it has been found that empagliflozin in group (C) significantly increases the level of GSH compared to group (B), as shown in Figure (3.4).

Dapagliflozin + MTX in group (D) increases the GSH level significantly compared to group (B) **(Bora *et al.*, 2021).** The results of the current study suggest that dapagliflozin prevents damage caused by an oxidative attack by increasing antioxidant mechanisms and reducing lipid peroxidation in tubular damage. Dapagliflozin SGLT2 inhibitors show potent antioxidant properties. **(Bora *et al.*, 2021).** Another study states that dapagliflozin ameliorates GSH levels and has antioxidant features. **(Chen *et al.*, 2023).**

Dapagliflozin treatment resulted in a 32.9% reduction in lipid peroxide levels and increased GSH/GSSG ratio and GPx activity to 82.2% and 78.1% of the control values, respectively. Dapagliflozin increased the upstream Nrf2 and its effector HO-1 levels to 92.3% and 95% of their control values to enhance the GSH/GSSG ratio and GPx antioxidant defences. Dapagliflozin-induced oxidative stress mitigation was facilitated by activating the Nrf2/HO-1 pathway.**(Arab, Al-Shorbagy and Saad, 2021). (Doaa I. Mohamed *et al.*, 2019)**

Ertugliflozin + MTX in group (E) resulted in a significant rise in GSH levels compared to group (B); it was not significant when compared to group (A), as shown in Table (3.5) and Figure (3.4). Ertugliflozin prevented mitochondrial dysfunction, leading to a correction of ATP production, an improvement in myocardial energetics, and a reduction in hydrogen peroxide production. **(Bodnar *et al.*, 2023).**

4.2 Effect of Methotrexate, Empagliflozin, Dapagliflozin, and Ertugliflozin on the Kidney Function Parameters

4.2.1 Effects on Creatinine

The final byproduct of the metabolism of creatine and creatine phosphate is creatinine. Glycine, arginine, and methionine are the amino acids that produce creatine. This nitrogenous organic acid is mainly produced in the kidney and liver and somewhat in the pancreas. This process consumes up to 10% of the daily glycine intake, 22% of arginine, and 42% of methionine. This substance's presence in the blood suggests that the kidneys are damaged **(Kashani, Rosner and Ostermann, 2020).**

Table 3.3 and Figure 3.2 show a significant increase in creatinine levels in the MTX group (B) compared to group (A). These findings align with previous studies **(Tiwari *et al.*, 2015)(Schmidt *et al.*, 2019).** They demonstrated that a rise in serum creatinine level is associated with renal impairment and delayed methotrexate elimination.

The precipitation of MTX and its metabolites inside the renal tubules may be the cause of the renal impairment that resulted in these outcomes, and this could explain the MTX-induced kidney damage. Researchers identified renal clearance as the primary mechanism for MTX excretion. Urine contains between 70% and 90% of the MTX dosage that is eliminated unchanged. Renal tubular cells tend to precipitate and crystallize, making MTX and its 7-hydroxy metabolite hazardous to them. Three key factors—an acidic pH, low urine volume, and high MTX concentration—are responsible for MTX crystallization and precipitation in the renal tubules. Particularly susceptible to toxicity are the proximal convoluted tubules (PCT), which have a high capacity for drug absorption and metabolism **(Mahmoud *et al.*, 2019)(Sami, Hammo and Athavale, 2022).**

Furthermore, the results of this study show that empagliflozin in group (C) in doses 10mg/kg for 14 days produced a significant decrease ($P<0.05$) in creatinine levels as compared to group (B), not significant compared to group (A) as shown

in Figure 3.3. This result goes in agreement with a previous study **(Wang et al., 2022),** which reported that creatinine level (133.5±12.2 μmol/L) in the disease group was significantly reduced (70.2±10.3 μmol/L) after empagliflozin treatment. Significant effects of SGLT2 inhibition may be associated with modifications in sodium reabsorption in the proximal tubule of the tubule. Blood pressure decreases and intraglomerular hypertension, which likely explains the typical early minor fall in eGFR and the quick and long-lasting reduction in albuminuria linked to SGLT2 inhibition, are among these consequences. **(Cherney *et al.*, 2017)**

Dapagliflozin reduced the creatinine levels, thus significantly reducing the risk of a composite of end-stage kidney disease, death from renal causes, and a sustained decline in the estimated GFR of at least 50% in patients with chronic kidney disease, regardless of whether or not they also had diabetes. **(Heerspink *et al.*, 2020)**. In the present study, dapagliflozin in group (D) significantly reduced the creatinine levels compared to group (B). It was not significant when compared to group (A), as shown in Table (3.3) and Figure (3.2). (**Wheeler *et al.*, 2021)**

Ertugliflozin decreased the risk of the prespecified exploratory renal composite, which included renal death, chronic renal replacement therapy, and a sustained 40% decline in eGFR; participants with microalbuminuria or macroalbuminuria at baseline had a significantly lower urine albumin/creatinine ratio (UACR) compared to placebo; kidney function was preserved, particularly in those with macroalbuminuria who were at the highest risk of developing diabetic kidney disease (DKD); and the renal safety profile was in line with known SGLT2 inhibitor side effects. **(Cherney *et al.*, 2021).** In the current study, the findings showed that pretreatment with 20mg/kg of ertugliflozin (group E) resulted in a significant decrease ($p<0.05$) in creatinine levels compared to group (B) and also resulted in a nonsignificant difference when compared to group (A) as shown in

table (3.3) and figure (3.2). These results align with a previous study that demonstrated that ertugliflozin renal protection is achieved via stimulating tubule-glomerular feedback, and ertugliflozin decreases renal hyperfiltration. This results in afferent arteriolar vasoconstriction and a drop in intraglomerular pressure.**(Cherney *et al.*, 2020) (Groothof *et al.*, 2022).**

4.2.2 Effects on Urea

Increased blood urea levels indicate impaired renal function and should be considered when assessing and evaluating kidney function. Figure (3.1) and Table (3.2) show that MTX in group (B) shows an increase in urea levels significantly compared to group (A). These findings are similar to previous studies **(Sherif, Al-Shaalan and Sabry, 2019).**

Both low and high doses of MTX therapy may cause kidney damage. High doses of MTX cause two types of kidney damage: a decrease in filtration rate and injury to the renal tubule due to MTX precipitation **(Asci *et al.*, 2017).**

Empagliflozin +MTX in group (C) showed a highly significant decrease in urea levels compared to group (B), as described in Figure (3.1) and Table (3.2). Also, this reduction after treatment with empagliflozin was significant compared to group (A). These results are similar to the previous studies **(Kuno *et al.*, 2020)(Maayah *et al.*, 2021).**

Empagliflozin increases distal sodium supply to the macula densa by decreasing sodium reabsorption in the proximal tubule. This increases tubuloglomerular feedback, which causes afferent vasomodulation and a reduction in hyperfiltration. In patients with type I diabetes, empagliflozin has been demonstrated to lower intraglomerular pressure, improve hyperfiltration, and increase the glomerular

filtration rate (GFR). These could lead to better renal outcomes**. (Said and Abdallah, 2021)**.

Pretreatment with dapagliflozin 10mg/kg for 14 days demonstrated a highly significant reduction in urea level compared to group (B) and a significant increase compared to group (A), as shown in Figure (3.1) and Table (3.2). These results are consistent with previous studies. **(Park *et al.*, 2018).**

The mechanism by which dapagliflozin reduces urea levels is similar to empagliflozin. **(Kohan *et al.*, 2016).**

Ertugliflozin + MTX in group (E) produces a highly significant reduction in urea levels compared to group (B). Also, this reduction is significant when compared to group (A). As Shown in Figure (3.1) and Table (3.2). There are no specific studies that support the results of the current research regarding ertugliflozin and its effects on urea levels. Still, many studies state that SGLT2 inhibitors have renal protection. Normally, SGLT2 is increased in circumstances such as hyperglycemia. Increased salt and glucose absorption triggered the activation of Na+-K+ ATPase, increasing oxygen consumption and ATP use and causing damage to the mitochondria. Due to the enhanced salt resorption, the low sodium content in the macula densa triggered tubuloglomerular feedback, which in turn vasodilated the afferent arterioles and raised intraglomerular pressure. SGLT2 inhibitors, including ertugliflozin, reverse these changes and result in the renal protective effect **(Huang *et al.*, 2022)**

4.2.3 Effects on Total Protein

Depletion of protein stored in the body or reduction occurs in advanced CKD. **(Sabatino *et al.*, 2017).** The current study shows that MTX in group (B) causes a highly significant reduction in total protein levels compared to group (A) ($p<0.001$), as shown in Figure (3.5). These results are consistent with the previous

study. **(Tousson *et al.*, 2014)**. MTX causes CKD in a way already mentioned in the current study; CKD patients experience metabolic acidosis. Loss of lean body mass, negative nitrogen balance, and increased protein catabolism are all related to metabolic acidosis. So MTX reduces Total protein levels by causing CKD. **(Zha and Qian, 2017).**

Empagliflozin + MTX in group (C) shows a significant increase in total protein level compared to group (B) and not significant compared to group (A), as shown in Figure (3.5) and Table (3.6) these results align with a previous study. **(Mujalli *et al.*, 2023)**. The exact methods by which empagliflozin improves total protein levels in CKD patients may include numerous components. However, this improvement in blood total protein levels is achieved by maintaining normal renal filtration and lowering protein loss in urine.

Pretreatment with 10mg/kg of dapagliflozin for 14 days in group (D) resulted in a significant rise in total protein levels compared to group (B) and no significant rise compared to group (A), as shown in Figure (3.5), and Table (3.6). These results are in line with another study. **(Chen *et al.*, 2016)**. Because dapagliflozin reduces proteinuria, it may improve total protein levels in CKD patients. **(Xue *et al.*, 2023)**. Also, dapagliflozin's ability to maintain total protein levels in individuals with chronic kidney disease (CKD) may be partly attributed to its benefits in lowering blood pressure and improving cardiovascular function.

In the current study, ertugliflozin in group (E) was associated with significant improvement in total protein levels compared to group (B) and was considered not significant rise in total protein levels compared to group (A), as shown in Figure (3.5), and Table (3.6). There are no other previous studies that agree with the

current study. Also, ertugliflozin, like other SGLT2 inhibitors, is known to have pleiotropic effects, including reducing the protein loss in urine; this effect and others may contribute to its improvement in total protein levels in CKD patients. **(Del Vecchio *et al.*, 2021)**.

4.3 Effect of Methotrexate, Empagliflozin, Dapagliflozin, and Ertugliflozin on Inflammatory Markers

Increased tumor necrosis factor-alpha (TNF-α) is a marker for inflammation in patients with kidney injury. **(Lousa *et al.*, 2021**). Also, interleukin-1bata (IL-1B) is a proinflammatory cytokine considered a biomarker for inflammation in case of kidney injury. **(Buraczynska *et al.*, 2019)**. In the present study, MTX in group (B) causes a significant increase in TNF-α and IL-1B levels as compared to group (A), as shown in Figure (3.6) and Figure (3.7), which was in agreement with the previous study. **(Dar *et al.*, 2021).** Through its impact on nuclear factor kappa-light-chain enhancer of activated B cell (NF-kB) transcription, MTX can raise levels of TNF-α and IL-1B. MTX prevents the replication of DNA and the growth of all cells, including immune cells. Consequently, adenosine levels drop, which often promote NF-kB activation. Reduced adenosine levels facilitate the activation of NF-kB, which in turn increases the transcription of pro-inflammatory cytokines such as TNF-α and IL-1β. **(Maksimovic *et al.*, 2020).**

Empagliflozin + MTX (group C), empagliflozin approved to have an anti-inflammatory effect in the present study as it decreases TNF-α and IL-1B significantly compared to the group (B) of MTX alone, as shown in Figure (3.6) and Figure (3.7). These results were inconsistent with other previous studies **(Kabel, Estfanous and Alrobaian, 2020)(Quagliariello *et al.*, 2021).** It has been demonstrated that empagliflozin inhibits NF-κB activation in a variety of cell types

and tissues. One crucial transcription factor that controls inflammatory reactions is NF-κB. Empagliflozin may lessen the production of pro-inflammatory genes, such as cytokines like TNF-α and IL-1β, by blocking NF-κB activation. **(Dashek et al., 2022)**.

Like empagliflozin, dapagliflozin prevents the activation of NF-κB and, therefore, reduces the production of pro-inflammatory cytokines like IL-1B and TNF-α, so it has an anti-inflammatory effect. **(Quagliariello et al., 2023)**. In the present study, dapagliflozin in group (D) decreases TNF-α and IL-1B significantly compared to group (B), as shown in Figure (3.6) and Figure (3.7). These results are in line with the previous study. **(Winiarska *et al.*, 2021).**

Pretreatment with ertugliflozin (group E) causes a significant reduction in TNF-α and IL-1B levels compared to group (B), as shown in Figure (3.6) and Figure (3.7), which reflected the anti-inflammatory effect of ertugliflozin. These results align with a previous study conducted in 2023, which states that ertugliflozin exhibits its anti-inflammatory effect by inhibiting NF-κB activation.**(Abd and Hassan, 2023)**

The objectives from Table (3.9) are a comparison among selected SGLT2 inhibitors to determine which one is superior to another, and the results revealed that no one is superior to another in terms of the present parameters.

4.4 Histological Alterations

It has been discovered that MTX exhibits severe inflammation and notable morphological changes (marked vascular congestion, chronic inflammatory cell infiltration, Bowman space widening, and Tubular cell vacuolation). Comparing group (B) to control group (A), MTX produced inflammation and showed histological changes in the rat model's kidneys, as shown in figures (3.12, 3.13,

3.14, 3.15, and 3.16). These results were consistent with the previous studies, which concluded that the MTX administration induced histological aberration in the kidneys with Tubular dilatation, atrophy in some tubules, glomerular congestion, and inflammatory cell infiltration in perivascular and intertubular regions **(Savran *et al.*, 2017**). MTX induce severe vacuolation **(Abdel-Daim *et al.*, 2017).**

Empagliflozin in group (C) showed mild vascular congestion, normal glomeruli to mild bowman space widening, and a bland look of the tubular structures, so it reduced the inflammation to a milder degree as compared to group (B), as shown in Figures (3.17, 3.18, and 3.19). These results were in agreement with the previous studies. **(Ala *et al.*, 2022)(Awad and Younis, 2023)**

Dapagliflozin in group (D) showed a seminormal look of the tubular structure and glomeruli as compared to group (B), as shown in Figures (3.20 and 3.21). As in other study **(Doaa I Mohamed *et al.*, 2019)**

Ertugliflozin +MTX in group (E) also showed a bland look of the glomerular and tubular structures as compared to group (B), as shown in Figures (3.22 and 3.23). No previous studies agreed with the current study up to our research.

Chapter Five

Conclusions and Recommendations

Conclusions

1. The selected SGLT2I (empagliflozin, dapagliflozin, and ertugliflozin) preserve renal function via decreasing urea and creatinine levels and increasing total protein level.

2. Empagliflozin, dapagliflozin, and ertugliflozin possess antioxidant properties that can minimize the pro-oxidant induction by MTX via decreasing malondialdehyde level and increasing reduced glutathione level.

3. Empagliflozin, dapagliflozin, and ertugliflozin have shown anti-inflammatory effects via decreased inflammatory mechanisms by decreasing tumor necrosis factor-α level and interleukin-1B level.

Recommendations

1. Future studies should focus on and involve more kidney samples for histopathological examination and implement a standardized scoring system which enable more accurate comparative studies across different experimental groups.

2. Future studies may benefit more from using different or the same protocols with more time.

3. Likewise, more effort is required to explore the full range of oxidative stress and inflammatory markers, with the addition of measures of superoxide dismutase activity(SOD), glutathione peroxidase activity, nitric oxide levels, total antioxidant capacity, Interleukin-1, and Interleukin -6.

4. Future studies should use kidney injury molecule-1 (KIM-1), estimated glomerular filteration rate (eGFR) and albumin/creatinine ratio as a parameter for kidney functions.

References

References:

- Abd, U.A.Q. and Hassan, E.S. (2023) 'Protective Effect of Ertugliflozin against Acute Lung Injury Caused by Endotoxemia Model in Mice', *Iranian Journal of War and Public Health*, 15(1), pp. 67–75.
- Abdel-Daim, M.M. *et al.* (2017) 'Diosmin Attenuates Methotrexate-Induced Hepatic, Renal, and Cardiac Injury: A Biochemical and Histopathological Study in Mice', *Oxidative Medicine and Cellular Longevity*, 2017.
- Ahmed, W., Zaki, A. and Nabil, T. (2015) 'Prevention of methotrexate-induced nephrotoxicity by concomitant administration of garlic aqueous extract in rat', *Turkish Journal of Medical Sciences*, 45(3), pp. 507–516.
- Al-Abdaly, Y.Z., Saeed, M.G. and Al-Hashemi, H.M. (2021) 'Effect of methotrexate and aspirin interaction and its relationship to oxidative stress in rats', *Iraqi Journal of Veterinary Sciences*, 35(1), pp. 151–156.
- Al-Naimi, M. *et al.* (2019) 'Nephrotoxicity: Role and significance of renal biomarkers in the early detection of acute renal injury', *Journal of Advanced Pharmaceutical Technology and Research*, 10(3), pp. 95–99.
- Ala, M. *et al.* (2022) 'Empagliflozin Enhances Autophagy , Mitochondrial Biogenesis , and Antioxidant Defense and Ameliorates Renal Ischemia / Reperfusion in Nondiabetic Rats', 2022.
- Alam, M.N., Bristi, N.J. and Rafiquzzaman, M. (2013) 'Review on in vivo and in vitro methods evaluation of antioxidant activity', *Saudi Pharmaceutical Journal*, 21(2), pp. 143–152.
- Ali, N. *et al.* (2017) *Protective effect of Chlorogenic acid against methotrexate induced oxidative stress, inflammation and apoptosis in rat liver: An experimental approach*, *Chemico-Biological Interactions*. Elsevier

Ireland Ltd.

- Alsahli, M. and Gerich, J.E. (2017) 'Renal glucose metabolism in normal physiological conditions and in diabetes', *Diabetes Research and Clinical Practice,*133, pp. 1–9.
- Alshanwani, A.R. *et al.* (2021) 'Cyanocobalamin and/or calcitriol mitigate renal damage-mediated by tamoxifen in rats: Implication of caspase-3/NF-κB signaling pathways', *Life Sciences*, 277(April), p. 119512.
- Alvirdizadeh, S. *et al.* (2020) 'A prospective study on total protein , plant protein and animal protein in relation to the risk of incident chronic kidney disease', pp. 1–7.
- Amin, N.B. *et al.* (2015) 'Blood pressure-lowering effect of the sodium glucose co-transporter-2 inhibitor ertugliflozin, assessed via ambulatory blood pressure monitoring in patients with type 2 diabetes and hypertension', *Diabetes, Obesity and Metabolism*, 17(8), pp. 805–808.
- Arab, H.H., Al-Shorbagy, M.Y. and Saad, M.A. (2021) 'Activation of autophagy and suppression of apoptosis by dapagliflozin attenuates experimental inflammatory bowel disease in rats: Targeting AMPK/mTOR, HMGB1/RAGE and Nrf2/HO-1 pathways', *Chemico-Biological Interactions*, 335(January), p. 109368.
- Asci, H. *et al.* (2017) 'The impact of gallic acid on the methotrexate-induced kidney damage in rats', *Journal of Food and Drug Analysis*, 25(4), pp. 890–897.
- Awad, M.M.Y. and Younis, A.M. (2023) 'Empagliflozin alleviates diabetic nephropathy in albino rats through its antioxidative and anti - inflammatory action and use of laboratory animals .', 17(1), pp. 0–4.
- Azadnasab, R. *et al.* (2021) 'Epicatechin ameliorative effects on

methotrexate-induced hepatotoxicity in mice', *Human and Experimental Toxicology*, 40(12_suppl), pp. S603–S610.

- Bailey, C.J., Day, C. and Bellary, S. (2022) 'Renal Protection with SGLT2 Inhibitors: Effects in Acute and Chronic Kidney Disease', *Current Diabetes Reports*, 22(1), pp. 39–52.
- Bedoui, Y. *et al.* (2019) 'Methotrexate an old drug with new tricks', *International Journal of Molecular Sciences*, 20(20).
- Bodnar, P. *et al.* (2023) 'The Impact of Pharmacotherapy for Heart Failure on Oxidative Stress—Role of New Drugs, Flozins', *Biomedicines*, 11(8), pp. 1–32.
- Bora, E.S. *et al.* (2021) 'Protective effect of dapagliflozin on colistin-induced renal toxicity', *Signa Vitae*, 17(4), pp. 92–97.
- Boulton, D.W. *et al.* (2013) 'Simultaneous oral therapeutic and intravenous 14C-microdoses to determine the absolute oral bioavailability of saxagliptin and dapagliflozin', *British Journal of Clinical Pharmacology*, 75(3), pp. 763–768.
- Boyer, N. *et al.* (2022) 'Critical Care Nephrology and Acute Kidney Injury Postoperative Acute Kidney Injury', 17(Table 2), pp. 1535–1545.
- Buraczynska, M. *et al.* (2019) 'Interleukin-1β Gene (IL1B) Polymorphism and Risk of Developing Diabetic Nephropathy', *Immunological Investigations*, 48(6), pp. 577–584.
- Chen, L. *et al.* (2016) 'Effect of Dapagliflozin Treatment on Fluid and Electrolyte Balance in Diabetic Rats', *American Journal of the Medical Sciences*, 352(5), pp. 517–523.
- Chen, W. *et al.* (2023) 'Dapagliflozin alleviates myocardial ischemia/reperfusion injury by reducing ferroptosis via MAPK signaling

inhibition', *Frontiers in Pharmacology*, 14(February), pp. 1–15.

- Chen, X. *et al.* (2023) 'Cellular and Molecular Effects of Antidiabetics Beyond Glycemic Control Renoprotective effects of empagli fl ozin are linked to activation of the tubuloglomerular feedback mechanism and blunting of the complement system', (February), pp. 951–962.
- Cherney, D.Z.I. *et al.* (2017) 'Effects of empagliflozin on the urinary albumin-to-creatinine ratio in patients with type 2 diabetes and established cardiovascular disease: an exploratory analysis from the EMPA-REG OUTCOME randomised, placebo-controlled trial', *The Lancet Diabetes and Endocrinology*, 5(8), pp. 610–621.
- Cherney, D.Z.I. *et al.* (2020) 'Effects of ertugliflozin on renal function over 104 weeks of treatment: a post hoc analysis of two randomised controlled trials', *Diabetologia*, 63(6), pp. 1128–1140.
- Cherney, D.Z.I. *et al.* (2021) 'Effects of ertugliflozin on kidney composite outcomes, renal function and albuminuria in patients with type 2 diabetes mellitus: an analysis from the randomised VERTIS CV trial', *Diabetologia*, 64(6), pp. 1256–1267.
- Croteau, D. *et al.* (2021) 'Effects of sodium-glucose linked transporter 2 inhibition with ertugliflozin on mitochondrial function, energetics, and metabolic gene expression in the presence and absence of diabetes mellitus in mice', *Journal of the American Heart Association*, 10(13).
- Dar, A.A. *et al.* (2021) 'The protective role of luteolin against the methotrexate-induced hepato-renal toxicity via its antioxidative, anti-inflammatory, and anti-apoptotic effects in rats', *Human and Experimental Toxicology*, 40(7), pp. 1194–1207.
- Dashek, R. *et al.* (1924) 'Effects of Empagliflozin on Intermittent Hypoxia-

Induced TRAF3IP2-Dependent Human Aortic Smooth Muscle Cell Proliferation Published : October 31 , 2022 Citation : Dashek R , Higash Y , et al ., 2022 . Effects of Empagliflozin on Intermittent Dependent Hum', pp. 1–17.

- DeFronzo, R.A., Norton, L. and Abdul-Ghani, M. (2017) 'Renal, metabolic and cardiovascular considerations of SGLT2 inhibition', *Nature Reviews Nephrology*, 13(1), pp. 11–26.
- Denic, A. *et al.* (2017) 'The substantial loss of nephrons in healthy human kidneys with aging', *Journal of the American Society of Nephrology*, 28(1), pp. 313–320.
- Fala, L. (2015) 'Jardiance (Empagliflozin), an SGLT2 Inhibitor, Receives FDA Approval for the Treatment of Patients with Type 2 Diabetes.', *American health & drug benefits*, 8(Spec Feature), pp. 92–5.
- Franken, G.A.C. *et al.* (2021) 'Mechanisms coupling sodium and magnesium reabsorption in the distal convoluted tubule of the kidney', *Acta Physiologica*, 231(2), pp. 1–15.
- Garlanda, C., Dinarello, C.A. and Mantovani, A. (2013) 'Review The Interleukin-1 Family : Back to the Future', pp. 1003–1018.
- Griffin, B.R., Faubel, S. and Edelstein, C.L. (2019) 'Biomarkers of drug-induced kidney toxicity', *Therapeutic Drug Monitoring*, 41(2), pp. 213–226.
- Groothof, D. *et al.* (2022) 'Ertugliflozin, renoprotection and potential confounding by muscle wasting', *Diabetologia*, 65(5), pp. 906–907.
- Hamed, K.M. *et al.* (2022) 'Overview of Methotrexate Toxicity : A Comprehensive Literature Review', 14(9).
- Den Hartogh, D.J. and Tsiani, E. (2019) *Health benefits of resveratrol in kidney disease: Evidence from in vitro and in vivo studies*, *Nutrients*.

- Hashkes, P.J. *et al.* (2014) 'Methotrexate: New uses for an old drug', *Journal of Pediatrics*, 164(2), pp. 231–236.
- Heerspink, H.J.L. *et al.* (2020) 'Dapagliflozin in Patients with Chronic Kidney Disease', *New England Journal of Medicine*, 383(15), pp. 1436–1446.
- Heymsfield, B. and Of, M.U.I. (2018) 'in Nutrition Measurement of muscle mass in humans : validity of the 24-hour urinary creatinine Thliuif', (February), pp. 478–494.
- Hristov, B.D. (2022) 'The Role of Glutathione Metabolism in Chronic Illness Development and Its Potential Use as a Novel Therapeutic Target', 14(9).
- Huang, W. *et al.* (2022) 'Recent Advances in the Emerging Therapeutic Strategies for Diabetic Kidney Diseases', *International Journal of Molecular Sciences*, 23(18).
- Izzedine, H. and Perazella, M.A. (2017) 'Anticancer Drug-Induced Acute Kidney Injury', *Advances in Clinical Chemistry*, 81(4), pp. 504–514.
- Jalili, C. *et al.* (2020) 'Toxic effects of methotrexate on rat kidney recovered by crocin as a consequence of antioxidant activity and lipid peroxidation prevention', *Iranian Biomedical Journal*, 24(1), pp. 39–46.
- Kabel, A.M., Estfanous, R.S. and Alrobaian, M.M. (2020) 'Targeting oxidative stress, proinflammatory cytokines, apoptosis and toll like receptor 4 by empagliflozin to ameliorate bleomycin-induced lung fibrosis', *Respiratory Physiology and Neurobiology*, 273, p. 103316.
- Kapusta, A., Kuczyńska, B. and Puppel, K. (2018) 'Relationship between the degree of antioxidant protection and the level of malondialdehyde in high-performance polish holstein-Friesian cows in peak of lactation', *PLoS ONE*, 13(3), pp. 1–13.
- Kardasz, S. (2015) 'The function of the nephron and the formation of urine',

Anaesthesia and Intensive Care Medicine, 16(6), pp. 286–291.

- Kashani, K., Rosner, M.H. and Ostermann, M. (2020) 'Creatinine: From physiology to clinical application', *European Journal of Internal Medicine*, 72(October), pp. 9–14.
- Kasichayanula, S. *et al.* (2014) 'Clinical pharmacokinetics and pharmacodynamics of dapagliflozin, a selective inhibitor of sodium-glucose Co-transporter type 2', *Clinical Pharmacokinetics*, 53(1), pp. 17–27.
- Kim, H.J. *et al.* (2021) 'PLOS ONE Effects of blood urea nitrogen independent of the estimated glomerular filtration rate on the development of anemia in non-dialysis chronic kidney disease : The results of the KNOW-CKD study', pp. 1–21.
- Kohan, D.E. *et al.* (2016) 'The effect of dapagliflozin on renal function in patients with type 2 diabetes', *Journal of Nephrology*, 29(3), pp. 391–400.
- Kuno, A. *et al.* (2020) 'Empagliflozin attenuates acute kidney injury after myocardial infarction in diabetic rats', *Scientific Reports*, 10(1), pp. 1–9.
- Kwiatkowska, E. *et al.* (2021) 'The mechanism of drug nephrotoxicity and the methods for preventing kidney damage', *International Journal of Molecular Sciences*, 22(11).
- Lindgren, D., Sjölund, J. and Axelson, H. (2018) 'Tracing Renal Cell Carcinomas back to the Nephron', *Trends in Cancer*, 4(7), pp. 472–484.
- Liu, H. *et al.* (2021) 'Markers of Kidney Injury, Inflammation, and Fibrosis Associated With Ertugliflozin in Patients With CKD and Diabetes', *Kidney International Reports*, 6(8), pp. 2095–2104.
- Liu, J., Lee, T.W. and DeFronzo, R.A. (2012) 'Why do SGLT2 inhibitors inhibit only 30-50% of renal glucose reabsorption in humans?', *Diabetes*, 61(9), pp. 2199–2204.

- Liu, X. *et al.* (2020) 'Nutrition , Metabolism & Cardiovascular Diseases The associations of plant-based protein intake with all-cause and cardiovascular mortality in patients on peritoneal dialysis', *Nutrition, Metabolism and Cardiovascular Diseases* [Preprint], (xxxx).
- Lousa, I. *et al.* (2021) 'New potential biomarkers for chronic kidney disease management — A review of the literature', *International Journal of Molecular Sciences*, 22(1), pp. 1–37.
- Lu, S.C. (2013) 'Glutathione synthesis', *Biochimica et Biophysica Acta - General Subjects*, 1830(5), pp. 3143–3153.
- Luciano, R.L. and Perazella, M.A. (2018) 'Drug-Induced Acute Kidney Injury'.
- Maayah, Z.H. *et al.* (2021) 'Empagliflozin suppresses inflammation and protects against acute septic renal injury', *Inflammopharmacology*, 29(1), pp. 269–279.
- Mahmoud, A.M. *et al.* (2019) 'Ferulic acid protects against methotrexate nephrotoxicity: Via activation of Nrf2/ARE/HO-1 signaling and PPARγ, and suppression of NF-κB/NLRP3 inflammasome axis', *Food and Function*, 10(8), pp. 4593–4607.
- Maksimovic, V. *et al.* (2020) 'Molecular mechanism of action and pharmacokinetic properties of methotrexate', *Molecular Biology Reports*, 47(6), pp. 4699–4708.
- Malínská, H. *et al.* (2022) 'Beneficial Effects of Empagliflozin Are Mediated by Reduced Renal Inflammation and Oxidative Stress in Spontaneously Hypertensive Rats Expressing Human C-Reactive Protein', *Biomedicines*, 10(9).
- Markham, A. (2018) 'Ertugliflozin: First Global Approval', *Drugs*, 78(4), pp.

513–519.

- Miao, Z. *et al.* (2013) ‘Pharmacokinetics, metabolism, and excretion of the antidiabetic agent ertugliflozin (PF-04971729) in healthy male subjectss’, *Drug Metabolism and Disposition*, 41(2), pp. 445–456.
- Mody, H. *et al.* (2020) ‘A Review on Drug-Induced Nephrotoxicity: Pathophysiological Mechanisms, Drug Classes, Clinical Management, and Recent Advances in Mathematical Modeling and Simulation Approaches’, *Clinical Pharmacology in Drug Development*, 9(8), pp. 896–909.
- Mohamed, Doaa I *et al.* (2019) ‘Potential protective effects of Dapagliflozin in gentamicin induced nephrotoxicity rat model via modulation of apoptosis associated miRNAs’, *Gene*, 707(April), pp. 198–204.
- Moodi, H. *et al.* (2020) ‘Ethanolic extract of Iris songarica rhizome attenuates methotrexate-induced liver and kidney damages in rats.’, *Avicenna journal of phytomedicine*, 10(4), pp. 372–383.
- Morya, R., Kumar, K. and Kumar, P. (2018) ‘Anatomical and Physiological Similarities of Kidney in Different Experimental Animals Used for Basic Studies’, *Journal of Clinical & Experimental Nephrology*, 03(02), pp. 1–6.
- Mujalli, A. *et al.* (2023) ‘Improved Glycaemic Control and Nephroprotective Effects of Empagliflozin and Paricalcitol Co-Therapy in Mice with Type 2 Diabetes Mellitus’, *International Journal of Molecular Sciences*, 24(24).
- Ndefo, U.A. *et al.* (2015) ‘Empagliflozin (Jardiance): A Novel SGLT2 Inhibitor for the Treatment of Type-2 Diabetes.’, *P & T : a peer-reviewed journal for formulary management*, 40(6), pp. 364–8.
- Owumi, S.E., Ajijola, I.J. and Agbeti, O.M. (2019) ‘Hepatorenal protective effects of protocatechuic acid in rats administered with anticancer drug methotrexate’, *Human and Experimental Toxicology*, 38(11), pp. 1254–1265.

- Park, H.S. *et al.* (2018) 'Use of dapagliflozin in patients with advanced diabetic kidney disease', *Kidney Research and Clinical Practice*, 37(3), pp. 292–297.
- Paueksakon, P. and Fogo, A.B. (2017) 'Drug-induced nephropathies', *Histopathology*, 70(1), pp. 94–108.
- Quagliariello, V. *et al.* (2021) 'The SGLT-2 inhibitor empagliflozin improves myocardial strain, reduces cardiac fibrosis and pro-inflammatory cytokines in non-diabetic mice treated with doxorubicin', *Cardiovascular Diabetology*, 20(1), pp. 1–20.
- Quagliariello, V. *et al.* (no date) 'Dapagliflozin prevents ejection fraction reduction , reduces myocardial and renal NF- κ B expression and systemic pro-inflammatory biomarkers in models of short-term doxorubicin cardiotoxicity'.
- Rieg, T. and Vallon, V. (2018) 'Development of SGLT1 and SGLT2 inhibitors', *Diabetologia*, 61(10), pp. 2079–2086.
- Rosenstock, J. *et al.* (no date) 'No 主観的健康感を中心とした在宅高齢者における 健康関連指標に関する共分散構造分析Title'.
- Rubino, F.M. (2001) 'Separation methods for methotrexate, its structural analogues and metabolites', *Journal of Chromatography B: Biomedical Sciences and Applications*, 764(1–2), pp. 217–254.
- Sabatino, A. *et al.* (2017) 'Protein-energy wasting and nutritional supplementation in patients with end-stage renal disease on hemodialysis', *Clinical Nutrition*, 36(3), pp. 663–671.
- Safaei, F. *et al.* (2018) 'Protective effects of gallic acid against methotrexate-induced toxicity in rats', *Acta Chirurgica Belgica*, 118(3), pp. 152–160.
- Sahasrabudhe, V. *et al.* (2018) 'A Phase 1, Randomized, Placebo- and Active-

Controlled Crossover Study to Determine the Effect of Single-Dose Ertugliflozin on QTc Interval in Healthy Volunteers', *Clinical Pharmacology in Drug Development*, 7(5), pp. 513–523.

- Sahindokuyucu-Kocasari, F. *et al.* (2021) 'Apigenin alleviates methotrexate-induced liver and kidney injury in mice', *Human and Experimental Toxicology*, 40(10), pp. 1721–1731.
- Said, M. and Abdallah, H. (2021) 'Potential mechanisms underlying the renoprotective effect of empagliflozin, a novel selective sodium glucose co-transporter (SGLT) 2 inhibitor, against diabetic nephropathy in streptozotocin induced diabetic rats', *Bulletin of Egyptian Society for Physiological Sciences*, 0(0), pp. 344–357.
- Saini, V. (2022) 'The role of oxidative stress in kidney diseases', *Novel Therapeutic Approaches Targeting Oxidative Stress*, pp. 119–141.
- Sales, G.T.M. and Foresto, R.D. (2020) 'Drug-induced nephrotoxicity', *Revista da Associacao Medica Brasileira*, 66(Suppl 1), pp. 82–90.
- Sami, F.L., Hammo, H. and Athavale, A. (2022) 'Crystalline Nephropathy With High-Dose Methotrexate in a Patient With Primary CNS Lymphoma: A Case Report', *Cureus*, 14(6), pp. 2–8.
- Santhakumar, P. *et al.* (2021) 'Ethanolic extract of capparis decidua fruit ameliorates methotrexate-induced hepatotoxicity by activating NrF2/HO-1 and PPARγ mediated pathways', *Indian Journal of Pharmaceutical Education and Research*, 55(1), pp. s265–s274.
- Savran, M. *et al.* (2017) 'Vitamin C attenuates methotrexate-induced oxidative stress in kidney and liver of rats', *Physiology International*, 104(2), pp. 139–149.
- Schett, G., Dayer, J. and Manger, B. (2015) 'Interleukin-1 function and role

in rheumatic disease', *Nature Publishing Group*, (Il), pp. 1–11.

- Schmidt, D. *et al.* (2019) 'Plasma creatinine as predictor of delayed elimination of high-dose methotrexate in childhood acute lymphoblastic leukemia: A Danish population-based study', *Pediatric Blood and Cancer*, 66(6).
- Sethi, J.K. and Hotamisligil, G.S. (2021) 'Metabolic Messengers: tumour necrosis factor', *Nature Metabolism*, 3(10), pp. 1302–1312.
- Sharma, S. *et al.* (2020) 'Ameliorative effect of a standardized polyherbal combination in methotrexate-induced nephrotoxicity in the rat', *Pharmaceutical Biology*, 58(1), pp. 184–199.
- Sherif, I.O., Al-Shaalan, N.H. and Sabry, D. (2019) 'Ginkgo biloba extract alleviates methotrexate-induced renal injury: New impact on pi3k/akt/mtor signaling and malat1 expression', *Biomolecules*, 9(11), pp. 4–6.
- Song, J. *et al.* (2019) 'Understanding kidney injury molecule 1: A novel immune factor in kidney pathophysiology', *American Journal of Translational Research*, 11(3), pp. 1219–1229.
- Steiner, S. (2016) 'Empagliflozin, cardiovascular outcomes, and mortality in type 2 diabetes', *Zeitschrift fur Gefassmedizin*, 13(1), pp. 17–18.
- Theodorou, C., Leatherby, R. and Dhanda, R. (2021) 'Function of the nephron and the formation of urine', *Anaesthesia and Intensive Care Medicine*, 22(7), pp. 434–438.
- Tiwari, P. *et al.* (2015) 'Serum Creatinine Versus Plasma Methotrexate Levels to Predict Toxicities in Children Receiving High-dose Methotrexate', *Pediatric Hematology and Oncology*, 32(8), pp. 576–584.
- Tousson, E. *et al.* (2014) 'Methotrexate-induced Hepatic and Renal Toxicity: Role of L-carnitine in Treatment', *Biomedicine and Biotechnology*, 2(4), pp.

85–92.

- Update, A.D.A. *et al.* (2023) ‘Malondialdehyde as a Potential Oxidative Stress Marker for’, pp. 1–22.
- Vallon, V. (2011) ‘The proximal tubule in the pathophysiology of the diabetic kidney’, *American Journal of Physiology - Regulatory Integrative and Comparative Physiology*, 300(5).
- Vallon, V. and Thomson, S.C. (2017) ‘Targeting renal glucose reabsorption to treat hyperglycaemia: the pleiotropic effects of SGLT2 inhibition’, *Diabetologia*, 60(2), pp. 215–225.
- Del Vecchio, L. *et al.* (2021) ‘A Role for SGLT-2 Inhibitors in Treating Non-diabetic Chronic Kidney Disease’, *Drugs*, 81(13), pp. 1491–1511.
- Vielhauer, V. and Mayadas, T.N. (2007) ‘Functions of TNF and its Receptors in Renal Disease : Distinct Roles in Inflammatory’, 27(3), pp. 286–308.
- Wang, Q. *et al.* (2022) ‘Empagliflozin protects against renal ischemia/reperfusion injury in mice’, *Scientific Reports*, 12(1), pp. 1–15.
- Weber, A. *et al.* (2010) ‘Interleukin-1 □ (IL-1 □) Processing Pathway’, 3(105), pp. 3–5.
- Wheeler, D.C. *et al.* (2021) ‘A pre-specified analysis of the DAPA-CKD trial demonstrates the effects of dapagliflozin on major adverse kidney events in patients with IgA nephropathy’, *Kidney International*, 100(1), pp. 215–224.
- Winiarska, A. *et al.* (2021) ‘Inflammation and oxidative stress in diabetic kidney disease: The targets for SGLT2 inhibitors and GLP-1 receptor agonists’, *International Journal of Molecular Sciences*, 22(19), pp. 1–38.
- Wiviott, S.D. *et al.* (2019) ‘Dapagliflozin and Cardiovascular Outcomes in Type 2 Diabetes’, *New England Journal of Medicine*, 380(4), pp. 347–357.
- Xue, S. *et al.* (2023) ‘Dapagliflozin can alleviate renal fibrosis in rats with

streptozotocin-induced type 2 diabetes mellitus', *Experimental and Therapeutic Medicine*, 26(6), pp. 1–10.

- Yaribeygi, H. *et al.* (2019) 'Sodium–glucose cotransporter inhibitors and oxidative stress: An update', *Journal of Cellular Physiology*, 234(4), pp. 3231–3237.
- Yaribeygi, H. *et al.* (2023) 'Sodium Glucose Cotransporter-2 Inhibitor Empagliflozin Increases Antioxidative Capacity and Improves Renal Function in Diabetic Rats', *Journal of Clinical Medicine*, 12(11), pp. 1–12.
- Zha, Y. and Qian, Q. (2017) 'Protein nutrition and malnutrition in CKD and ESRD', *Nutrients*, 9(3), pp. 1–19.
-

في المجموعات العلاجيه الثلاثه كانت نسب كل من(TNF-a, IL-1B, Urea, Creatinine, MDA) قد انخفضت بشكل كبير بينما نسب(GSH و Total protein) قد ازدادت بشكل كبير مقارنه مع المجموعه (ب).

احداث المرض بواسطه ماده MTX يصاحبه التهاب شديد وتغيرات نسيجيه ملحوظه (احتقان الاوعيه الدمويه, اتساع فتحة بومان, خلايا ملتهبه, خلايا انبوبيه مفرغه) كل هذه الاعراض في المجموعه (ب) ولاتوجد في المجموعه (ا).

وجدت هذه الدراسه بان ادويه (Dapagliflozin , Empagliflozin, Ertugliflozin) تخفف من الاضرار النسيجيه المرضيه والالتهابات ايظا مقارنه مع المجموعه (ب).

في الختام نستنتج من الدراسه الحاليه بان هذه المجموعه العلاجيه لها تاثيرات وقائيه مضاده للالتهابات ومضاده للاكسده وتوفر حمايه للكلى. كما هو مبين في الاختبارات البيوكيميائيه والنتائج النسيجيه .

الخلاصه

تعتبر السمية الكلوية هي السبب الثالث الأكثر شيوعا لأمراض الكلى الحادة، والتي ازدادت سوءا في العقود الأخيرة نتيجة لتعاطي المخدرات التي تنطوي على مخاطر أعلى لتلف الكلى. أظهرت الدراسات أن ما يصل إلى 20 ٪ من المرضى المصابين بأمراض خطيرة يستخدمون الأدوية السامة للكلية. في حين أن اختبارات السلامة مطلوبة قبل طرح الأدوية الجديدة في السوق ، لا يتم اكتشاف الآثار الضارة في كثير من الأحيان إلا بعد طرح الدواء في السوق واستخدامه من قبل مختلف السكان في جميع أنحاء العالم. يؤدي إفراز الكلى للأدوية إلى تعريض الهياكل التي تتطلب طاقة عالية في الكلى ، الكبيبات والأنابيب ، لتركيزات كبيرة من المواد الكيميائية الأجنبية ، وهو ما يفسر سبب ارتفاع معدلات إصابة الكلى الناتجة عن الأدوية. يعد فقدان معدل الترشيح الكبيبي علامة متأخرة لإصابة الكلى ، ويتم البحث عن مؤشرات حيوية أخرى للسماح بتدخل مبكر ، مما قد يحسن تشخيص هؤلاء المرضى.

مثبطات نواقل الصوديوم والكلوكوز 2 هو فئة من الأسرة المضادة لمرض السكر التي لديها حماية الكلى. استكشفت هذه الدراسة آثار (Empagliflozin ، Dapagliflozin ، Ertugliflozin) كمضاد للأكسدة ، مضاد للالتهابات وحماة الكلى.

تم تسجيل خمسين فئران ألبينو من الذكور البالغين ، وتم تقسيم الفئران المختارة إلى خمس مجموعات ، مع عشرة فئران في كل مجموعة. المجموعة (أ) لم تتعرض MTX ولم تتلق أي علاج ، في حين تعرضت المجموعة (ب) إلى 10 ملغ/كغ من MTX في اليوم العاشر من التجربة. تلقت المجموعة (ج) 10 مجم/كجم من Empagliflozin عن طريق التزقيم الفموي لمدة أربعة عشر يوما و 10 مجم/كجم من MTX في اليوم 10 من التجربة. تعرضت المجموعة (د) ل Dapagliflozin 10 مجم/كجم عن طريق التزقيم الفموي لمدة أربعة عشر يوما و 10مجم/كجم من MTX في اليوم العاشر من التجربة. تلقت المجموعة (هـ) 20 مجم/كجم من Ertugliflozin عن طريق التزقيم الفموي لمدة أربعة عشر يوما وتعرضت لـ 10 مجم/كجم من MTX في اليوم العاشر من التجربة.

تم قياس التاثير الوقائي الكلوي لمثبطات نواقل الصوديوم والكلوكوز 2 من خلال قياس نسبة (TNF-a, IL-1B, MDA, GSH, Creatinine, Urea, Total protein) في الدم . في المجموعه (ب) كانت نسب (TNF-a, IL-1B, Urea, Creatinine, MDA) تزيد بصوره كبيره جدا مقارنه مع نسبها في المجموعه (ا) بينما نسب(GSH و Total protein) انخفضت بصوره كبيره مقارنه مع المجموعه (ا).

جمهورية العراق

وزارة التعليم العالي والبحث العلمي

جامعة بابل/ كلية الطب

التأثيرات الوقائية المحتملة لمثبطات SGLT2 ضد السمية الكلوية الناتجة عن الميثوتريكسات في النموذج حيواني

رسالة

مقدمـــة إلـــى مجلس كليـــة الطـــب / جامعـــة بابـــل

كجزء من متطلبـات نيل درجـة الماجستير في الادويه /الادويه والسموم

من قبل

رامي ثامر كريم عبد الائمه الحسيني

بكالوريوس صيدلة

الرافدين الجامعه (2016-2017) كلية

إشراف

م.د	ا. مساعد
احمد راجي	ماجد كاظم عباس
دكتوراه علم الانسجه	ماجستير علم الادويه
1445 هـ	2024 م